Quantum Magnetism, Interacting Bosons, and Low Dimensionality

Edmond Orignac

ÉCOLE NORMALE SUPÉRIEURE DE LYON

Mémoire d'Habilitation à diriger des recherches
Version of March 24, 2014

Spécialité: Physique

Edmond ORIGNAC

SUJET: **Magnétisme Quantique, Bosons en interaction et basse dimensionnalité**

Composition de la commission d'examen

MM. B. Douçot *Rapporteur*
T. Jolicoeur *Rapporteur*
P. Holdsworth *Examinateur*
F. Mila *Rapporteur*
S. Eggert *Examinateur*

Laboratoire de Physique de l'École Normale Supérieure de Lyon
46, Allée d'Italie, 69007 Lyon France
Edmond.Orignac@ens-lyon.fr

Contents

General introduction

I began my research experience in the field of correlated low-dimensional systems during my PhD thesis under the direction of Thierry Giamarchi from 1994 to 1998 at the Laboratoire de Physique des solides of the University Paris-Sud. The subject of my thesis was the effect of disorder in ladder systems, and was in part motivated by the discovery of superconductivity in the ladder material $Sr_{14}Cu_{24}O_{41}$ under high pressure. During that period, I became acquainted with the bosonization technique and the renormalization group.

After the PhD, I moved to Rutgers University (Piscataway, New Jersey) for a postdoctoral fellowship. During that period, I got interested in the spin-tube system as well as Kondo-Heisenberg chains. The work with Natan Andrei led me the learn integrable models and conformal field theory techniques. During that period, I started to collaborate with R. Citro (U. Salerno, Italy). I was hired in 1999 by CNRS, at the laboratoire de Physique theorique de l'Ecole Normale Superieure. During that period, I worked with P. Lecheminant (University of Cergy) and R. Chitra (then at Université Pierre et Marie Curie, now at ETH Zurich). My principal fields of study was then quantum magnetism in low dimensions, and I was partially supported by an ACI grant from the French Ministry of Research jointly with R. Moessner. I stayed in Paris until 2005, then moved to the ENS-Lyon. There, I started a collaboration with David Carpentier on transport in mesoscopic spin glasses and more recently on topological insulators. In parallel, I started to work on interacting boson systems, motivated in part by experiments on ultracold gases. In the present habilitation thesis, I have chosen to focus on the closely related topics of quantum magnetism and interacting bosons in low dimensionality. In a first part, I will introduce the field of interacting systems in one-dimension. I will review the bosonization technique as well as the theory of the quantum sine-Gordon model. In a second part, I will describe my work on quantum spin systems, starting with two leg ladder systems, and ending with the spin-Peierls transition. In the last part, I will describe the research on interacting bosons.

Note concerning this version of the manuscript

The thesis that was reviewed before the habilitation defense also included copies of articles published in peer-reviewed journals. For copyright reasons, the articles cannot be included in this version. Instead, when necessary, I have introduced a note in a boxed frame at the beginning of the chapter indicating on which articles it is based.

Part I

Introduction to one-dimensional systems

Chapter 1

one-dimensional fermions and bosonization

In three dimensional systems of interacting fermions, such as electrons in a metal or liquid ^{3}He, the thermodynamics and the low energy response can be described in terms of the Landau Fermi liquid theory.[1, 2, 3, 4] In Landau Fermi liquid theory, the elementary excitations of the system are fermionic quasiparticles possessing a residual interaction. The energy of an excited state is:

$$\delta E = \sum_{k,\sigma} \epsilon(k,\sigma)\delta n_{k,\sigma} + \frac{1}{2}\sum_{\substack{k,k'\\ \sigma,\sigma'}} f(k,\sigma;k',\sigma')\delta n_{k,\sigma}\delta n_{k',\sigma'}, \tag{1.1}$$

where $\epsilon(k,\sigma)$ is a renormalized dispersion for the quasiparticles,[1], $\delta n(k,\sigma)$ is the variation of quasiparticle occupation number in the state k,σ and $f(k,\sigma;k',\sigma')$ is the residual interaction. Eq.(1.1) leads to a specific heat behaving as:

$$C_v = \frac{\pi^2 k_B^2 T}{3}\rho(\epsilon_F), \tag{1.2}$$

where $\rho(\epsilon)$ is the density of states resulting from the renormalized dispersion $\epsilon(k,\sigma)$. Considering a variation of the density, one finds that[4]:

$$\frac{\partial\mu}{\partial N} = \frac{\pi^2}{L^3 k_F m^*} + \int \frac{d\Omega}{8\pi} f(\mathbf{k},\mathbf{k}'), \tag{1.3}$$

i. e. the residual interactions between the quasiparticles renormalizes the compressibility of the Fermi liquid. The magnetic susceptibility χ_M is also renormalized[4], with:

$$\frac{(g\mu_B)^2}{\chi_M} = \frac{4\pi^2}{m^* k_F} + \frac{L^3}{2\pi}\int d\Omega[f(\mathbf{k},\uparrow,\mathbf{k}',\uparrow) - f(\mathbf{k},\uparrow,\mathbf{k}',\downarrow)] \tag{1.4}$$

[1]often taken in the form $\epsilon(k) = v_F(k_F)(k-k_F)$ with $v_F = k_F/m^*$, m^* being an effective mass different from the electron mass, containing renormalizations coming from the interactions

The Landau Fermi liquid theory can be justified in the framework of many-body diagrammatic perturbation theory from some plausible hypotheses[5] and experiments on heavy fermion materials have shown that quasiparticles with a mass 100 times the electron mass could account for the thermodynamics of these systems, indicating that in strongly correlated systems very strong renormalizations of the dispersion can be obtained without a breakdown of the Fermi liquid state. Despite its robustness, the Fermi liquid theory is known to break down in low-dimensional systems. The most well known examples are the fractional quantum hall effect, where the physical properties can be described in terms of quasiparticles of fractional charge possessing anyonic statistics and the one-dimensional systems where the quasiparticles are replaced by collective charge and spin excitations propagating at different velocities, the so-called Tomonaga-Luttinger liquid.[6, 7] The case of one-dimensional systems is not only a theoretical counterexample to Landau Fermi liquid theory. It is also relevant to various experimental systems such as the organic conductors $(TMTTF)_2X$, $(TMTSF)_2X$ inorganic conductors such as $Li_{0.9}Mo_6O_{17}$, or carbon nanotubes. Moreover, the Tomonaga-Luttinger liquid concept is not restricted to fermionic systems, but is also applicable to spin systems and systems of interacting bosons. As a result, it has found applications to low dimensional quantum antiferromagnets such as $KCuF_3$ as well as ultracold atomic gases. In the rest of this chapter, I will review the solution the the Tomonaga-Luttinger model, and I will introduce the spin-charge separation concept. I will then discuss the extension of the Tomonaga-Luttinger liquid concept to spin systems and interacting bosons. I will then turn to perturbations of the Tomonaga-Luttinger model, and introduce the concept of the Luther-Emery liquid and the quantum sine-Gordon model. I will end with a survey of the experimental systems.

1.1 The Tomonaga-Luttinger model

1.1.1 Definition of the model

To obtain the Tomonaga-Luttinger model, we start with a model on one-dimensional interacting spinless fermions with Hamiltonian:

$$\begin{aligned} H &= H_0 + V && (1.5)\\ H_0 &= \sum_k \epsilon(k) c_k^\dagger c_k && (1.6)\\ V &= \frac{1}{L}\sum_{k_1,k_2,q} V(q) c_{k_1+q}^\dagger c_{k_2-q}^\dagger c_{k_2} c_{k_1}. && (1.7) \end{aligned}$$

Our aim is to understand the low-energy spectrum of the Hamiltonian (1.5). Since we are restricting to low energy excitations, it is justified to linearize the spectrum around the two Fermi points $\pm k_F$, as shown on the Fig. 1.1. Our Hamiltonian can then be rewritten in terms of left moving $(-)$ and right moving $(+)$ fermions as:

$$H = \sum_{k,r} v_F r k c_{k,r}^\dagger c_{k,r} \quad (1.8)$$

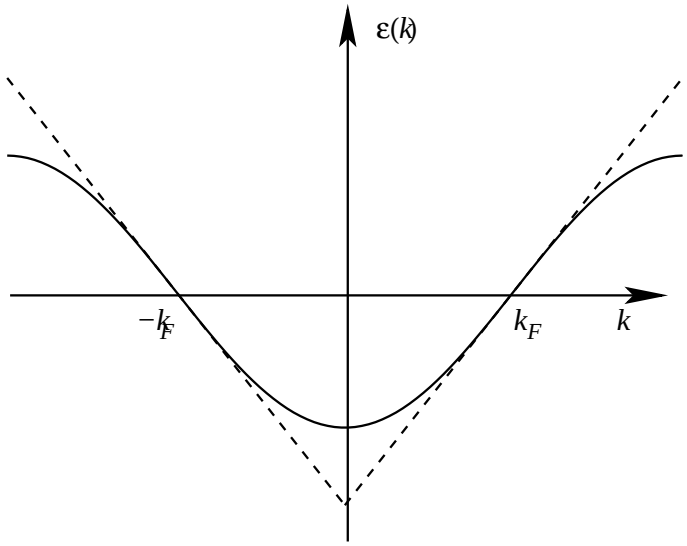

Figure 1.1: The dispersion of a one-dimensional model of fermions (solid line) and the dispersion linearized near the Fermi points.

$$+\frac{1}{L}\sum_q [g_4 \sum_r \rho_r(q)\rho_r(-q) + g_2\rho_r(q)\rho_{-r}(-q)], \tag{1.9}$$

where $c_{k,\pm} = c_{\pm k_F + k}$, and:

$$\rho_r(q) = \sum_k c^\dagger_{k+q,r} c_{k,r} \tag{1.10}$$

$$g_4 = V(0), \tag{1.11}$$

$$g_2 = V(0) - V(2k_F) \tag{1.12}$$

1.1.2 Diagonalization of the model using the density variables

The remarkable insight of Tomonaga[8] and Luttinger[9] was to attempt to rewrite the non-interacting Hamiltonian entirely in terms of the Fourier components $\rho_r(q)$ of the density. Indeed, because of the linearized form of the spectrum, the action of the density operator $\rho_\pm(\mp q)$ on an eigenstate of the Hamiltonian creates another eigenstate of the Hamiltonian with energy shifted by $v_F q$. Moreover, the calculation of the commutator of the density operators yields a particularly simple result,

$$[\rho_r(-q), \rho_r(q')] = r\delta_{q,q'}\frac{qL}{2\pi} \tag{1.13}$$

that allows the rewriting of the non-interacting Hamiltonian H_0 as a quadratic form in the Fourier components of the density:

$$H_0 = \frac{\pi v_F}{L}\sum_q [\rho_+(q)\rho_+(-q) + \rho_-(-q)\rho_-(q)] \tag{1.14}$$

It has been shown[10] that the partition functions calculated from the Hamiltonian (1.14) and from the original fermion Hamiltonian are identical, proving that they share the same spectrum. So the original fermion Hamiltonian can be rewritten entirely in terms of the density operators. The relation (1.13) is very similar to the commutation relation of boson operators, and in fact it is possible for $q \neq 0$ to reexpress $\rho_\pm(q)$ in terms of boson creation $b_q^\dagger$ and annihilation b_q operators:

$$\rho_r(q) = \sqrt{\frac{|q|L}{2\pi}} \left[\theta(rq) b_{rq}^\dagger + \theta(-rq) b_{-rq}\right], \tag{1.15}$$

so that in the limit of $L \to +\infty$ the Hamiltonian (1.14) can be rewritten as a sum of independent harmonic oscillators Hamiltonians. The transformation leading to (1.14) is called *bosonization* for that reason.

The usefulness of bosonization stems from the fact that the full interacting Hamiltonian $H = H_0 + V$ remains quadratic in the density variables and thus can be diagonalized by a Bogoliubov transformation. A computationally more convenient approach is to introduce the chiral fields:

$$\begin{aligned} \rho_\pm(x) &= \frac{1}{L}\sum_q \rho_\pm(q) e^{iqx}, & (1.16)\\ \phi_\pm &= -2\pi \int^x dx' \rho_\pm(x'), \\ &= \phi_\pm^0 - \frac{2\pi N_r}{L} + \frac{1}{L}\sum_{q\neq 0} \frac{2i\pi\rho_r(q)}{q} e^{iqx}, & (1.17) \end{aligned}$$

where N_r is the number of fermions added near the Fermi point rk_F and the integration constant $\phi_\pm^0$ is an operator such that $[N_r, \phi_0^r] = ir$. The chiral fields have the commutation relations:

$$\begin{aligned} [\rho_r(x), \rho_{r'}(x')] &= -\frac{ir}{2\pi}\delta_{r,r'}\partial_x(\delta(x-x')), & (1.18)\\ [\phi_r(x), \rho_r(x')] &= -ir\delta(x-x'). & (1.19) \end{aligned}$$

The introduction of the integration constants in Eq. (1.16) is necessary to ensure that these commutation relations are valid also for a finite size system.

so that the non-interacting Hamiltonian becomes:

$$H_0 = \int dx \frac{v_F}{4\pi} \left[(\partial_x\phi_+)^2 + (\partial_x\phi_-)^2\right]. \tag{1.20}$$

Then, one can introduce another set of fields,

$$\begin{aligned} \Pi(x) &= \rho_+(x) - \rho_-(x), & (1.21)\\ \phi(x) &= (\phi_+(x) + \phi_-(x))/2, & (1.22) \end{aligned}$$

having Fourier decomposition:

$$\Pi(x) = \frac{J}{L} + \frac{1}{L}\sum_{q\neq 0}[\rho_+(q) - \rho_-(q)]e^{iqx}, \tag{1.23}$$

$$\phi(x) = \frac{1}{2}(\phi_+^0 + \phi_0^-) - \frac{\pi N x}{L} - \frac{\pi}{L}\sum_q \frac{\rho_+(q) + \rho_-(q)}{iq}e^{iqx}, \tag{1.24}$$

with $J = N_+ - N_-$ and $N = N_+ + N_-$. The fields defined in (1.21) satisfy the canonical commutation relation $[\phi(x), \Pi(x')] = i\delta(x - x')$ and allow the rewriting of the non-interacting Hamiltonian in the form:

$$H_0 = v_F \int \frac{dx}{2\pi}\left[(\pi\Pi)^2 + (\partial_x\phi)^2\right], \tag{1.25}$$

and of the interaction term in the form:

$$V = \int dx \frac{g_4}{2}\left(\Pi^2 + \frac{(\partial_x\phi)^2}{\pi}^2\right) + \int dx \frac{g_2}{2}\left(-\Pi^2 + \frac{(\partial_x\phi)^2}{\pi}^2\right), \tag{1.26}$$

giving for the full Hamiltonian:

$$H = \int \frac{dx}{2\pi}\left[uK(\pi\Pi)^2 + \frac{u}{K}(\partial_x\phi)^2\right], \tag{1.27}$$

where:

$$u^2 = \left(v_F + \frac{g_4}{\pi}\right)^2 - \left(\frac{2g_2}{\pi}\right)^2 \tag{1.28}$$

$$K = \sqrt{\frac{\pi v_F + g_4 - 2g_2}{\pi V_F + g_4 + 2g_2}} \tag{1.29}$$

The Hamiltonian can be brought back to the non-interacting form by a simple rescaling of the fields, $\tilde{\phi} = \phi/\sqrt{K}$ and $\tilde{\Pi} = \sqrt{K}\Pi$, which is equivalent to the Bogoliubov transformation. In the form (1.27), the Hamiltonian describes one-dimensional phonons, with a displacement field $\phi(x)$ and a momentum density $\Pi(x)$. Indeed, if we consider a one-dimensional harmonic chain, with Hamiltonian:

$$H = \sum_n \left[\frac{p_n^2}{2m} + \frac{k}{2}(u_n - u_{n+1})^2\right], \tag{1.30}$$

and $[u_n, p_m] = i\delta_{n,m}$, calling a the lattice spacing, we can introduce the continuum fields $P(na) = p_n/a$ and $u(na) = u_n$, and obtain the commutation relation $[u(x), P(x')] = i\delta(x - x')$ with the continuum Hamiltonian:

$$H = \int dx \left[\frac{P^2}{2\rho} + \frac{\kappa}{2}(\partial_x u)^2\right], \tag{1.31}$$

where we have defined $\rho = m/a$ and $\kappa = ka$, which is precisely the form (1.27). The analogy can be pushed further by noting that with our definitions, the density $\rho(x) = \rho_+(x) + \rho_-(x) = -\partial_x\phi/\pi$, which corresponds to the usual definition of the density[11] as a function of the displacement in elasticity theory, $\rho(x) = -\partial_x u$. Following that analogy, we can view bosonization as a consequence of having particles moving along a line. When a particle is moving, it is forced to interact with its neighbors, and exchange some momentum with them. As a result, the individual motion of a particle is quickly transformed into a collective motion represented by a compression wave.

1.1.3 Expressing the operators in terms of the density variables

Having found the spectrum, the next step is to calculate the correlation functions of the model. In particular, it is useful to determine the fermion Green's functions. To do that, one can remark that the commutation relations of the density with the fermion annihilation operator are:

$$[\rho(x), \psi(x)] = \delta(x - x')\psi(x) \tag{1.32}$$

Thus, the fermion annihilation operator has the same commutation relation with the density as the exponential $e^{-ir\phi_r(x)}$, and it is expected that $\psi_r(x) \sim e^{-ir\phi_r(x)}$.

Indeed, the fermion annihilation and creation operators can be written[12, 10]:

$$\psi_+(x) = \frac{1}{\sqrt{L}} :e^{-i\phi_+(x)}:, \tag{1.33}$$

$$\psi_-(x) = \frac{1}{\sqrt{L}} :e^{i\phi_-(x)}:, \tag{1.34}$$

where $: \ldots :$ indicates normal ordering. Using the relations:

$$[\phi_r(x), \psi_r(x')] = i\pi r\delta(x - x'), [\phi_+(x), \phi_-(x')] = i\pi, \tag{1.35}$$

where the last commutator is a consequence of the choice of commutator $[\phi_+^0, \phi_-^0] = i\pi$, and using the Glauber identity $e^A e^B = e^{A+B}e^{\frac{1}{2}[A,B]}$ valid for $[A, [A, B]] = [B, [A, B]] = 0$, one can check that (1.33) indeed reproduce the commutation relations of the fermion operators.

A less rigorous version of (1.33) is obtained keeping the cutoff finite and neglecting the normal ordering. One can then write:

$$\psi_+(x) = \frac{e^{i(\theta-\phi)}}{\sqrt{2\pi\alpha}}, \tag{1.36}$$

$$\psi_-(x) = \frac{e^{i(\theta+\phi)}}{\sqrt{2\pi\alpha}}, \tag{1.37}$$

where we have introduced $\theta = (\phi_- - \phi_+)/2$. With (1.36) and , the retardated Green's function at $T = 0$ of right moving fermions is obtained in the form:

$$G_+(x, t) = \frac{1}{2\pi(x - ut - i0_+)} \left(\frac{\alpha^2}{x^2 - (ut + i0_+)^2}\right)^{(\sqrt{K}-1/\sqrt{K})^2/4} \tag{1.38}$$

taking the Fourier transform of the Green's function, the spectral function is[13]:

$$A_+(k,\omega) = \frac{\pi}{\Gamma(\lambda)\Gamma(\lambda+1)}\left[\left(\frac{\omega\alpha}{v}\right)^2 - (q\alpha)^2\right]^{K-1/K}\frac{\Theta(\omega-vq)\Theta(\omega+vq)}{\omega-vq} \tag{1.39}$$

The delta peak at $\omega = vq$ is changed into a power-law singularity that indicated that the Fermion excitations have become incoherent, the true long lived excitations being the density modes (1.16). Also, a threshold is present for $\omega = -vq$ which is a sign of the interaction of the two Fermi points. The calculation of the momentum distribution shows also that the step at the Fermi energy is replaced by a power law singularity $n(k) \sim \frac{1}{2} + C|k-k_F|^{\frac{1}{2}(K+1/K-2)}\mathrm{sign}(k_F-k)$. The energy distribution obeys the same law, $n(\epsilon) \sim \frac{1}{2} + C|\epsilon-\epsilon_F|^{\frac{1}{2}(K+1/K-2)}\mathrm{sign}(\epsilon_F-\epsilon)$.

For finite temperature, the spectral functions can be derived in a similar manner. The Green's function takes the form:

$$G_+(x,t) = \frac{-i}{2\pi\alpha}\left(\frac{\pi T\alpha}{iu\sinh\frac{\pi T}{u}(x-ut)}\right)^{\frac{1}{4}(K+\frac{1}{K}+2)}\left(\frac{\pi T\alpha}{-iu\sinh\frac{\pi T}{u}(x+ut)}\right)^{\frac{1}{4}(K+\frac{1}{K}-2)}, \tag{1.40}$$

Leading to the spectral function[14]:

$$A_+(k,\omega) \sim \left(\frac{\pi T\alpha}{u}\right)^{\frac{1}{2}(K+K^{-1})}\mathrm{Re}\left[(2i)^\gamma B\left(\frac{\gamma}{2} - i\frac{uq-\omega}{4\pi T}, 1-\gamma\right)\right]\mathrm{Re}\left[(2i)^{\gamma+1}B\left(\frac{\gamma+1}{2} - i\frac{uq+\omega}{4\pi T}, -\gamma\right)\right], \tag{1.41}$$

where we have defined $\gamma = (K + K^{-1} - 2)/4$. In the case of finite size, the Fermion Green's functions have been obtained at $T = 0$ as well as for finite temperature[15]. The derivation requires a more careful treatment of the boundary conditions and of the zero modes than in the present introduction.

Besides the obtention of the Fermion Green's function, the Eq. (1.36) also allow us to obtain a more complete representation of the density operator. Indeed, since $\psi(x) = e^{ik_Fx}\psi_+(x) + e^{-ik_Fx}\phi_-(x)$, we can write the density as:

$$\begin{aligned}
\rho(x) &= \psi^\dagger(x)\psi(x), &(1.42)\\
&= \sum_r \psi_r^\dagger(x)\psi_r(x)e^{2ik_Fx}\psi_-^\dagger(x)\psi_+(x) + e^{2ik_Fx}\psi_+^\dagger(x)\psi_-(x), &(1.43)\\
&= -\frac{1}{\pi}\partial_x\phi + \frac{\sin(2\phi(x) - 2k_Fx)}{\pi\alpha}, &(1.44)
\end{aligned}$$

Therefore, an oscillating component of the density, of wavevector $\pm 2k_F$ is also present. This component is the order parameter for $2k_F$ charge density wave ordering. Using Wick's theorem, it can be shown that for zero temperature:

$$\langle T_\tau e^{2i\phi(x,\tau)}e^{-2i\phi(0,0)}\rangle = e^{-2\langle T_\tau(\phi(x,\tau)-\phi(0,0))^2\rangle}\left(\frac{\alpha^2}{x^2+(u\tau)^2}\right)^K, \tag{1.45}$$

so that no long range order, but only quasi-long range order is possible in the ground state, in agreement with the Mermin-Wagner-Hohenberg theorem.[16, 17, 18] The order parameter for superconductivity, $O_{SC} = \psi_+(x)\psi_-(x) \sim \frac{e^{2i\theta(x)}}{2\pi\alpha}$ can also be considered. One has:

$$\langle T_\tau e^{i2\theta(x,\tau)} e^{-2i\theta(0,0)} \rangle = \left(\frac{\alpha^2}{x^2 + (u\tau)^2} \right)^{1/K}, \tag{1.46}$$

so that superfluid correlations are also quasi-long range ordered. The superfluid exponent is the inverse of the density wave exponent. This can be understood as the consequence of a duality property. Indeed, the Hamiltonian (1.27) can be rewritten:

$$H = \int \frac{dx}{2\pi} \left[\frac{u}{K} (\pi P)^2 + uK(\partial_x \theta)^2 \right], \tag{1.47}$$

where $\partial_x \phi = \pi P$. One has the commutation relations $[\theta(x), P(x')] = i\delta(x - x')$ so that the Hamiltonian (1.47) can be changed into (1.27) by the substitution $\theta(x) \to \phi(x)$, $P(x) \to \Pi(x)$ and $K \to 1/K$. As a result, the correlations of exponentials of the θ field are obtained from the correlation of the ϕ fields by the substitution $K \to 1/K$. In general, with the Hamiltonian (1.27) the two-point ground state correlation functions are of the form:

$$\langle T_\tau e^{i\lambda\phi(x,\tau)} e^{-i\lambda\phi(0,0)} \rangle = e^{-\lambda^2 \langle T_\tau (\phi(x,\tau) - \phi(0,0))^2 \rangle / 2} = \left(\frac{\alpha^2}{x^2 + (u|\tau| + \alpha)^2} \right)^{\lambda^2 K/4} \tag{1.48}$$

$$\langle e^{i\lambda\theta(x,\tau)} e^{-i\lambda\theta(0,0)} \rangle = e^{-\lambda^2 \langle T_\tau (\phi(x,\tau) - \phi(0,0))^2 \rangle / 2} = \left(\frac{\alpha^2}{x^2 + (u|\tau| + \alpha)^2} \right)^{\lambda^2 K^{-1}/4} \tag{1.49}$$

In the language of the renormalization group, the operator $e^{i\lambda\phi}$ has the scaling dimension $\lambda^2 K/4$ while the operator $e^{i\lambda\theta}$ has scaling dimension $\lambda^2/(4K)$. An operator $e^{i(\alpha\theta + \lambda\phi)}$ has a scaling dimension $(\alpha^2/K + \lambda^2 K)/4$, but its correlation function also contains a phase factor. The Fourier transform of the correlation functions (1.48) gives the Matsubara response functions. For a general correlation function of the form:

$$\langle T_\tau O(x,\tau) O(0,0) \rangle = \left(\frac{\alpha^2}{x^2 + (u\tau)^2} \right)^\gamma, \tag{1.50}$$

The Fourier transform is (for $\gamma < 1$):

$$\chi_O(q, i\omega) = \frac{\pi 2^{2(1-\gamma)\Gamma(1-\gamma)}}{u\Gamma(\gamma)} \alpha^{2\gamma} \left(q^2 + \frac{\omega^2}{u^2} \right)^{(\gamma-1)}, \tag{1.51}$$

giving after analytic continuation $i\omega \to \omega + i0$ the response function. For $\gamma < 1$, the response function is divergent. This implies a divergent density-wave response for $K < 1$ (*i. e.* repulsive interactions) and a divergent superconducting response for $K > 1$ (*i. e.* attractive interactions).

For positive temperature, the correlation functions take the form:

$$\langle T_\tau(\phi(x,\tau)-\phi(0,0))^2\rangle = -\frac{K}{2}\ln\left[\frac{x^2+(u|\tau|+\alpha)^2}{\alpha^2}\frac{\Gamma^4\left(1+\frac{\alpha}{\beta u}\right)}{\Gamma\left(1+\frac{\alpha-iz}{\beta u}\right)\Gamma\left(1+\frac{\alpha+iz}{\beta u}\right)\Gamma\left(1+\frac{\alpha-i\bar{z}}{\beta u}\right)\Gamma\left(1+\frac{\alpha+i\bar{z}}{\beta u}\right)}\right]$$

$$\langle T_\tau(\theta(x,\tau)-\theta(0,0))^2\rangle = -\frac{1}{2K}\ln\left[\frac{x^2+(u|\tau|+\alpha)^2}{\alpha^2}\frac{\Gamma^4\left(1+\frac{\alpha}{\beta u}\right)}{\Gamma\left(1+\frac{\alpha-iz}{\beta u}\right)\Gamma\left(1+\frac{\alpha+iz}{\beta u}\right)\Gamma\left(1+\frac{\alpha-i\bar{z}}{\beta u}\right)\Gamma\left(1+\frac{\alpha+i\bar{z}}{\beta u}\right)}\right]$$

where $\beta = 1/(k_B T)$, $z = x - iu\tau$, $\bar{z} = x + iu\tau$ and Γ is the Gamma function[19]. As a function of Matsubara time, the correlation functions are periodic of period β, as required by the Kubo-Martin-Schwinger condition[20]. In the limit $\alpha \ll \beta u, |z|$, the expressions (1.52) can be simplified, using the identity (6.1.17) in [19] yielding the approximate correlation functions:

$$\langle T_\tau e^{i\lambda\phi(x,\tau)}e^{-i\lambda\phi(0,0)}\rangle \simeq \left[\frac{\pi^2\alpha^2}{\beta^2u^2\sinh\left(\frac{\pi z}{\beta u}\right)\sinh\left(\frac{\pi\bar{z}}{\beta u}\right)}\right]^{\lambda^2K/4}, \tag{1.54}$$

$$\langle T_\tau e^{i\lambda\theta(x,\tau)}e^{-i\lambda\theta(0,0)}\rangle \simeq \left[\frac{\pi^2\alpha^2}{\beta^2u^2\sinh\left(\frac{\pi z}{\beta u}\right)\sinh\left(\frac{\pi\bar{z}}{\beta u}\right)}\right]^{\lambda^2K^{-1}/4}. \tag{1.55}$$

For long distances, the correlation functions (1.54) decay exponentially with distance. The characteristic length $\pi u/(k_B T)$ is the thermal length. The result (1.54) can be derived with conformal field theory[21] by mapping the plane on a cylinder of circumference β. In that language, the origin of the exponential decay of the correlation functions is the fact that the system has the same correlation functions as a quasi-one dimensional system. The response functions corresponding to (1.54) have been obtained[22, 23] from the integral (convergent for $\gamma < 1/2$):

$$\begin{aligned} I_\gamma(q,\omega) &= \int_{-\infty}^{+\infty}dx\int_0^\beta d\tau\frac{e^{i(qx-\omega\tau)}}{\left|\sinh\left(\frac{\pi(x+iu\tau)}{\beta u}\right)\right|^{2\gamma}} \\ &= \frac{\beta^2u\sin(\pi\gamma)}{(2\pi)^2}B\left(1-\gamma,\frac{\gamma}{2}+\frac{\beta(|\omega_n|+iuq)}{4\pi}\right)B\left(1-\gamma,\frac{\gamma}{2}+\frac{\beta(|\omega_n|-iuq)}{4\pi}\right) \end{aligned} \tag{1.56}$$

The finite temperature response functions are finite for $q, \omega \to 0$, however they diverge as a power law of temperature when $T \to 0$.

To summarize that section: We have seen that with spinless fermions in one dimension, the long-lived low energy excitations are not fermionic quasiparticles as in the three dimensional case, but instead are bosonic collective modes analogous to sound waves. These modes are described by a one-dimensional harmonic Hamiltonian. The fermion excitations are incoherent, and the ground state superconducting and density wave correlations have only quasi-long range order, with corresponding power law divergences of the response functions.

1.2 The XXZ spin-chain model

1.2.1 Jordan-Wigner transformation and derivation of a bosonized Hamiltonian

The Tomonaga-Luttinger liquid Hamiltonian (1.27) is also applicable to the study of spin-1/2 chains. That can be understood by considering the Jordan-Wigner transformation[24]:

$$S_n^+ = (-)^n c_n^\dagger e^{i\pi \sum_{m<n} c_m^\dagger c_m}, \tag{1.57}$$

$$S_n^z = c_n^\dagger c_n - \frac{1}{2}, \tag{1.58}$$

where $S_n^{x,y,z}$ are spin-1/2 operators, $S_n^+ = S_n^x + iS_n^y$, and the c_n are fermion annihilation operators. While spin-1/2 operators anticommute on the same site, but commute on different site, fermion operators always anticommute. The Jordan-Wigner operator:

$$e^{i\pi \sum_{m<n} c_m^\dagger c_m} \tag{1.59}$$

compensates the anticommutation relation of the fermion operators on different sites and thus permits to reproduce exactly the spin-1/2 operator algebra.

As a result, the Hamiltonian of the XXZ spin chain:

$$H = \sum_n \left[J(S_n^x S_{n+1}^x + S_n^y S_{n+1}^y) + J_z S_n^z S_{n+1}^z - h S_n^z \right], \tag{1.60}$$

is mapped to the $t - V$ model of interacting fermions.

$$H = \sum_n \left[-t(c_{n+1}^\dagger c_n + c_n^\dagger c_{n+1}) + V(c_n^\dagger c_n - 1/2)(c_{n+1}^\dagger c_{n+1} - 1/2) - \mu c_n^\dagger c_n \right], \tag{1.61}$$

with $t = J/2$, $V = J_z$ and $\mu = h$. The phase factor $(-)^n$ in (1.57) has been inserted to ensure that for $V = 0$ the minimum of the kinetic energy is at $k = 0$. In the limit $V \ll t$, a bosonized representation of the Hamiltonian (1.61) can be derived. For $V = 0$, we will have two Fermi points at $\pm k_F$ with $\mu = -2t\cos(k_F a)$ where a is the lattice spacing of our model. We can also relate the Fermi wavevector to the magnetization of the XXZ model using: $m = \langle S^z \rangle = k_F/\pi - 1/2$. For $h \neq 0$, we can take the continuum limit as we did for Eq. (1.5), and we obtain a bosonized Hamiltonian of the for (1.27). For $h = 0$, a more careful treatment is required. Indeed, for $h = 0$, the $t - V$ model is at half-filling and $k_F = \pi/(2a)$ so that:

$$c_n^\dagger c_n = a \left[\sum_r \psi_r^\dagger \psi_r + e^{i\pi \frac{x}{a}} \sum_r \psi_r^\dagger \psi_{-r} \right], \tag{1.62}$$

and since we have a discrete sum in (1.61), the terms $\psi_+^\dagger \psi_+^\dagger \psi_- \psi_- + \text{H.c.}$ do not drop out from the Hamiltonian. In more physical terms, when $k_F = \pi/(2a)$, we have $4k_F = 2\pi/a$ i.e. $4k_F$ is

a reciprocal lattice vectors, and interactions can include umklapp terms[25]. Using (1.36), we can nevertheless derive a bosonized representation of the Hamiltonian (1.61):

$$H = \int \frac{dx}{2\pi} \left[uK(\pi\Pi)^2 + \frac{u}{K}(\partial_x \phi)^2 \right] - \frac{2V}{(2\pi\alpha)^2} \int dx \cos 4\phi, \tag{1.63}$$

Since the scaling dimension of $\cos 4\phi$ is $4K$, this term is irrelevant in the renormalization group sense as long as $K > 1/2$. Within the perturbative treatment, $K \simeq 1$, so the renormalization group fixed point is a still Hamiltonian of the form (1.27) with renormalized parameters u^* and K^*.

1.2.2 Derivation of a bosonized representation for spin operators

Using the relations (1.57), it is possible to derive a bosonized representation of the spin operators. First, we need to use a slightly modified expression of the Jordan-Wigner operator compared with (1.59), that has the advantage to yield a hermitian expression in the continuum limit[26], i. e.

$$e^{i\pi \sum_{m<n} c_m^\dagger c_m} = \cos \left[\pi \sum_{m<n} c_m^\dagger c_m \right]. \tag{1.64}$$

On the lattice, the expressions (1.59) and (1.64) are completely equivalent, but (1.64) becomes after bosonization:

$$\cos(\phi - k_F x), \tag{1.65}$$

while (1.59) would give a non-hermitian expression. The reason for such difference is that we have approximated a field taking only discrete values by a field taking its value in a continuum. Using the bosonized expressions of the fermion operators, we derive a bosonized representation of the spin operators:

$$S^+(x) = \frac{S_n^+}{\alpha} = \frac{e^{i\theta(x)}}{\sqrt{\pi\alpha}} \left[(-)^{x/a} + \cos(2\phi(x) - 2k_F x + \pi x/a) \right], \tag{1.66}$$

$$S^z(x) = \frac{S_n^z}{a} = -\frac{1}{\pi}\partial_x \phi - \frac{1}{\pi\alpha} \sin(2\phi - 2k_F x), \tag{1.67}$$

In the representation (1.66), θ plays the role of an azimuthal angle. To derive (1.67), the Glauber identity and the commutators (1.35) have been used to express the products $\psi_R^\dagger \psi_L + \text{H.c.}$. It is also possible to derive a bosonized representation of the operator $S_{n+1}^+ S_n^-$ of the form:

$$S_{n+1}^+ S_n = \frac{u}{2\pi} \left[(\pi\Pi)^2 + (\partial_x \phi)^2 \right] + \frac{\cos(2\phi - 2k_F x)}{\pi\alpha}. \tag{1.68}$$

Such representation allows us to find the correlation functions of the XXZ spin chain at $T = 0$ and find that it has only quasi-long range order in the vicinity of $J_z = 0$.

1.3 Hard core bosons

Using the Holstein Primakoff representation[27], one can write a spin S operator as:

$$S_n^z = b_n^\dagger b_n - S, \tag{1.69}$$

$$S_n^+ = b_n^\dagger \sqrt{2S - b_n^\dagger b_n}, \tag{1.70}$$

with the constraint $b_n^\dagger b_n \leq 2S$. For $S = 1/2$, Eq. (1.69) shows that a spin-1/2 is equivalent to a hard core boson. In particular, the Jordan-Wigner transformation (1.57) can also be used to represent hard core bosons in terms of fermions.[2] The Eqs. (1.66)– (1.67) thus also yield a bosonized representation of hard-core bosons. It is important to note that the representation thus obtained is non-trivial. The bosonic modes that enter the problem can be understood as the density modes of the hard core boson system as we discussed previously for fermions. Hard core bosons can also be considered directly in the continuum [28] and the bosonized representation that we have derived is also applicable.

Another instructive manner to arrive at the bosonized representation of boson operators is by considering the number-phase representation. In that representation, we first consider the number operator $N_n = b_n^\dagger b_n$ and define its canonically conjugate variable θ_n such that $[N_n, \theta_n] = i$. We can then rewrite the boson annihilation operator as $b_n = e^{i\theta_n}\sqrt{N_n}$ and the boson creation operator as $b_n^\dagger = \sqrt{N_n}e^{-i\theta_n}$.[3] Taking the continuum limit, we find the annihilation operator in the form $\psi_B(x) = b_n/\sqrt{\alpha} = e^{i\theta}\sqrt{\rho_B(x)}$, where $\rho_B(x)$ is the bosonic particle density, and $\theta(x)$ is the superfluid phase of the boson field. The commutator becomes $[\rho(x), \theta(x')] = i\delta(x - x')$. This result is also consistent with the form of the order parameter for superfluidity of the spinless fermions. Moreover, in a model of interacting bosons such as the Lieb-Liniger model[29]:

$$H = \int dx \left[\frac{1}{2m} \partial_x \psi_B^\dagger \partial_x \psi_B(x) - \mu \psi_B^\dagger \psi_B(x) + \frac{g}{2} \psi_B^\dagger \psi_B^\dagger \psi_B \psi_B(x) \right] \tag{1.71}$$

the number phase representation leads to the Hamiltonian:

$$H = \int dx \left[\frac{1}{2m} \left(\frac{(\partial_x \rho_B)^2}{4\rho_B} + \sqrt{\rho_B}(\partial_x \theta)^2 \sqrt{\rho_B} \right) - \mu \rho_B + \frac{g}{2} \rho_B^2 \right]. \tag{1.72}$$

Minimizing the classical energy with respect to the boson density, we obtain an average boson density $\langle \rho_B \rangle = \mu/g$. Replacing in (1.72) the operator ρ_B by $\langle \rho_B \rangle \delta\rho_B$ and expanding to quadratic order, we obtain a Hamiltonian:

$$H = \int dx \left[\frac{1}{2m} \left(\frac{(\partial_x \delta\rho_B)^2}{4\langle \rho_B \rangle} + \langle \rho_B \rangle (\partial_x \theta)^2 \right) + \frac{g}{2} (\delta\rho_B)^2 \right] \tag{1.73}$$

[2] In that case the phase factor $(-)^n$ can be removed, provided that the kinetic energy of the bosons without hard core interaction is minimal for $k = 0$

[3] With that representation, we are actually enlarging the Hilbert space adding an unphysical space where N_n takes negative values. However, the b_n operators annihilate the states with $N_n = 0$, so that no admixture between the physical and unphysical Hilbert space can take place when the boson Hamiltonian is normal ordered.

Neglecting the $(\partial_x \delta\rho_B)^2$ term, the Hamiltonian (1.73) reduces to a Hamiltonian of the form (1.47) with $uK = \pi\langle\rho_B\rangle/m$, $u/K = g/\pi$, $\delta\rho = -\pi P$. The Hamiltonian (1.73) yields the same dispersion relation for the low-energy modes as the Bogoliubov approximation, but does not rely on the incorrect assumption of Bose condensation. If we return to the Hamiltonian (1.71) and derive equations of motion for the fields θ and ρ, we obtain:

$$\partial_t \rho + \partial_x(\rho \partial_x \theta/m) = 0 \tag{1.74}$$

$$\partial_t \theta + \frac{(\partial_x\theta)^2}{2m} = \frac{\delta}{\delta\rho}\left(-\mu\rho + g\rho^2/2 + (\partial_x\rho)^2/(8m\rho)\right) \tag{1.75}$$

The first equation is the continuity equation, the second one is the Euler equation with velocity potential θ/m. This shows that bosonization can be viewed as linearized quantum hydrodynamics, and that the linearly dispersing excitations predicted by bosonization can be viewed as sound modes, as already suggested by the one-dimensional phonon analogy (1.30). In this picture, we can view the Tomonaga-Luttinger liquid as a one-dimensional crystal melt by quantum fluctuations. Such hydrodynamic interpretation is independent of particle statistics. When considering the picture obtained from the phase representation, we can alternatively view the Tomonaga-Luttinger liquid as a superfluid whose long range order is turned into quasi-long range order by quantum fluctuations. Thus, the absence of ordering breaking the continuous $U(1)$ translation symmetry and $U(1)$ global gauge symmetry appears to place one-dimensional systems of interacting particles in a kind of "fluctuating supersolid" state, with both quasi-long range crystalline and superfluid order.

1.4 The Tomonaga-Luttinger liquid concept

Until now, we have discussed the solution of the Tomonaga-Luttinger model within a perturbative framework. However, it has been argued by Luther[30] and Haldane[31] that the bosonized Hamiltonian offered a more general description of the low energy physics of interacting particles in one-dimension than suggested by the perturbative treatment. Indeed, the theoretical treatment shows that the Tomonaga-Luttinger model is scale invariant, and can be viewed as a renormalization group fixed point[6]. This suggests that the Hamiltonian can be viewed in general as the fixed point Hamiltonian of a gapless model of interacting particles. Such a fixed point is characterized by two parameters, the velocity of excitations and the Luttinger parameter. The fixed point is called the Tomonaga-Luttinger liquid. In a more modern language, one would note that a model in which the low energy dispersion of excitation is linear is at a renormalization group fixed point with a dynamical exponent $z = 1$. For such a fixed point, space and rescaled Matsubara time are equivalent, and as a result, the scale invariance of the fixed point implies the full conformal invariance of the model.[32] Conformal field theory allows for a classification of the conformally invariant fixed points. Since the model has $U(1)$ symmetry, a plausible fixed point is the $c = 1$ conformal field theory generated by the $U(1)$ Katz-Moody algebra the Hamiltonian of which is precisely (1.27). The interpretation of K in the language of conformal field theory is simply that K is the compactification radius of the conformal field theory. From a practical point of view, in order to characterize a system in

the Tomonaga-Luttinger liquid state, one has to determine the velocity of excitations and the Tomonaga-Luttinger parameter from the macroscopic observables. A simple approach is to calculate the charge (or spin) stiffness and the compressibility with the help of the fixed point Hamiltonian and relate them with the exact quantities. First, if we consider the compressibility, with the help of (1.23), we see that adding one particle to our system is going to make $\phi(x) \to -\pi x/L$. Using the Hamiltonian (1.27), we see that this is going to shift the energy by the amount $\pi u/(2KL)$. If we consider the ground state energy change, since in an extensive system the ground state energy $E_0(N,L) - \mu N$ behaves as: $E_0(N,L) = Le(N/L) - \mu N$, we find that the ground state energy changes by: $e'(N/L) - \mu + e"(N/L)/(2L)$, so that, since $e'(N/L) = \mu$, we have:

$$e"(N/L) = \frac{\pi u}{K} \tag{1.76}$$

Using the definition of the compressibility as:

$$\kappa = -\frac{1}{L}\left(\frac{\partial L}{\partial P}\right)_N \tag{1.77}$$

$$= -\frac{1}{\rho_0(\partial P/\partial \rho_0)}, \tag{1.78}$$

where the pressure $P = -(\partial E_0/\partial L)_N$, we find that $\kappa = 1/(\rho_0^2 e"(\rho_0)) = K/(\pi u \rho_0^2)$. Now, if we turn to the stiffness, we have to consider our system under a change of boundary conditions such that $\psi(L) = e^{i\varphi}\psi(0)$. Such a change of boundary condition amounts to making $\theta(x) \to \theta(x) + \varphi x/L$ giving a shift of the ground state energy from (1.27) equal to $uK\varphi^2/(2\pi L)$. This gives us the second relation:

$$\pi L \frac{\partial^2 E_0}{\partial^2 \varphi} = uK. \tag{1.79}$$

In the case of a Galilean invariant model, the relation (1.79) can be further simplified. Indeed, under a Galilean boost, $\psi(x,t) \to e^{imvx - mv^2 t/2}\psi(x,t)$ so that $\theta(x,t) \to \theta(x,t) + mvx - mv^2 t/2$ and $\pi\Pi \to \pi\Pi + mv$. In the Hamiltonian (1.27), this gives a shift of the energy equal to $uK(mv)^2 L/(2\pi)$. But in a Galilean invariant model, the energy is simply shifted by $Nmv^2/2$ in the moving frame. Equating the two quantities, we find that $uK = \pi N/(mL)$ i. e.

$$uK = \frac{\pi \rho_0}{m}. \tag{1.80}$$

Such an approach has been applied to the $t - V$ model (or equivalently the XXZ chain) of Eq. (1.61) by Haldane. The $t - V$ model is integrable by the Bethe Ansatz (BA), and the low energy spectrum as well as the stiffness and the compressibility can be obtained non-perturbatively. The Tomonaga-Luttinger theory then fixes relation between the velocity of excitations u, the compressibility and the stiffness which have been checked on the BA solution. For $h = 0$, an analytic expression of u, K is available:

$$K = \frac{1}{2 - \frac{2}{\pi}\arccos\frac{V}{2t}}$$

$$u = \pi \frac{\sqrt{t^2 - \frac{V^2}{4}}}{\arccos\left(\frac{V}{2t}\right)} \tag{1.81}$$

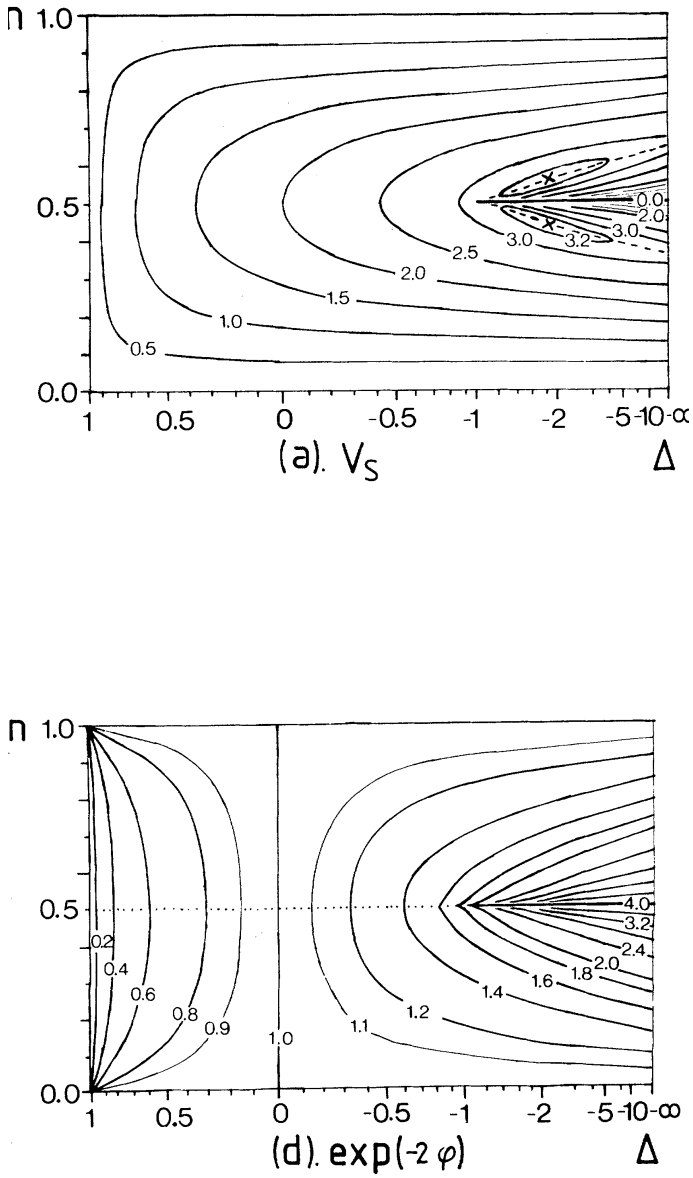

Figure 1.2: Contour plots of (a) the excitation velocity u and (d) the Luttinger parameter K in the plane (n,$\Delta = V/2t$) for the $t-V$ model after F. D. M. Haldane, Phys. Rev. Lett. **45**, 1358 (1980). In the notation of Haldane, $v_s = u$ and $K = e^{-2\varphi}$.

which becomes in the case of the XXZ chain:

$$K = \frac{1}{2 - \frac{2}{\pi}\arccos\frac{J_z}{J}}$$
$$u = \frac{\pi\sqrt{J^2 - J_z^2}}{2\arccos\left(\frac{J_z}{J}\right)} \tag{1.82}$$

These expressions are defined only for $|J_z| < J$ (or $|V| < 2t$ in the $t - V$ model). For $J_z < -J$, the XXZ chain has a ferromagnetic long range order, and for $J_z > J$ it has an antiferromagnetic long range order. The phase transitions from the Luttinger liquid state to the ferromagnet and to the antiferromagnet belong to different universality classes. In the case of the transition to the ferromagnetic state, the Luttinger exponent is diverging at the transition, while the velocity is vanishing[33, 34]. On the ferromagnetic side, the dispersion of excitations is gapless and quadratic. In the case of the transition to the antiferromagnetic state, both the velocity and the Luttinger exponent remain finite at the transition, but the excitations become gapful on the antiferromagnetic side. The latter type of transition belong to the Berezinskii-Kosterlitz-Thouless[35, 36] to be discussed in chapter 2. For now, let us just note that for $J = J_z$ the scaling dimensions of the operators $e^{i\theta}$ and $\cos 2\phi$, as well as $e^{i\theta}\cos 2\phi$ and $\partial_x\phi$ in (1.66) and (1.67) become respectively 1/2 and 1, as we would expect from $SU(2)$ invariance. The quantities u, K have also been derived for the Lieb-Liniger model.[37] They only depend on the dimensionless parameter $\gamma = mg/\rho_0$. For $\gamma \ll 1$, their behavior follows the prediction from the Bogoliubov approximation (1.73). For $\gamma \to \infty$, the bosons behave as hard core bosons and $K \to 1$, $u \to \pi\rho_0/m$. There are two ways to reach that limit, the first one is by sending g to infinity, the second one is by sending the density to zero.

The Tomonaga-Luttinger exponent has also been obtained for the non-integrable Bose-Hubbard model[38].

Besides knowing the expression of the fixed point bosonized Hamiltonian, we also need a representation of the density and particle creation and annihilation operators in terms of the fields that enter the Hamiltonian (1.27). Haldane[39] proposed the following arguments to justify such a representation.

First, we will consider classical particles along a line, and call x_m the positions of the particles. We will then define a field $\phi(x)$ such that $\phi(x_m) = m\pi$ and $\phi(x)$ is an increasing function of x. The particle density will then be given by

$$\rho(x) = \sum_{m=-\infty}^{\infty} \delta(x - \phi^{-1}(m\pi)), \tag{1.83}$$
$$= \sum_{m=-\infty}^{\infty} \delta(\phi(x) - m\pi)\frac{d\phi}{dx}, \tag{1.84}$$
$$= \frac{1}{\pi}\sum_{k=-\infty}^{\infty} e^{2ik\phi(x)}\frac{d\phi}{dx}, \tag{1.85}$$

where in the last line we have applied the Poisson summation formula. For a given average density of particles ρ_0, there are $\rho_0 x$ particles between the position 0 and the position $x > 0$,

so we expect that $\phi(x) = \pi\rho_0 x - \hat{\phi}(x)$, yielding:

$$\rho(x) = \left(\rho_0 - \frac{1}{\pi}\partial_x\hat{\phi}\right)\sum_{k=-\infty}^{\infty} e^{2ik(\pi\rho_0 x - \hat{\phi}(x))}. \tag{1.86}$$

That formula is analogous to the formula giving the particle density in Eq. (1.42). It is assumed that for the quantum system, a similar formula holds, with:

$$\rho(x) = \rho_0 - \frac{1}{\pi}\partial_x\phi + \sum_m A_m e^{2im(\phi(x) - 2\pi\rho_0 x)}. \tag{1.87}$$

The coefficients A_m cannot in general be predicted from bosonization as they depend on the details of the model. In perturbative bosonization, only the terms $A_{\pm 1}$ are nonzero. The origin of the higher order terms can be understood by the following argument.

The $4k_F$ component of the density is given by an operator $\rho(4k_F) = \sum_q c^\dagger_{k_F+q} c_{-3k_F+q}$. In first order perturbation theory, the ground state of the interacting system is given by:

$$|0\rangle + \frac{V(2k_F - q - q')}{\epsilon(3k_F - q') + \epsilon(k_F - q') - \epsilon(k_F - q) - \epsilon(k_F + q)} c^\dagger_{-3k_F+q'} c^\dagger_{k_F-q'} c_{-k_F+q} c_{-k_F+q}|0\rangle + \ldots \tag{1.88}$$

Acting on that state with $\rho(4k_F)$ and neglecting approximating $\epsilon(nk_F + q) \sim \epsilon(nk_F)$, $V(2k_F + q) \sim V(2k_F)$ yields a contribution proportional to:

$$\rho(4k_F) \sim \frac{V(2k_F)}{\epsilon(3k_F) - \epsilon(k_F)} \sum_{q,q'} c^\dagger_{k_F+q'} c^\dagger_{k_F-q'} c_{-k_F+q} c_{-k_F+q} \tag{1.89}$$

$$\tag{1.90}$$

the bosonized expression of which is:

$$\rho_{4k_F}(x) \sim \frac{V(2k_F)}{\epsilon(3k_F) - \epsilon(k_F)} e^{4i(\phi(x) - \pi\rho_0 x)} \tag{1.91}$$

Turning to the expression of the particle annihilation operator, one can start from the phase representation (1.72) encountered, with:

$$\psi_B(x) = e^{i\theta(x)}\sqrt{\rho(x)} \tag{1.92}$$

It is of course difficult to define properly the square root of an operator which is a sum of delta functions. However, since $\rho(x)$ is a periodic function of $\phi(x)$, the square root should preserve that property. This leads to the representation:

$$\psi_B(x) = e^{i\theta(x)}\left[\sum_{m=-\infty}^{\infty} B_m e^{i2m(\phi(x) - \pi\rho_0 x)}\right], \tag{1.93}$$

where again the parameters B_m are not universal. In the perturbative approach, only B_0 and B_1 are nonzero. With the help of the Jordan-Wigner transformation (1.57), the corresponding representation for fermions is:

$$\psi_F(x) = e^{i\theta(x)} \left[\sum_{m=-\infty}^{\infty} B_m e^{i(2m+1)(\phi(x)-\pi\rho_0 x)} \right], \tag{1.94}$$

The non-universal amplitudes have been computed for the XXZ spin chain[40]. One has:

$$\sigma_n^+ = e^{i\theta} \left[(-)^n \sqrt{\frac{A}{2}} + \sqrt{\frac{\tilde{A}}{2}} \cos 2\phi + \dots \right] \tag{1.95}$$

$$\sigma_n^z = -\frac{1}{\pi}\partial_x\phi + (-)^n \sqrt{\frac{A_z}{2}} \cos 2\phi + \dots \tag{1.96}$$

with:

$$A = \frac{2K^2}{(2K-1)^2} \left[\frac{\Gamma\left(\frac{1}{4K-2}\right)}{2\sqrt{\pi}\Gamma\left(\frac{K}{2K-1}\right)} \right]^{\frac{1}{2K}} \exp\left[-\int_0^\infty \frac{dt}{t} \left(\frac{\sinh\left(\frac{t}{2K}\right)}{\sinh t \cosh\left(1-\frac{1}{2K}\right) t} - \frac{e^{-2t}}{2K} \right) \right] \tag{1.97}$$

$$\tilde{A} = \frac{8K^2}{2K-1} \left[\frac{\Gamma\left(\frac{1}{4K-2}\right)}{2\sqrt{\pi}\Gamma\left(\frac{K}{2K-1}\right)} \right]^{2K+\frac{1}{2K}} \times \exp\left[-\int_0^\infty \frac{dt}{t} \left(\frac{\cosh\left(\frac{t}{K}\right) e^{-2t} - 1}{2\sinh\frac{t}{2K}\sinh t\cosh\left(1-\frac{1}{2K}\right) t} + \frac{1}{\sinh\frac{t}{2K}} - \left(2K+\frac{1}{2K}\right) e^{-2t} \right) \right] \tag{1.98}$$

$$A_z = \frac{8}{\pi^2} \left[\frac{\Gamma\left(\frac{1}{4K-2}\right)}{2\sqrt{\pi}\Gamma\left(\frac{K}{2K-1}\right)} \right]^{2K} \exp\left[-\int_0^\infty \frac{dt}{t} \left(\frac{\sinh\left(\frac{1}{K}-1\right) t}{\sinh\frac{t}{2K}\cosh\left(1-\frac{1}{2K}\right) t} - 2(1-K)e^{-2t} \right) \right] \tag{1.99}$$

The expressions of the higher order terms can be found in [40]. The amplitudes in (1.97) are divergent in the limit $K = 1/2$. This is an indication of the presence of logarithmic corrections to the correlation functions in the SU(2) symmetric case.[41] We will defer their discussion to Chapter 2.

1.5 Multicomponent systems

1.5.1 The case of fermions with spin

Derivation of the bosonized Hamiltonian

In the case of non-interacting fermions with spin, we can separately obtain a boson representation of the type (1.36) of the spin up and spin down fermions, with two separate Hamiltonians

of the form (1.27) for each spin. However, when considering a Hubbard type interaction:

$$H_{int} = g\int dx\rho_{\uparrow}(x)\rho\downarrow(x) \tag{1.100}$$

$$= g\int dx\left[-\frac{1}{\pi}\partial_x\phi_{\uparrow}+\frac{\cos(2\phi_{\uparrow}-2k_{F,\uparrow}x)}{\pi\alpha}\right]\left[-\frac{1}{\pi}\partial_x\phi_{\downarrow}+\frac{\cos(2\phi_{\downarrow}-2k_{F,\downarrow}x)}{\pi\alpha}\right], \tag{1.101}$$

when $k_{F,\uparrow}=k_{F,\downarrow}$, we note that there is an extra term in the Hamiltonian, of the form:

$$\cos 2(\phi_{\uparrow}-\phi_{\downarrow}) \tag{1.102}$$

Also, when $k_{F,\uparrow}+k_{F,\downarrow}=2\pi/a$ in a system of spin-1/2 fermions on a lattice (of lattice spacing a) a term of the form:

$$\cos(\phi_{\uparrow}+\phi_{\downarrow}) \tag{1.103}$$

is present in the Hamiltonian.

Introducing the new canonically conjugate operators,

$$\phi_{\rho} = \frac{\phi_{\uparrow}+\phi_{\downarrow}}{\sqrt{2}}, \Pi_{\rho}=\frac{\Pi_{\uparrow}+\Pi_{\downarrow}}{\sqrt{2}}, \tag{1.104}$$

$$\phi_{\sigma} = \frac{\phi_{\uparrow}-\phi_{\downarrow}}{\sqrt{2}}, \Pi_{\sigma}=\frac{\Pi_{\uparrow}-\Pi_{\downarrow}}{\sqrt{2}}, \tag{1.105}$$

it is possible to rewrite the Hamiltonian in the form:

$$H = H_{\rho}+H_{\sigma}, \tag{1.106}$$

$$H_{\rho} = \int\frac{dx}{2\pi}\left[u_{\rho}K_{\rho}(\pi\Pi_{\rho})^2+\frac{u_{\rho}}{K_{\rho}}(\partial_x\phi_{\rho})^2\right], \tag{1.107}$$

$$H_{\sigma} = \int\frac{dx}{2\pi}\left[u_{\sigma}K_{\sigma}(\pi\Pi_{\sigma})^2+\frac{u_{\sigma}}{K_{\sigma}}(\partial_x\phi_{\sigma})^2\right]-\frac{2g_{1\perp}}{(2\pi\alpha)^2}\int dx\cos\sqrt{8}\phi_{\sigma}, \tag{1.108}$$

in which the charge excitations (ρ) and the spin excitations (σ) are decoupled. We note that $\cos\sqrt{8}\phi_{\rho}$ and $\cos\sqrt{8}\phi_{\sigma}$ are marginal perturbations in the vicinity of the non-interacting point. We will defer the renormalization group treatment to a later section, but we already note that a marginally irrelevant operator can give rise to logarithmic corrections to the power-law behavior of the correlation functions. It should be noted that by the rescaling $\phi_{\sigma}=\sqrt{2}\phi$, $\theta_{\sigma}=\theta/\sqrt{2}$ and $K_{\sigma}=2K$, the bosonized spin Hamiltonian is mapped on the spin chain Hamiltonian.

Derivation of the bosonized expression of the operators

The fermion creation and annihilation operators take the form:

$$\psi_{r,\sigma}=\frac{e^{\frac{i}{\sqrt{2}}[\theta_{\rho}-r\phi_{\rho}+\sigma(\theta_{\sigma}-r\phi_{\sigma})]}}{\sqrt{2\pi\alpha}}\eta_{\sigma}, \tag{1.109}$$

where the operators η_σ are Majorana fermion operators with the anticommutation relation $\eta_\sigma\eta_{\sigma'} + \eta_{\sigma'}\eta_\sigma = \delta_{\sigma\sigma'}$. It is necessary to introduce the operators to ensure the anticommutation of fermion operators of opposite spins.[4] With Eq. (1.109), it is possible to rewrite the charge and spin density in the form:

$$\rho(x) = \sum_{r,\sigma} \psi^\dagger_{r,\sigma}\psi_{r,\sigma} \tag{1.110}$$

$$= -\frac{\sqrt{2}}{\pi}\partial_x\phi_\rho + \frac{2}{\pi\alpha}\cos(\sqrt{2}\phi_\rho - 2k_F x)\cos\sqrt{2}\phi_\sigma \tag{1.111}$$

$$\sigma^+(x) = \sum_r \psi^\dagger_{r,\uparrow}\psi_{r,\downarrow} \tag{1.112}$$

$$= \frac{e^{i\sqrt{2}(\theta_\sigma-\phi_\sigma)}}{2\pi\alpha}\eta_\uparrow\eta_\downarrow + \frac{e^{i\sqrt{2}(\theta_\sigma-\phi_\sigma)}}{2\pi\alpha}\eta_\uparrow\eta_\downarrow + e^{i\sqrt{2}\theta_\sigma}\cos(\sqrt{2}\phi_\rho - 2k_F x)\eta_\uparrow\eta_\downarrow \tag{1.113}$$

$$\sigma^z(x) = \frac{1}{2}\sum_{r,\sigma}\sigma\psi^\dagger_{r,\sigma}\psi_{r,\sigma} \tag{1.114}$$

$$= -\frac{1}{\pi\sqrt{2}}\partial_x\phi_\sigma + \frac{2}{\pi\alpha}\cos(\sqrt{2}\phi_\rho - 2k_F x)\sin\sqrt{2}\phi_\sigma \tag{1.115}$$

Using the rescaling $\theta_\sigma = \sqrt{2}\phi, \theta_\sigma = \theta/\sqrt{2}$, the expressions of the spin density can be brought to a form reminiscent of Eqs. (1.66)–(1.67). The difference between the two expressions is coming from the factor $e^{i2k_F x - \sqrt{2}\phi_\rho}$. In the case of lattice fermions at half filling $k_F = \pi/2a$ and a charge gap opens for repulsive interactions giving $\langle\phi_\rho\rangle = 0$, so that the expression (1.112) becomes identical to the bosonized representation of the spin chain. In that way, the equivalence between a system of spin-1/2 fermions with a Mott gap and an antiferromagnet is recovered. When the system is not at half filling, the presence of the operator ϕ_ρ is the expression (1.112) is an indication that the carriers of the magnetic moments can have a fluctuating position[43, 44] when charge degrees of freedom are not frozen.

If we consider the spin-spin correlation functions, we observe that the scaling dimensions of the operators forming the uniform and staggered parts of σ^+ and σ^z are identical only when $K_\sigma = 1$, so that $K_\sigma = 1$ is a necessary condition for spin rotational invariance. This condition corresponds to $K = 1/2$ in the XXZ spin-1/2 chain, in agreement with Eq. (1.82). As a result, in a case with $SU(2)$ invariance, only 3 parameters u_ρ, K_ρ and u_σ have to be determine to define non-perturbatively the fixed point bosonized Hamiltonian. For the Hubbard model, these parameters have been determined from the Bethe Ansatz[45]. It has been shown that $K_\rho > 1/2$ for any U.

In the case of a non-integrable model such as the extended Hubbard model at quarter filling, the Tomonaga-Luttinger parameters have been obtained from numerical computation[46].

[4] Actually, Eq. (1.109) is not a fully rigorous representation. A more correct treatment would use operators that change the fermion number[31, 42], of which the Majorana fermion representation is only an approximation.

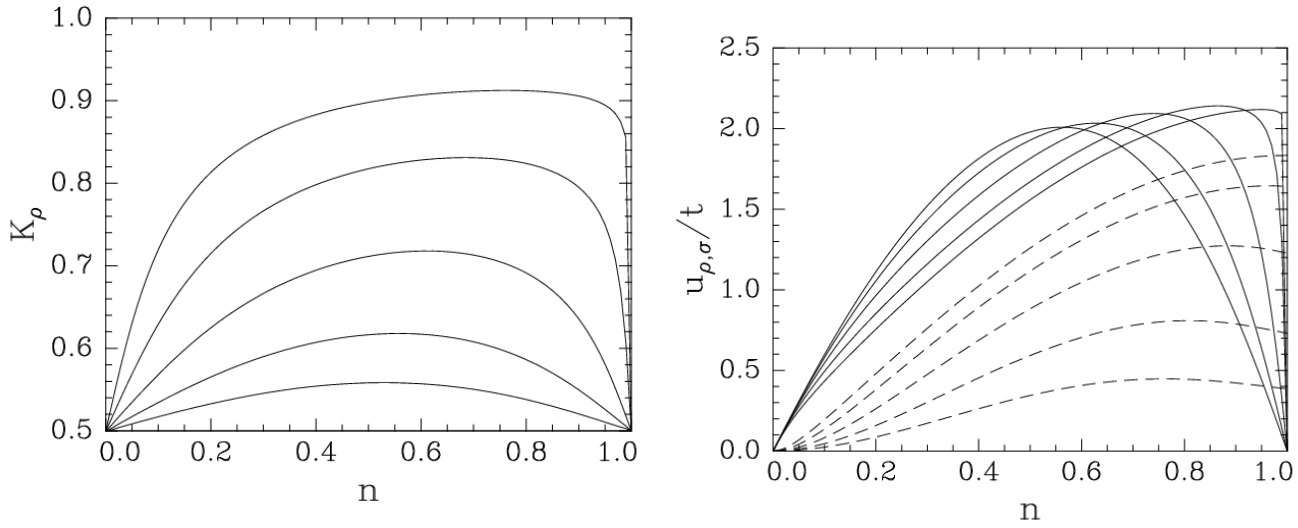

Figure 1.3: The Tomonaga-Luttinger charge exponent K_ρ and the charge u_ρ (solid line) and spin u_σ (dashed line) velocities in the repulsive Hubbard model as a function of density for different values of U/t. From top to bottom $U/t = 16, 8, 4, 2, 1$ for K_ρ, u_σ and u_ρ (in the left part of the figure). After [45].

In the case of the Hubbard model under a magnetic field[47, 48], where $SU(2)$ symmetry is lost but integrability is preserved the fixed point bosonized Hamiltonian has also been determined. We will defer its discussion to Sec.1.5.2.

The order parameters for singlet superconductivity and triplet superconductivity are obtained in the form:

$$O_{SS} = \psi^\dagger_{+,\alpha}(-i\sigma_y)_{\alpha\beta}\psi_{-\beta} = \frac{1}{\pi\alpha}e^{i\sqrt{2}\theta_\rho}\cos\sqrt{2}\phi_\sigma \quad (1.116)$$

$$O_{TS^x} = \psi^\dagger_{+,\alpha}(-i\sigma_y\sigma_x)_{\alpha\beta}\psi_{-\beta} = \frac{1}{\pi\alpha}e^{i\sqrt{2}\theta_\rho}\cos\sqrt{2}\theta_\sigma \quad (1.117)$$

$$O_{TS^y} = \psi^\dagger_{+,\alpha}(-i\sigma_y\sigma_y)_{\alpha\beta}\psi_{-\beta} = \frac{1}{\pi\alpha}e^{i\sqrt{2}\theta_\rho}sin\sqrt{2}\theta_\sigma \quad (1.118)$$

$$O_{TS^z} = \psi^\dagger_{+,\alpha}(-i\sigma_y\sigma_z)_{\alpha\beta}\psi_{-\beta} = \frac{1}{\pi\alpha}e^{i\sqrt{2}\theta_\rho}\sin\sqrt{2}\phi_\sigma \quad (1.119)$$

The duality transformation $\phi_\rho \leftrightarrow \theta_\rho$ exchanges the singlet superconductivity order parameter O_{SS} with the charge-density wave order parameter O_{CDW} and the triplet order parameters $O_{TS^{x,y,z}}$ with the spin density wave order parameters $O_{SDW^{x,y,z}}$.

The expressions (1.109), (1.110), (1.112) and (1.116) are obtained in the framework of perturbative bosonization. Non perturbative expressions including higher order harmonics can be obtained by applying (1.87) to spin up and spin down fermions and forming combinations. This would give a density of the form:

$$\rho(x) = \rho_0 - \frac{\sqrt{2}}{\pi}\partial_x\phi_\rho + \sum_m A_m e^{im(\sqrt{2}\phi_\rho - 2\pi\rho_0 x)}\cos m\sqrt{2}\phi_\sigma. \quad (1.120)$$

However, this expression must be corrected to take into account the presence of the term $\cos\sqrt{8}\phi_\sigma$. In perturbative expansions, powers of this term cancel the $\cos 2m\sqrt{2}\phi_\sigma$ in (1.120) leading to the corrected expression:

$$\rho(x) = \rho_0 - \frac{\sqrt{2}}{\pi}\partial_x\phi_\rho + \sum_m A'_{2m+1}e^{i(2m+1)(\sqrt{2}\phi_\rho - 2\pi\rho_0 x)}\cos\sqrt{2}\phi_\sigma + \sum_m A'_{2m}e^{i2m(\sqrt{2}\phi_\rho - 2\pi\rho_0 x)} \quad (1.121)$$

Concerning the spin density, a similar procedure leads to:

$$\begin{aligned} S^+(x) &\sim e^{i\sqrt{2}\theta_\sigma}\sum_m A_{2m+1,x}e^{i(2m+1)(\sqrt{2}\phi_\rho - 2k_F x)} \\ &\quad + e^{i\sqrt{2}\theta_\sigma}\cos\sqrt{2}\phi_\sigma\sum_m A_{2m,x}e^{i2m(\sqrt{2}\phi_\rho - 2k_F x)}. \quad (1.122) \\ S^z(x) &= -\frac{1}{\pi\sqrt{2}}\partial_x\phi_\sigma\sum_m A_{2m,z}\sin 2m(\sqrt{2}\phi_\rho - 2k_F x) \\ &\quad + \sum_m A_{2m+1,z}\sin\sqrt{2}\phi_\sigma\sin(2m+1)(\sqrt{2}\phi_\rho - 2k_F x). \quad (1.123) \end{aligned}$$

It should be noted that in the limit of $U/t \to +\infty$, in the Hubbard model, the spins up and down cannot occupy the same site. The charge density is then the same as the one of a system of spinless fermions having a density equal to the sum of the density of spins up and spins down. Meanwhile, the spin excitations become highly degenerate with a vanishing u_σ. As a result, although the total charge excitations can still be described by bosonization, the spin excitations require a completely different description. Such limit is called the spin-incoherent Tomonaga-Luttinger liquid.[49, 50, 51] and requires a special treatment.

Correlation functions

The ground state response functions for the case of general K_ρ and K_σ have been obtained in [52] in terms of the Appell generalized hypergeometric function of two variables F_1.[53] Starting from the general correlation function:

$$\langle T_\tau O(x,\tau)O(0,0)\rangle = \left(\frac{\alpha^2}{(x^2+(u_\rho\tau)^2}\right)^{\eta_\rho}\left(\frac{\alpha^2}{(x^2+(u_\sigma\tau)^2}\right)^{\eta_\sigma}, \quad (1.124)$$

the Feynman identity[54]:

$$\frac{1}{\prod_{j=1}^n A_j^{\alpha_j}} = \frac{\Gamma\left(\sum_j\alpha_j\right)}{\prod_j\Gamma(\alpha_j)}\int\prod_{j=1}^n du_j u_j^{\alpha_j-1}\frac{\delta\left(1-\sum_j u_j\right)}{\left(\sum_{j=1}^n u_j A_j\right)^{-\sum_j\alpha_j}}, \quad (1.125)$$

is used to rewrite the Fourier transform of the Matsubara correlation function (1.124) in the form:

$$\chi_O(q,\omega) = \int dx d\tau\int dv v^{\eta_\rho-1}(1-v)^{\eta_\sigma-1}\frac{\alpha^{2(\eta_\rho+\eta_\sigma)}e^{iqx-\omega\tau}}{\left(x^2+vu_\rho^2\tau^2+(1-v)u_\sigma^2\tau^2\right)^{\eta_\rho+\eta_\sigma}}, \quad (1.126)$$

leading with the help of (1.51) to:

$$\chi(q,\omega) = \frac{\pi 2^{2(1-\eta_\rho-\eta_\sigma)}\alpha^{2(\eta_\rho+\eta_\sigma)\Gamma(1-\eta_\rho-\eta_\sigma)}}{\Gamma(\eta_\rho+\eta_\sigma)u_\sigma^{2(\eta_\rho+\eta_\sigma-1)}}(\omega^2+u_\sigma^2q^2)^{\eta_\rho+\eta_\sigma-1} \times F_1\left(\eta_\rho;\eta_\rho+\eta_\sigma-1/2,1-\eta_\rho-\eta_\sigma;\eta_\rho+\eta_\sigma,1-u_\rho^2/u_\sigma^2,\frac{(u_\sigma^2-u_\rho^2)q^2}{\omega^2+u_\sigma^2q^2}\right) \quad (1.127)$$

After analytic continuation, power-law singularities appear in the response function for $\omega = u_\sigma q$ and $\omega = u_\rho q$. Such singularities mark the presence of a spin and a charge continuum.

In the ground state, and for the spin-isotropic case of $K_\sigma = 1$, the spectral functions can be expressed in terms of the Gauss hypergeometric functions[55]. In the case $u_\rho > u_\sigma$ and with $\gamma_\rho = (K_\rho + K_\rho^{-1} - 2)/8$ we have for $\omega > u_\rho q$

$$A_{+,s}(q,\omega) = \frac{\alpha^{2\gamma_\rho}}{\Gamma(\gamma_\rho)\Gamma(\gamma_\rho+1)}\frac{(\omega+u_\rho q)^{\gamma_\rho}(\omega-u_\sigma q)^{\gamma_\rho-1}}{(2u_\rho)^{\gamma_\rho+1/2}(u_\rho+u_\sigma)^{\gamma_\rho-1/2}}{}_2F_1\left(1-\gamma_\rho,\gamma_\rho+\frac{1}{2};\gamma_\rho+1;\frac{u_\rho-u_\sigma}{2u_\rho}\frac{\omega+u_\rho q}{\omega-u_\sigma q}\right), \quad (1.128)$$

for $u_\sigma q < \omega < u_\rho q$,

$$A_{+,s}(q,\omega) = \frac{\alpha^{2\gamma_\rho}}{\Gamma(1/2)\Gamma(2\gamma_\rho+1/2)}\frac{(\omega+u_\rho q)^{-1/2}(\omega-u_\sigma q)^{2\gamma_\rho-1/2}}{(u_\rho+u_\sigma)^{\gamma_\rho-1/2}(u_\rho-u_\sigma)^{\gamma_\rho+1/2}}{}_2F_1\left(\frac{1}{2},\gamma_\rho+\frac{1}{2};2\gamma_\rho+\frac{1}{2};\frac{2u_\rho}{u_\rho-u_\sigma}\frac{\omega-u_\sigma}{\omega+u_\rho}\right) \quad (1$$

and for $\omega < -u_\rho q$,

$$A_{+,\sigma}(q,\omega) = \frac{\alpha^{2\gamma_\rho}}{\Gamma(\gamma_\rho)\Gamma(\gamma_\rho+1)}\frac{|\omega-u_\sigma q|^{\gamma_\rho-1}|\omega+u_\rho q|^{\gamma_\rho}}{(u_\rho+u_\sigma)^{\gamma_\rho-1/2}(2u_\rho)^{\gamma_\rho+1/2}}{}_2F_1\left(1-\gamma_\rho,\gamma_\rho+\frac{1}{2};\gamma_\rho+1;\frac{u_\rho-u_\sigma}{2u_\rho}\frac{\omega+u_\rho q}{\omega-u_\sigma q}\right). \quad (1.130)$$

In the articles [56, 57], we expressed the spectral functions of the general two-component model in terms of Appell F_2 and F_1 functions.

For $0 < u_\sigma q < \omega < u_\rho q$, the spectral function is expressed as:

$$A_s(k_{F,s}+q,\omega)|_{u_\sigma q<\omega<u_\rho q} = \frac{(\alpha/\Delta u)^{\bar\nu_s-1}(|\omega|-u_\sigma q)^{\nu_{s,\rho}+\nu'_{s,\sigma}+\nu'_{s,\rho}-1}(-|\omega|+u_\rho q)^{\nu_{s,\sigma}+\nu'_{s,\sigma}+\nu'_{s,\rho}-1}}{\Gamma(\nu_{s,\rho}+\nu'_{s,\rho}+\nu'_{s,\sigma})\Gamma(\nu_{s,\sigma})(|\omega|+u_\rho q)^{\nu'_{s,\rho}}(|\omega|+u_\sigma q)^{\nu'_{s,\sigma}}} \times F_1\left(\bar\nu_s-1;\nu'_{s,\rho},\nu'_{s,\sigma};\nu_{s,\rho}+\nu'_{s,\rho}+\nu'_{s,\sigma};\frac{2u_\rho(|\omega|-u_\sigma q)}{\Delta u(|\omega|+u_\rho q)},\frac{2\bar u(|\omega|-u_\sigma q)}{\Delta u(|\omega|+u_\sigma q)}\right), \quad (1.131)$$

and for $\omega > u_\rho q$, as:

$$A_s(k_{F,s}+q,\omega)|_{\omega>u_\rho q} = \frac{(\alpha/2u_\rho)^{\bar\nu_s-1}(|\omega|-u_\rho q)^{\nu_{s,\sigma}+\nu'_{s,\rho}+\nu'_{s,\sigma}-1}(|\omega|+u_\rho q)^{\nu_{s,\rho}+\nu_{s,\sigma}+\nu'_{s,\sigma}-1}}{\Gamma(\nu_{s,\rho}+\nu_{s,\sigma})\Gamma(\nu'_{s,\rho}+\nu'_{s,\sigma})(|\omega|-u_\sigma q)^{\nu_{s,\sigma}}(|\omega|+u_\sigma q)^{\nu'_{s,\sigma}}} \times F_2\left(\bar\nu_s-1;\,\nu_{s,\sigma},\,\nu'_{s,\sigma},\,\nu_{s,\rho}+\nu_{s,\sigma},\,\nu'_{s,\rho}+\nu'_{s,\sigma};\,\frac{\Delta u(|\omega|+u_\rho q)}{2u_\rho(|\omega|-u_\sigma q)},\,\frac{\Delta u(|\omega|-u_\rho q)}{2u_\rho(|\omega|+u_\sigma q)}\right) \quad (1.132)$$

where $\bar{u} = u_\rho + u_\sigma$, $\Delta u = u_\rho - u_\sigma > 0$, $\nu_{s,\beta} = (\sqrt{K_\beta} - 1/\sqrt{K_\beta})^2/8$, $\nu'_{s,\beta} = (\sqrt{K_\beta} + 1/\sqrt{K_\beta})^2/8$, $\bar{\nu}_s = \sum_\beta (\nu_{s,\beta} + \nu'_{s,\beta})$ and $F_1(\alpha;\beta,\beta';\gamma;x,y)$ and $F_2(\alpha;\beta,\beta';\gamma,\gamma';x,y)$ are respectively the first and second Appell hypergeometric functions [53]. For $\omega < 0$ the spectral function for $-u_\rho q < \omega < -u_\sigma q$ and for $\omega < -u_\rho q$ is obtained by interchanging (1.131) and (1.132) respectively [56]. We find $A_s(k_{F,s} + q, \omega) = 0$ for $|\omega| < u_\sigma q$. The singularities of the spectral functions[58, 59] can be recovered from these expressions. We have:

$$A_{R,s}(q,\omega) \propto \begin{cases} |\omega - u_\rho q|^{\beta_{s,\rho}} & (\text{for } \omega \to +u_\rho q \pm 0) \\ (\omega - u_\sigma q)^{\beta_{s,\sigma}} & (\text{for } \omega \to +u_\sigma q + 0) \\ (\omega + u_\sigma q)^{\beta'_{s,\sigma}} & (\text{for } \omega \to -u_\sigma q - 0) \\ C + |\omega + u_\rho q|^{\beta'_{s,\rho}} & (\text{for } \omega \to -u_\rho q \pm 0) \end{cases}, \tag{1.133}$$

where

$$\beta_{s,\rho} \equiv \frac{1}{8}(K_\rho + K_\rho^{-1} + 2K_\sigma + 2K_\sigma^{-1} - 2) - 1, \tag{1.134}$$

$$\beta_{s,\sigma} \equiv , \frac{1}{8}(2K_\rho + 2K_\rho^{-1} + K_\sigma + K_\sigma^{-1} - 2) - 1 \tag{1.135}$$

$$\beta'_{s,\sigma} \equiv \frac{1}{8}(2K_\rho + 2K_\rho^{-1} + K_\sigma + K_\sigma^{-1} + 2) - 1, \tag{1.136}$$

$$\beta'_{s,\rho} \equiv \frac{1}{8}(K_\rho + K_\rho^{-1} + 2K_\sigma + 2K_\sigma^{-1} + 2) - 1, \tag{1.137}$$

We have $\beta'_{s,\rho/\sigma} > 0$, so that the singularities for $\omega = -u_{\rho,\sigma} q$ are cusp singularities, while $\beta_{s,\rho/\sigma} = \beta'_{s,\rho} - 1/2$. For weak interactions, the singularities at $\omega = +u_{\rho,\sigma} q$ are peak singularities, and turn into cusp singularities for stronger interaction. For finite temperature, spectral functions and response functions have been expressed as convolution integrals in [14] but no closed form expression is known in the general case. The integrals giving the spectral functions have been considered numerically in [60].

1.5.2 General multicomponent models

Bosonization is of course also applicable to multicomponent models. Such models can be encountered for instance in ladder or nanotube systems (that will be discussed later) or in Kugel-Khomskii models.[61] In the case where all densities are incommensurate, the low-energy Hamiltonian takes the form:

$$H = \int \frac{dx}{2\pi} \sum_{a,b} \left[\pi^2 M_{ab} \Pi_a \Pi_b + N_{ab} \partial_x \phi_a \partial_x \phi_b \right], \tag{1.138}$$

with $[\phi_a(x), \Pi_b(x')] = i\delta_{ab}\delta(x - x')$. In (1.138) the matrices M and N are real symmetric and are defined in terms of the variations of the ground state energy E_{GS} of a finite system of size L from (respectively) change of boundary conditions $\psi_a(L) = e^{i\varphi_a}\psi_a(0)$ and change of particle densities $\rho_a = N_a/L$:

$$M_{ab} = \pi L \frac{\partial^2 E_{GS}}{\partial \varphi_a \partial \varphi_b}, \tag{1.139}$$

$$N_{ab} = \frac{1}{\pi L}\frac{\partial^2 E_{GS}}{\partial\rho_a \partial\rho_b}. \tag{1.140}$$

The fields ϕ_a and θ_a have the decomposition:

$$\begin{aligned}
\phi_a(x) &= \phi_0^{(a)} - \frac{\pi N_a}{L}x + \frac{1}{\sqrt{L}}\sum_{q\neq 0}\phi_a(q)e^{iqx} \\
\theta_a(x) &= \theta_0^{(a)} - \frac{\pi J_a}{L}x + \frac{1}{\sqrt{L}}\sum_{q\neq 0}\theta_a(q)e^{iqx}
\end{aligned} \tag{1.141}$$

where $\pi\Pi_a(x) = \partial_x\theta_a$, $[\phi_a(q), \theta_a(-q')] = -\delta_{ab}\delta_{q,q'}/q$, $[\phi_0^{(a)}, J_b] = -i\delta_{ab}$ and $[\theta_0^{(a)}, N_b] = -i\delta_{ab}$.

The spectrum of the general bosonized Hamiltonian (1.138) is obtained by a linear transformation[62] of the fields Π_a and ϕ_a:

$$\Pi_b = \sum_\beta P_{b\beta}\tilde{\Pi}_\beta, \tag{1.142}$$

$$\phi_a = \sum_\alpha Q_{a\alpha}\tilde{\phi}_\alpha, \tag{1.143}$$

where $P^tQ = 1$ in order to preserve the canonical commutation relations.[63] The matrices P and Q are calculated explicitly by applying a succession of linear transformations. We define the rotation matrix R_1 that diagonalizes M, *i. e.* ${}^tR_1MR_1 = \Delta_1$ with Δ_1 a diagonal matrix, and the matrix $N_1 = {}^tR_1NR_1$. Since the matrix $\Delta_1^{1/2}N_1\Delta_1^{1/2}$ is symmetric, it can be diagonalized by a second rotation R_2, *i.e.* $\Delta_1^{1/2}N_1\Delta_1^{1/2} = R_2\Delta_2{}^tR_2$ with Δ_2 a second diagonal matrix. The transformations P and Q are then:

$$P = R_1\Delta_1^{-1/2}R_2(\Delta_2)^{1/4}, \tag{1.144}$$

$$Q = R_1\Delta_1^{1/2}R_2(\Delta_2)^{-1/4}, \tag{1.145}$$

and we have: ${}^tPMP = (\Delta_2)^{1/2}$ and ${}^tQNQ = (\Delta_2)^{1/2}$, giving the transformed Hamiltonian:

$$H = \int \frac{dx}{2\pi}\left[\pi^2\,{}^t\tilde{\mathbf{\Pi}}(\Delta_2)^{1/2}\tilde{\mathbf{\Pi}} + {}^t(\partial_x\tilde{\phi})(\Delta_2)^{1/2}(\partial_x\tilde{\phi})\right]. \tag{1.146}$$

In this last equation, the elements on the diagonal of $(\Delta_2)^{1/2}$ are the velocities u_β of the decoupled modes of the Hamiltonian (1.138).

The definition (1.144) implies in particular that: ${}^tPMNQ = \Delta_2$ i.e. $Q^{-1}MNQ = \Delta_2$, and by taking the transpose, $P^{-1}NMP = \Delta_2$.

The stability of the multicomponent TL liquid state requires that all the velocities are real, i.e., that the matrix MN has only positive eigenvalues.

With the notations of [47, 48], the matrices P and Q are $Q = U^{-1}Z$, $P = {}^tU^t(Z^{-1})$ where:

$$U = \begin{pmatrix} 1 & 1 \\ 0 & 1 \end{pmatrix}, \tag{1.147}$$

and:

$$Z = \begin{pmatrix} Z_{cc} & Z_{cs} \\ Z_{sc} & Z_{ss} \end{pmatrix}. \tag{1.148}$$

The result (1.146) implies that the correlation functions of operators $e^{i\sum_a(\lambda_a\phi_a+\mu_a\theta_a)}$ can be factorized into products of correlators. We have for zero temperature:

$$\langle T_\tau e^{i\sum_{a=1}^n(\lambda_a\phi_a+\mu_a\theta_a)(x,\tau)} e^{i\sum_{a=1}^n(\lambda_a\phi_a+\mu_a\theta_a)(x,\tau)}\rangle \quad = \tag{1.149}$$

$$\prod_{\beta=1}^{n}\prod_{r=\pm}\left(\frac{\alpha}{\alpha+u_\beta\tau+irx}\right)^{2\Delta_\beta^{(r)}}, \tag{1.150}$$

where:

$$2\Delta_\beta^{(r)} = \frac{1}{4}\left[\sum_{a=1}^{n}\mu_a P_{a\beta} + r\lambda_a Q_{a\beta}\right]^2. \tag{1.151}$$

Further details can be found in the articles [64, 56, 65].

Chapter 2

The sine-Gordon model

Until now, we have deferred the discussion of the sine-Gordon Hamiltonian that was obtained in systems with umklapp processes or with spin degrees of freedom. In the present chapter, we wish to review the main important results on the sine-Gordon model. We will write the sine-Gordon model in the form:

$$H = \int \frac{dx}{2\pi} \left[uK(\pi\Pi)^2 + \frac{u}{K}(\partial_x \phi)^2 \right] - \frac{2g}{(2\pi\alpha)^2} \cos\sqrt{8}\phi, \tag{2.1}$$

which is the one appropriate for the spin sector of the Hubbard model in one dimension. For the XXZ spin chain, the bosonized Hamiltonian can be brought to the form (2.1) by a rescaling of the fields. In the case of a dimerized spin-1/2 chain[66] one has to rescale $\phi \to \phi/\sqrt{2}$. The case of the spin chain in staggered field along x can also be reduced to (2.1) by a duality transformation.

Classically, the sine-Gordon model is integrable, and the solution of the sine-Gordon equations of motion can be described in terms of solitons, antisolitons and breathers[67]. At the classical level, the ground state of the sine Gordon Hamiltonian is given by $\phi = n\pi/\sqrt{2}$ with n integer. A soliton interpolates between the ground state with $\phi = n\pi/\sqrt{2}$ at $-\infty$ and the ground state with $\phi = (n+1)\pi/\sqrt{2}$ at $+\infty$, while an antisoliton interpolates between $\phi = (n+1)\pi/\sqrt{2}$ at $-\infty$, and $\phi = n\pi/\sqrt{2}$ at $+\infty$. Breathers are bound states of solitons and antisolitons. All these excitations have a relativistic-like dispersion $E = \sqrt{u^2p^2 + \Delta^2}$, where Δ is the mass of the excitation and p its momentum. In the classical case, the parameter K plays no role. By contrast, in the quantum case, the parameter K is important. As the renormalization group treatment will show, the parameter K determines whether the quantum sine-Gordon model is gapful or gapless. Moreover, in the gapful case, the parameter K also determines which excitations are present and how these excitations scatter.

2.1 Renormalization group approach

2.1.1 The operator product expansion approach

A very convenient method for deriving RG equations is the operator product expansion technique.[68] The Hamiltonian is written:

$$H = H_0 + \sum_i g_i \int dx d\tau O_i(x,\tau), \tag{2.2}$$

where H_0 is the fixed point Hamiltonian and O_i is an operator of scaling dimension d_i i. e.

$$\langle O_i(x,\tau) O_i(0,0)\rangle_{H_0} = \left(\frac{\alpha^2}{x^2+(u\tau)^2}\right)^{d_i}, \tag{2.3}$$

where α is a real space cutoff and u is a velocity. The evolution operator in Matsubara time is written:

$$U = \exp\left[-\sum_i g_i \int dx d\tau O_i(x,\tau)\right], \tag{2.4}$$

and we want to determine how the coupling constants g_i will change under a rescaling of the real space cutoff $\alpha \to \alpha e^{d\ell}$. The idea of the method is to consider the product of two normal ordered operators $O_i(z)$ and $O_j(z')$. The product can be expanded as:

$$O_i(x,\tau) O_j(0,0) = \sum_k \varphi_{ij}^k(x,\tau) O_k(0,0) + \text{regularterms}, \tag{2.5}$$

Then, if one expands the Matsubara evolution operator (2.4) to second order in the interactions, and change the cutoff, a correction to the coupling constants g_k will be generated by the integration over distances $\alpha^2 < x^2 + (u\tau)^2 < \alpha^2 e^{2d\ell}$. That step gives:

$$\delta g_k = -\frac{1}{2}\sum_{i,j} \int_{\alpha^2<x^2+(u\tau)^2<\alpha^2 e^{2d\ell}} dx d\tau \varphi_{ij}^k(x,\tau) g_j g_k, \tag{2.6}$$

$$= -\pi d\ell \sum_{i,j} C_{ij}^k g_i g_j, \tag{2.7}$$

where we have defined:

$$C_{ij}^k = \alpha^2 \int \frac{d\theta}{2\pi} \varphi(\alpha\cos\theta, \alpha\sin\theta/u) \tag{2.8}$$

The second step is a rescaling of the fields to restore the original cutoff. Under the rescaling, $g_k \to (1+(2-d_k)d\ell)g_k$, leading to the final renormalization group equations:

$$\frac{dg_k}{dl} = (2-d_k)g_k - \pi \sum_{i,j} C_{ij}^k g_i g_j \tag{2.9}$$

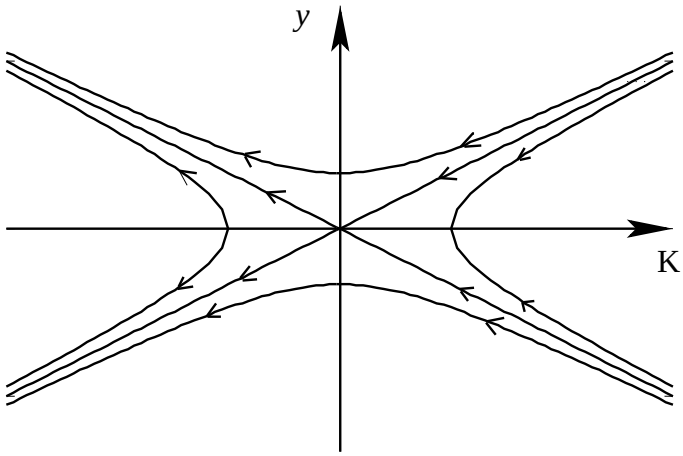

Figure 2.1: The renormalization group flow of the sine Gordon model. A stable fixed line exists for $K > 1$.

2.1.2 Renormalization group for the sine Gordon model

The operator product expansion of the operators:

$$\cos\beta\phi(x,\tau)\cos\beta\phi(0) = \left(\frac{\alpha^2}{x^2+(u\tau)^2}\right)^{\beta^2K/4}\left[1-\frac{\beta^2}{2}(x\partial_x\phi+\tau\partial_\tau\phi)^2+\ldots\right]+\ldots \tag{2.10}$$

leads to the Kosterlitz-Thouless renormalization group equations:

$$\frac{dK}{d\ell} = -\frac{K^2}{2}\left(\frac{g}{\pi u}\right)^2 \tag{2.11}$$

$$\frac{dg}{d\ell} = 2(1-K)g \tag{2.12}$$

It is convenient to introduce the dimensionless variable $y(\ell) = g(\ell)/(\pi u)$. Because the flow is symmetric under $y \to -y$ and $K \to K$, it is sufficient to discuss the case of $y > 0$. The flow diagram is represented on the Figure. 2.1.

When $K > 1$, the cosine operator is irrelevant and the Luttinger liquid fixed point is stable. When $K < 1$ the cosine is relevant, the system flows to a strong coupling fixed point. At the strong coupling fixed point, it is legitimate to expand the cosine around $\phi = 0$, yielding a mass term $\propto \phi^2$ which shows that the spectrum is fully gapped. For K far from 1, the RG flow is nearly vertical, and the gap behaves as $\Delta \sim u/\alpha(g/u)^{1/(2-2K)}$.

At the transition between the gapful and the gapless regime, there is a marginal flow, with the cosine being marginally irrelevant. On that line, $K(\ell) = 1 + y(\ell)/2$ and the RG equations reduce to a single equation:

$$\frac{dy}{d\ell} = -y(\ell)^2, \tag{2.13}$$

with solution:

$$y(\ell) = \frac{y(0)}{1+y(0)\ell}, \tag{2.14}$$

with $y(\ell) \to 0$ for $\ell \to \infty$. Such marginal flow gives rise to logarithmic correlations to the correlation functions[41, 69]. One has in particular:

$$\langle e^{i\sqrt{2}\theta(x,\tau)} e^{-i\sqrt{2}\theta(0,0)} \rangle = \frac{\alpha}{r} [\ln(r/\alpha)^{1/2}], \tag{2.15}$$

$$\langle \cos\sqrt{2}\phi(x,\tau) \cos\sqrt{2}\phi(0,0) \rangle = \frac{\alpha}{r} [\ln(r/\alpha)^{1/2}], \tag{2.16}$$

$$\langle \sin\sqrt{2}\phi(x,\tau) \sin\sqrt{2}\phi(0,0) \rangle = \frac{\alpha}{r} [\ln(r/\alpha)^{-3/2}], \tag{2.17}$$

so that fluctuations towards antiferromagnetic ordering are enhanced over the fluctuations towards dimer order in the spin-1/2 chain at the isotropic point. In the Hubbard model with repulsive interaction, this implies that spin density wave order dominates over charge density wave order. The logarithmic corrections also affect macroscopic observables such as the magnetic susceptibility. In, particular, in the spin-1/2 chain, with finite temperature, the RG flow has to stop when the running cutoff αe^{l^*} is of the order of the thermal length u/T giving at finite temperature

$$K(T) = 1 + \frac{1}{2} \frac{y(0)}{1 + y(0) \ln(u\alpha/T)} \simeq 1 + \frac{1}{2\ln(T_0/T)}, \tag{2.18}$$

giving a susceptibility varying as[70]

$$\chi(T) = \frac{1}{\pi^2 J} \left[1 + \frac{1}{2\ln(T_0/T)} \right] \tag{2.19}$$

A similar logarithmic dependence of the magnetic susceptibility on the magnetic field can be deduced from Eq.(2.14). There exists also a line of marginally relevant flow with $K = 1 - y/2$. Such a case is realized with the spin sector of the Hubbard model when $U < 0$, or the charge sector of the half-filled Hubbard model when $U > 0$ or with the frustrated antiferromagnetic spin-1/2 chain with nearest neighbor exchange J_1 and next-nearest neighbor exchange $J_2 > 0.24 J_1$. This time, the coupling constant is diverging at a scale $\ell^* = -1/y(0)$. The excitations of the sine-Gordon model are gapped.[66] and its spectrum is formed of massive solitons. In the $J_1 - J_2$ chain or the spin sector of the Hubbard model with $U < 0$, the massive solitons are spin-1/2 spinons. Since the total spin can only change by 1, these spinons are always formed or annihilated in pairs, giving a simple example of fractionnalized excitations.

2.2 The Luther-Emery point and the Ising model

2.2.1 Fermionization of the sine-Gordon model at the Luther-Emery point

An interesting special point of the sine Gordon model is the Luther-Emery point[71] obtained for $K = 1/2$. At that point, the sine-Gordon model is a bosonized representation of a model

of free gapful fermions. Indeed, under the rescaling $\phi = \tilde{\phi}/\sqrt{2}$ and $\Pi = \sqrt{2}\tilde{\Pi}$, the sine Gordon Hamiltonian becomes:

$$H = \int \frac{dx}{2\pi} u \left[(\pi\tilde{\Pi})^2 + (\partial_x \tilde{\phi})^2 \right] + \frac{2g}{(2\pi\alpha)^2} \cos 2\tilde{\phi}, \tag{2.20}$$

Undoing the bosonization transformation by introducing the free fermions $\tilde{\psi}_r = \frac{e^{i(\tilde{\theta} - r\tilde{\phi})}}{\sqrt{2\pi\alpha}}$ yields the Hamiltonian:

$$H = \int dx \left[-iu \sum_r r \tilde{\psi}_r^\dagger \partial_x \tilde{\psi}_r + \frac{g}{\pi\alpha} \sum_r \tilde{\psi}_r^\dagger \tilde{\psi}_{-r} \right], \tag{2.21}$$

with gapful spectrum $E(k) = \pm\sqrt{(uk)^2 + [g/(\pi\alpha)]^2}$.

2.2.2 The double Ising model and Dirac fermions in two dimensions

A mapping from the gapful free fermion model to a doubled Ising chain can be derived.[72, 73] For a single Ising chain,

$$H = -J \sum_j \sigma_j^x \sigma_{j+1}^x - h \sum_j \sigma_j^z, \tag{2.22}$$

there is a phase transition between a ferromagnetic phase with $\langle \sigma_j^x \rangle = \pm\sigma_0 \neq 0$ at small h and a paramagnetic phase $\langle \sigma_j^x \rangle = 0$ at large h. The Ising chain is known to possess a duality transformation:

$$\mu_j^z = 2\sigma_j^x \sigma_{j+1}^x, \tag{2.23}$$
$$\sigma_j^z = 2\mu_j^x \mu_{j+1}^x, \tag{2.24}$$

which exchanges J and $2h$. For $J = 2h$ the model is self-dual, indicating the transition point. The Jordan-Wigner transformation (1.57) allows to rewrite the Hamiltonian in terms of pseud-ofermions[1]:

$$H = -\frac{J}{4} \sum_j (c_j^\dagger - c_j)(c_{j+1}^\dagger + c_{j+1}) - h \sum_j (c_j^\dagger c_j - 1/2), \tag{2.25}$$

It is convenient to introduce the Majorana fermions operators:

$$\zeta_j = \frac{c_j^\dagger - c_j}{i\sqrt{2}}, \tag{2.26}$$
$$\eta_j = \frac{c_j^\dagger + c_j}{\sqrt{2}}, \tag{2.27}$$

[1] We don't include the $(-)^n$ factor in that case.

that satisfy $\zeta_j = \zeta_j^\dagger$, $\eta_= \eta_j^\dagger$ and the anticommutation relations $\{\zeta_j, \zeta_k\} = \delta_{jk}$ and $\{\eta_j, \eta_k\} = \delta_{jk}$ to rewrite:

$$H = -i\frac{J}{2}\sum_j \zeta_j \eta_{j+1} - ih\sum_j \zeta_j \eta_j. \tag{2.28}$$

In terms of the Majorana fermion operators,

$$\begin{aligned}
\sigma_j^x &= \frac{\eta_j}{\sqrt{2}}\prod_{k<j}(2i\eta_j\zeta_k) && (2.29)\\
\sigma_j^z &= i\zeta_j\eta_j, && (2.30)\\
\mu_j^z &= i\zeta_j\eta_{j+1}, && (2.31)\\
\mu_j^x &= \prod_{k<j}(2i\eta_j\zeta_k) && (2.32)
\end{aligned}$$

After a rotation in Majorana fermion space,

$$\begin{aligned}
\zeta_j &= \frac{1}{\sqrt{2}}(\psi_{R,j} - \psi_{L,j}), && (2.33)\\
\eta_j &= \frac{1}{\sqrt{2}}(\psi_{R,j} + \psi_{L,j}), && (2.34)
\end{aligned}$$

The Ising Hamiltonian is finally rewritten as:

$$H = -\frac{iJ}{4}\sum_j(\psi_{R,j}\psi_{R,j+1} - \psi_{L,j}\psi_{L,j+1}) + \sum_n\left(\frac{iJ}{2}\psi_{R,j+1}\psi_{L,j+1} - ih\psi_{R,j}\psi_{L,j}\right), \tag{2.35}$$

Taking the continuum limit, the Hamiltonian becomes:

$$H = -\frac{iJ}{4}\sum_j(\psi_R(x)\partial_x\psi_R(x) - \psi_L(x)\partial_x\psi_L(x)) + i(J/2-h)\int dx\psi_R(x)\psi_L(x), \tag{2.36}$$

indicating that the Ising transition is obtained when the Majorana fermions become massless. If we now consider two Ising chains,

$$\begin{aligned}
H &= H_1 + H_2 && (2.37)\\
H_n &= -J\sum_j \sigma_{j,n}^x\sigma_{j+1,n}^x - h\sum_j \sigma_{j,n}^z, && (2.38)
\end{aligned}$$

We can apply the previous mapping to each chain and derive a continuum representation of the form (2.36):

$$H = \sum_{n=1,2}\left[-\frac{iJ}{4}\sum_{j,n}(\psi_R^{(n)}(x)\partial_x\psi_R^{(n)}(x) - \psi_L^{(n)}(x)\partial_x\psi_L^{(n)}(x)) + i(J/2-h)\int dx\psi_R^{(n)}(x)\psi_L^{(n)}(x)\right] \tag{2.39}$$

which can be rewritten into a single Dirac fermion representation by introducing:

$$\Psi_{R/L} = \frac{1}{\sqrt{2}}(\psi^{(1)}_{R/L} + i\psi^{(1)}_{R/L}), \tag{2.40}$$

so that:

$$H = -iv\int dx(\Psi^\dagger_R\partial_x\Psi_R - \Psi^\dagger_L\partial_x\Psi_L) + im\int dx(\Psi^\dagger_R\Psi_L - \Psi^\dagger_L\Psi_R). \tag{2.41}$$

If we now turn to the disorder operators, we have that:

$$2\mu^x_{j,n} = \prod_{k<j}(2i\zeta_k\eta_k) = \prod_{k<j}(2i\psi^{(n)}_{R,j}\psi^{(n)}_{L,k}), \tag{2.42}$$

So:

$$\begin{aligned}
4\mu^x_{j,1}\mu^x_{j,2} &= \prod_{k<j}\prod_{n=1,2}(2i\psi^{(n)}_{R,j}\psi^{(n)}_{L,k}), && (2.43)\\
&= \prod_{k<j}(2\Psi^\dagger_{R,j}\Psi_{R,j} - 1)(2\Psi^\dagger_{L,j}\Psi_{L,j} - 1) && (2.44)\\
&= \prod_{k<j} e^{i\pi(\Psi^\dagger_{R,j}\Psi_{R,j} + \Psi^\dagger_{L,j}\Psi_{L,j})} && (2.45)\\
&= \cos\left[\pi\sum_{k<j}(\Psi^\dagger_{R,j}\Psi_{R,j} + \Psi^\dagger_{L,j}\Psi_{L,j})\right]. && (2.46)
\end{aligned}$$

We also have:

$$4\sigma^x_{j,1}\mu^x_{j,2} = (\psi^{(1)}_R + \psi^{(1)}_L)\cos\left[\pi\sum_{k<j}(\Psi^\dagger_{R,j}\Psi_{R,j} + \Psi^\dagger_{L,j}\Psi_{L,j})\right], \tag{2.47}$$

$$4\mu^x_{j,1}\sigma^x_{j,2} = (\psi^{(2)}_R + \psi^{(2)}_L)\cos\left[\pi\sum_{k<j}(\Psi^\dagger_{R,j}\Psi_{R,j} + \Psi^\dagger_{L,j}\Psi_{L,j})\right], \tag{2.48}$$

and:

$$4\sigma^x_{j,1}\sigma^x_{j,2} = (\psi^{(1)}_R + \psi^{(1)}_L)(\psi^{(2)}_R + \psi^{(2)}_L)\cos\left[\pi\sum_{k<j}(\Psi^\dagger_{R,j}\Psi_{R,j} + \Psi^\dagger_{L,j}\Psi_{L,j})\right], \tag{2.49}$$

Applying bosonization, we obtain the relations:

$$\begin{aligned}
\mu^x_1(x)\mu^x_2(x) &= \cos\phi(x) && (2.50)\\
\sigma^x_1(x)\mu^x_2(x) &= \cos\theta(x) && (2.51)\\
\mu^x_1(x)\sigma^x_2(x) &= \sin\theta(x) && (2.52)\\
\sigma^x_1(x)\sigma^x_2(x) &= \sin\phi(x) && (2.53)
\end{aligned}$$

The correlation functions of the two-dimensional Ising model in the vicinity of the critical point are known[74] to be expressible in terms of Painlevé III functions[75]. This allows us to obtain the correlation functions of the sine-Gordon fields at the Luther-Emery point. We see that the operators $e^{i\theta}$ always have short range order, while the operators $e^{i\phi}$ present a long range order.

2.3 Integrability of the sine-Gordon model and the Form-factor approach

The integrability of the classical sine-Gordon model persists at the quantum level. Indeed, the quantum sine-Gordon model can be mapped in all generality to the massive Thirring model which is known from the work of Bergknoff and Thacker to be integrable by the Bethe Ansatz[76, 77].

The excited states of the quantum sine-Gordon model can be described in terms of solitons of mass uM/α, antisolitons of mass uM/α and (possibly) breathers. The dimensionless mass M depends on g/u as[78] as:

$$M = \frac{2\Gamma\left(\frac{K}{2-2K}\right)}{\Gamma(1/2)\Gamma\left(\frac{1}{2-2K}\right)}\left[\frac{\Gamma(1-K)}{\Gamma(K)}\frac{g}{4\pi u}\right]^{\frac{1}{2-2K}}. \tag{2.54}$$

The ground state expectation value of the exponential fields is conjectured to be[79]:

$$\langle e^{in\sqrt{2}\phi}\rangle = \left[\frac{\pi\Gamma(1-K)}{\Gamma(K)}\frac{g}{4\pi^2 u}\right]^{\frac{n^2K}{(4-4K)}} \exp\left\{\int_0^\infty \frac{dt}{t}\left[\frac{\sinh^2(nKt)}{2\sinh(Kt)\sinh t\cosh(1-K)t} - \frac{n^2K}{2}e^{-2t}\right]\right\}, \tag{2.55}$$

with $n < 1/K$. However, in contrast to the classical sine-Gordon model, the breather masses uM_n/α are quantized and satisfy the condition:

$$M_n = 2M\sin\left(n\frac{\pi}{2}\frac{K}{1-K}\right) \tag{2.56}$$

with n an integer, taking values from 1 to the integer part of $1/K-1$. The condition (2.56) can be derived from a semiclassical analysis[80]. According to (2.56), the breathers exist only for $K < 1/2$ i. e. only below the Luther-Emery point. The interpretation of this result is that for $K < 1/2$ the interaction between the Luther-Emery fermions is repulsive. As a result, a bound state can be formed between a Luther-Emery hole (antisoliton) and a Luther-Emery fermion (soliton). For $K > 1/2$, the Luther-Emery fermion and the Luther-Emery hole repel each other and no bound state can form.

In the case of the Hubbard model for $U < 0$ and $|U| \ll t$, or the frustrated spin-1/2 chain, $K < 1$ and we have only massive spin-1/2 solitons. In the case of the dimerized spin-1/2 chain, $K = 1/4$, so that two breathers of masses $M_1 = 2M\sin(\pi/6) = M$ and $M_2 = 2M\sin(\pi/3) = M\sqrt{3}$ are present. The light breather of mass M and spin $S^z = 0$ forms a triplet with the the soliton of spin $S^z = 1$ and the antisoliton of spin $S^z = -1$. The heavy breather of mass $M_2 = M\sqrt{3}$ is a singlet excitation.[66, 81, 82]

2.3.1 S-matrix

The integrability of the quantum sine-Gordon model can be used to derive the exact free energy, but also to obtain the correlation functions using the Form factor expansion. To do that, it

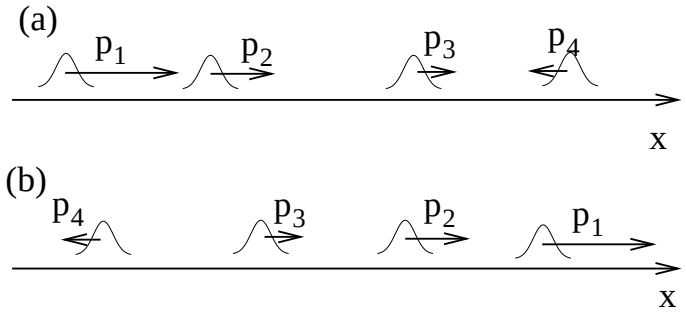

Figure 2.2: (a) an in-going state, with particle velocities in increasing order from left to right. (b) an outgoing state, with particle velocities in decreasing order from left to right. In both type of states, the particle are approximately localized in space forming wavepackets. p_1, p_2, p_3, p_4 are their approximate momenta.

is convenient to work from the S matrix.[83] The S-matrix relates the in-going states, which are wave-packets in which the particles are approximately localized, with their velocities in decreasing order from left to right, to the out-going states also wave-packets but with particle velocities in increasing ordered from left to right. If $|p_1, \dots p_m\rangle_{in}$ is an in state, and $|p'_1, \dots, p'_n\rangle_{out}$ is an out state, then

$$S(p'_1 \dots'_n ; p_1, \dots p_m) = {}_{out}\langle p'_1, \dots, p'_n || p_1, \dots p_m\rangle_{in} \tag{2.57}$$

The Bethe Ansatz integrability implies that no particle production can obtain so that the numbers of solitons, antisolitons and breathers are conserved, and the S-matrix is factorizable.[83] As a result, it is sufficient to know the S-matrix for collisions of two excitations. It is convenient to parameterize the S-matrix in terms of:

$$\nu = \frac{K}{1-K}, \tag{2.58}$$

and introduce the rapidity θ to parameterize the velocity $u \tanh\theta$, momentum $p = mu \sinh\theta$ and the energy $E = mu^2 \cosh\theta$ of a particle. When working with rapidities, for two particles, the invariant $(E_1 + E_2)^2/u^4 - (p_1 + p_2)^2/u^2 = m_1^2 + m_2^2 + 2m_1 m_2 \cosh(\theta_1 - \theta_2)$, so that the S matrix describing the collision of those particles depends only on $\theta = \theta_1 - \theta_2$. Another advantage of that representation is that the S-matrix can be analytically continued to complex values of the parameter θ. The S-matrix is a periodic function of θ of period $2i\pi$. Bound states of particles correspond to poles of the S-matrix for purely imaginary values of the parameter θ. When a bound state c is formed between two particles of masses M_a and M_b, the energy of the bound state can be written $M_c^2 = M_a^2 + M_b^2 + 2M_a M_b \cos(iU_{ab}^c)$. One has[83, 84]:

$$S(\theta_1 - \theta_2) = i \frac{(\Gamma_{ab}^c)^2}{\theta_1 - \theta_2 - iU_{ab}^c} \tag{2.59}$$

The S-matrix for the soliton-soliton or antisoliton-antisoliton collision is:

$$S_{ss}(\theta) \;=\; \exp\left[\int_0^{+\infty} \frac{dt}{t} \frac{\sinh\frac{1}{2}(1-\nu)t}{\sinh\frac{1}{2}\nu t \cosh\frac{t}{2}} \sinh t\frac{\theta}{i\pi}\right], \tag{2.60}$$

The S-matrix describing a collision between soliton and antisoliton without momentum exchange is:

$$S_{s\bar{s}}^{(t)}(\theta) = \frac{\sinh\theta/\nu}{\sinh(i\pi-\theta)/\nu} S_{ss}(\theta), \tag{2.61}$$

while the S-matrix describing a collision between soliton and antisoliton with momentum exchange is:

$$S_{s\bar{s}}^{(r)}(\theta) = \frac{\sinh i\pi/\nu}{\sinh(i\pi-\theta)/\nu} S_{ss}(\theta), \tag{2.62}$$

We notice that when $1/\nu$ is integer, the matrix describing reflection vanishes. The points are called reflectionless points.

When breathers exist, we also have soliton-breather:

$$S_{sb_k}(\theta) = (-)^k \exp\left[\int_0^{+\infty} \frac{dt}{t} \frac{2\cosh\frac{\nu}{2}t\sinh\frac{\nu}{2}kt}{\sinh\frac{1}{2}\nu t\cosh\frac{t}{2}} \sinh t\frac{\theta}{i\pi}\right], \tag{2.63}$$

and breather-breather ($k<l$):

$$S_{b_kb_l}(\theta) = (-)^k \exp\left[\int_0^{+\infty} \frac{dt}{t} \frac{4\cosh\frac{\nu}{2}t\sinh\frac{\nu}{2}kt\cosh\frac{1}{2}(1-\nu l)t}{\sinh\frac{1}{2}\nu t\cosh\frac{t}{2}} \sinh t\frac{\theta}{i\pi}\right], \tag{2.64}$$

$$S_{b_kb_k}(\theta) = (-)^k \exp\left[\int_0^{+\infty} \frac{dt}{t} 2\frac{\cosh\frac{\nu}{2}t\sinh\frac{1}{2}(2k\nu-1)t+\sinh\frac{1}{2}(1-\nu)t}{\sinh\frac{1}{2}\nu t\cosh\frac{t}{2}} \sinh t\frac{\theta}{i\pi}\right]. \tag{2.65}$$

2.3.2 Bethe Ansatz at the reflectionless points

At the reflectionless points, there is no backscattering of solitons, antisolitons or breathers and the S-matrix is simply describing a phase-shift of the particles after a collision. Such situation makes the description of the conditions to be satisfied by the rapidities of the particles when periodic boundary conditions are imposed particularly simple to write.[85] Indeed, if we consider a particle of rapidity θ_j and mass m_j going from position x to position $x+L\equiv x$ it will receive a phase-shift $e^{im_j\sinh\theta_j L}$ resulting from its momentum, and another phase-shift $\prod_{j\neq k} S_{jk}(\theta_k-\theta_j)$ from the collisions with the other particles. These phase shifts have to compensate each other so that the periodic boundary conditions are satisfied and:

$$e^{im_j\sinh\theta_j L}\prod_{k\neq j} S_{jk}(\theta_j-\theta_k) = 1. \tag{2.66}$$

Taking the logarithm of (2.66), we find:

$$m_jL\sinh\theta_j + \frac{1}{i}\sum_{j\neq k}\ln S_{jk}(\theta_k-\theta_j) = 2\pi I_j, \tag{2.67}$$

where the I_j's are integer. Introducing the densities of solitons, antisolitons and breathers, the equations (2.67) can be rewritten as integral equations[85]:

$$M_\alpha \cosh\theta + \sum_\beta \int_{-\infty}^{\infty} K_{\alpha\beta}(\theta-\theta')\rho_\beta(\theta') = 2\pi[\rho_\beta(\theta) + \rho^h_\beta(\theta')], \tag{2.68}$$

where $\alpha = s, \bar{s}, b_j$ indicates whether $\rho_\alpha(\theta)$ is a density of solitons (s), antisolitons ($\bar{s}$) or breathers (b_j), $\rho^h_\beta(\theta)$ being a density of unoccupied soliton, antisoliton or breather states. We have also defined:

$$K_{\alpha\beta}(\theta) = \frac{1}{i}\frac{d}{d\theta}\ln S_{\alpha\beta}(\theta). \tag{2.69}$$

The dimensionless free energy $F = (\alpha^2/u)\mathcal{F}$ is obtained from the method of Yang and Yang.[86, 87, 88] The total energy of an excited state is given by:

$$E = E_{GS} + \int d\theta \sum_\alpha M_\alpha \cosh\theta \rho_\alpha(\theta), \tag{2.70}$$

with the dimensionless ground state energy density E_{GS} given by:

$$E_{GS} = -\frac{M^2}{4}\tan\left(\frac{\pi K}{2-2K}\right) \tag{2.71}$$

while the entropy is given by:

$$S = \sum_\alpha \int d\theta[(\rho_\alpha + \rho^h_\alpha)(\theta)\ln(\rho_\alpha+\rho^h_\alpha)(\theta) - \rho_\alpha(\theta)\ln\rho_\alpha(\theta) - \rho^h_\alpha(\theta)\ln\rho^h_\alpha(\theta)]. \tag{2.72}$$

We have to minimize the free energy $F = E - TS$ with respect to the densities ρ and ρ^h subject to the condition (2.68). Introducing the pseudoenergies:

$$\frac{\rho_\alpha(\theta)}{\rho^h_\alpha(\theta)} = e^{-\epsilon_\alpha(\theta)/T}, \tag{2.73}$$

we find:

$$0 = \delta F = \sum_\alpha \left[m_\alpha \cosh\theta - T\ln(1+e^{\epsilon_\alpha(\theta)/T})\right]\delta\rho_\alpha - T\ln(1+e^{-\epsilon_\alpha(\theta)/T})\delta\rho^h_\alpha \tag{2.74}$$

$$\delta\rho^h_\alpha = -\delta\rho_\alpha + \frac{1}{2\pi}\sum_\beta \int d\theta' K_{\alpha\beta}(\theta-\theta')\delta\rho_\beta(\theta') \tag{2.75}$$

substituting the second line into the first equation, we obtain:

$$m_\alpha \cosh\theta = \epsilon_\alpha(\theta) - \frac{T}{2\pi}\int d\theta' \sum_\beta K_{\alpha\beta}(\theta-\theta')\ln(1+e^{-\epsilon_\beta(\theta')/T}). \tag{2.76}$$

The non-linear integral equations (2.76) must be solved in order to obtain the pseudoenergies. Once the pseudoenergies are known, it is possible to express the free energy using:

$$F = E_{GS} + \int d\theta \left[\sum_\alpha \int d\theta m_\alpha \cosh\theta - \epsilon_\alpha(\theta)\rho_\alpha(\theta) - T(\rho_\alpha + \rho_\alpha^h)\ln(1+e^{-\epsilon_\alpha/T}) \right] \quad (2.77)$$

$$= E_{GS} - \frac{T}{2\pi}\int d\theta \sum_\alpha m_\alpha \cosh\theta \ln(1+e^{-\epsilon_\alpha/T}), \quad (2.78)$$

where, to obtain the last line we have used the integral equations (2.76) and the condition (2.68).

2.3.3 The form factor expansion

The form factor expansion allows the calculation of correlation functions in integrable models. It has been applied to the calculation of conductivity in one-dimensional Mott insulators[89, 90, 91], spin-spin correlation functions in gapful spin chains [92, 93, 94, 95] and spectral functions in metals with spin gap[96]. In the present section, we will first describe the principle of the Form factor expansion, and we will then describe the calculation of the simplest form factors.

Principle of the method

For any translationally invariant system, the Matsubara correlation functions in the ground state can be written as:

$$\langle A(x,\tau)A(0,0)\rangle = \sum_n \langle 0|e^{-iPx+\tau H}Ae^{iPx-\tau H}|n><n|A|0> \quad (2.79)$$

$$= \sum_n |<n|A|0>|^2 e^{iP_n x - E_n \tau}, \quad (2.80)$$

where $|n>$ is a simultaneous eigenstate of the energy operator $H|n>=E_n|n>$ and of the momentum operator $P|n>=P_n|n>$. In a general model, the computation of all eigenvalues and eigenstates is a daunting task. However, in the case of an integrable model such as the sine-Gordon model, the problem is simpler. First, the eigenstates are simply described in terms of the rapidities of the solitons, antisolitons and breathers, and the eigenvalues are simply $P_n = \sum_j m_j \sinh\theta_j$ and $E_n = \sum_j m_j \cosh\theta_j$. Second, it is possible to obtain equations relating the matrix elements $F_A(\theta_1,\ldots,\theta_n) = \langle\theta_1,\ldots,\theta_n|A|0\rangle$ (these matrix elements are called form factors) to the S-matrix.[97] Solving these equations allows to write a series expansion of Eq. (2.79) the terms of which are indexed by the number of solitons, antisolitons and breathers in the expansion. Finally, for gapped models such as the sine-Gordon model, the term $e^{-E_n\tau}$ decays exponentially with τ over a scale inversely proportional to the sum of the masses of the breathers, solitons and antisolitons appearing in the eigenstate $|n>$. As a result, the first terms of the series already give an accurate approximation of the Matsubara correlation function (2.79). If we were considering the imaginary part of a response function, the situation would be even better. Indeed, the expression of the response function being:

$$I_A(q,\omega) = \sum_n |<n|A|0>|^2 \delta(q-P_n)\delta(\omega-E_n), \quad (2.81)$$

for $\omega < E_n$, the contribution of the eigenstate $|n>$ to the response function is exactly zero. So for fixed ω and with a gapful model, only the terms with a total mass of the excitations less than ω need to be summed in (2.81) to obtain the exact answer.

The equations defining the form factors

For the n-particle form factor, we define[97]:

$$\rangle 0|A(x)|\langle \theta_1, \dots \theta_n\rangle_{in} = e^{ix(m_1 \sinh\theta_1 + \dots + \sinh\theta_n)} F_A^{(n)}(\theta_1, \dots \theta_n) \tag{2.82}$$

As a result of the Lorentz-like invariance of the sine-Gordon model, $F_A(\{\theta_j\})$ depends only on the differences $\theta_j - \theta_k$. The form factor possesses invariance under the combination of charge conjugation, parity and time reversal, so that:

$$\rangle 0|A(x)|\langle \theta_1, \dots, \theta_n\rangle_{out} = F_A^{(n)}(-\theta_1, \dots, -\theta_n) \tag{2.83}$$

It also possesses the crossing symmetry, such that:

$$_{out}\langle \theta_1, \dots, \theta_m|A(x)|\langle \theta_{m+1}, \dots, \theta_n\rangle_{in} = F_A^{(n)} \tag{2.84}$$

If we consider the two-particle form-factor and insert a resolution of the identity in Eq. (2.82) using the out-going state as a basis, we find with (2.83) that:

$$F_A^{(2)}(\theta_2 - \theta_1) = S(\theta_1 - \theta_2) F_A(\theta_1 - \theta_2) \tag{2.85}$$

and from (2.84):

$$F_A(i\pi - \theta) = F_A(i\pi + \theta) \tag{2.86}$$

The equation (2.85) is called Watson's equation. It allows to find the two-particle form factor by solving a Riemann-Hilbert problem.[98] When the S matrix can be written as:

$$S(\theta) = \exp\left[\int_0^{+\infty} dt f(t) \sinh\frac{t\theta}{i\pi}\right], \tag{2.87}$$

The minimal solution of the Riemann Hilbert problem is given by[97, 99]:

$$F^{min.}(\theta) = \exp\left[\int_0^{+\infty} dt f(t) \frac{\sin^2[t(i\pi - \theta)/2\pi]}{\sinh t}\right] \tag{2.88}$$

The solution (2.88) is free from poles. The general solution is of the form:

$$F(\theta) = K(\theta) F^{min.}(\theta), \tag{2.89}$$

where $K(\theta) = K(-\theta) = K(\theta + 2i\pi)$. The factor $K(\theta)$ contains all the poles of the physical form factor.

In the case of the general multi-particle form-factors, the set of equations to be solved is discussed in[84, 100, 99]. This set of equation is:

$$F_A(\theta_1, \dots \theta_j, \theta_{j+1}, \dots, \theta_n) = S(\theta_j - \theta j + 1) F_A(\theta_1, \dots \theta_{j+1}, \theta_j, \dots, \theta_n) \tag{2.90}$$

$$F_A(2i\pi + \theta_1, \theta_2, \dots, \theta_n) = F_A(\theta_2, \dots, \theta_n, \theta_1) \tag{2.91}$$

To these equations, conditions fixing the position of the poles must be added. The first one is related to kinematic poles:

$$-i \lim_{\theta \to \theta'} (\theta - \theta') F_A(\theta' + i\pi, \theta, \theta_1, \dots, \theta_n) = \left(1 - \prod_{l=1}^{n} S(\theta - \theta_l)\right) F_A(\theta_1, \dots \theta_n), \tag{2.92}$$

where θ and θ' are the rapidities of a soliton and and an antisoliton. These poles correspond the annihilation of a particle and an antiparticle, the total energy being $4M^2 \cosh(i\pi/2)^2 = 0$ when $\theta - \theta' = i\pi$. These poles relate the $n+2$ particle form factor to the n particle form factor. The other one is related to bound state poles. When a bound state exists, one has the relation (with the same notations as in (2.59):

$$-i \lim_{\theta - \theta' \to i U^c_{ab}} F(\theta, \theta', \theta_1, \dots, \theta_n) = \Gamma^c_{ab} F\left(\frac{\theta + \theta'}{2}, \theta_1, \dots, \theta_n\right), \tag{2.93}$$

which relates the $n+1$ particles form factor to the n-particles form factor (the first particle being a bound state).

Chapter 3

A brief review of experimental systems

3.1 Quasi-one dimensional conductors

These systems are three-dimensional solids with a highly anisotropic structure that can be viewed as an an array of weakly coupled one-dimensional chains. As a result, they can be expected to show some Tomonaga-Luttinger liquid features. However, in all those quasi-one dimensional conductors, interchain couplings are relevant perturbations that destabilize the Luttinger liquid fixed point[101]. If we call $t_\perp$ the interchain hopping, a renormalization group argument shows that, when $t_\perp$ is relevant, below a temperature:

$$T_X \propto T_F \left(\frac{t_\perp}{E_F} \right)^{\frac{4K_\rho}{6K_\rho - K_\rho^2 - 1}}, \tag{3.1}$$

the one-dimensional chains cannot be considered decoupled and a Fermi liquid is restored.[101] One may hope that since $t_\perp$ is irrelevant for either $K_\rho < 3-2\sqrt{2}$ or $K_\rho > 3+2\sqrt{2}$ the Tomonaga-Luttinger liquid could be stable for large interactions. However, interchain exchange coupling and interchain Josephson coupling are also present[102, 103, 104] and become relevant for respectively $K_\rho < 1$ and $K_\rho > 1$ giving rise respectively to antiferromagnetic or superconducting long range order. As a result, the hints of Tomonaga-Luttinger liquid physics can only be observed in a regime of sufficiently large temperature or high frequency. With these limitations in mind, we discuss some of the hints of Tomonaga-Luttinger liquid properties in these materials.

3.1.1 TTF-TCNQ

The organic conductor TTF-TCNQ (tetrathiafulvalenium-tetracyanoquinodimethane) is made of chains of stacked organic molecules TTF and TCNQ. The structure is monoclinic, with space group $P2_{1/c}$, and lattice parameters $a = 12,298$ Å, $b = 3,819$ Å, $c = 18,468$ Ået $\beta = 104,46^o$. The electronic orbitals overlap most strongly along the b axis, and more weakly along the other directions. TCNQ is an electron acceptor molecule, while TTF is an electron donor molecule, and as a result of electron transfer, the TTF chains are hole doped ($n_h = 1.41$)while the TCNQ chains are electron doped ($n_e = 0.59$). A Peierls instability exists for $T < 54$K. It is know

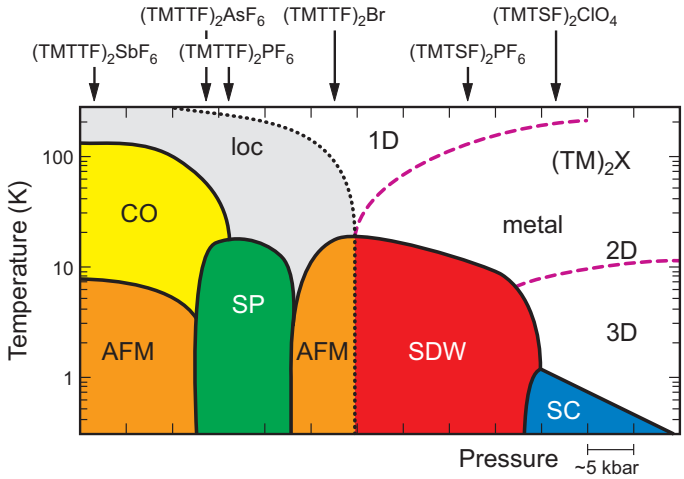

Figure 3.1: The universal phase diagram of organic conductors. The Bechgaard salts are more weakly correlated than the Fabre salts and correspond to higher effective pressure.

that $4k_F$ fluctuations of the charge density exist on the TTF chains[105] a signature of strong correlations in one dimension. Angle resolved photoemission spectroscopy measurements that give access to the electronic spectral functions of the TCNQ chains can be interpreted in terms of a one-dimensional Hubbard model with $U = 4.9t$.[106] However, the hole spectral functions on the TTF chains have to be interpreted in terms of a Hubbard model with $U < 0.2t$ in disagreement with the suggestion of stronger correlation on these chains coming from the $4k_F$ measurement.

3.1.2 The Bechgaard and Fabre salts

The Bechgaard salts $(TMTSF)_2X$ (tetramethyltetraselenafulvalene combined with an anion X^-) and the Fabre salts $(TMTTF)_2X$ (tetramethyltetrathiafulvalene combined with a anion X^-) are also examples of one quasi-dimensional conductors. The present a stacking of the TMTTF or TMTSF molecules forming chains. Since the formal charge of a molecule is +0.5, the chains are apparently three-quarter filled. However, a dimerization of the chains (giving 2 non-equivalent organic molecules in each unit cell) makes them actually half filled in the upper band. A universal phase diagram in the pressure temperature plane has been proposed based on experiments and is represented on Fig. 3.1. Under pressure, the organic molecules are brought closer to each other, increasing the overlap integrals and the kinetic energy of electrons, while the Coulomb repulsion is weakly affected. As a result, high pressure corresponds to smaller interaction to bandwidth ratio. The Fabre salts at ambient pressure present a larger interaction to bandwidth ratio than the Bechgaard salts and appear on the left of the phase diagram. They present a regime of charge localisation, where the conductance becomes activated, in agreement with the prediction of insulating state in a one-dimensional system at half filling. However, since the Fabre salts are already three-quarter filled in the absence of dimerization, the charge localization may also result from a three-quarter filled umklapp process[107] provided

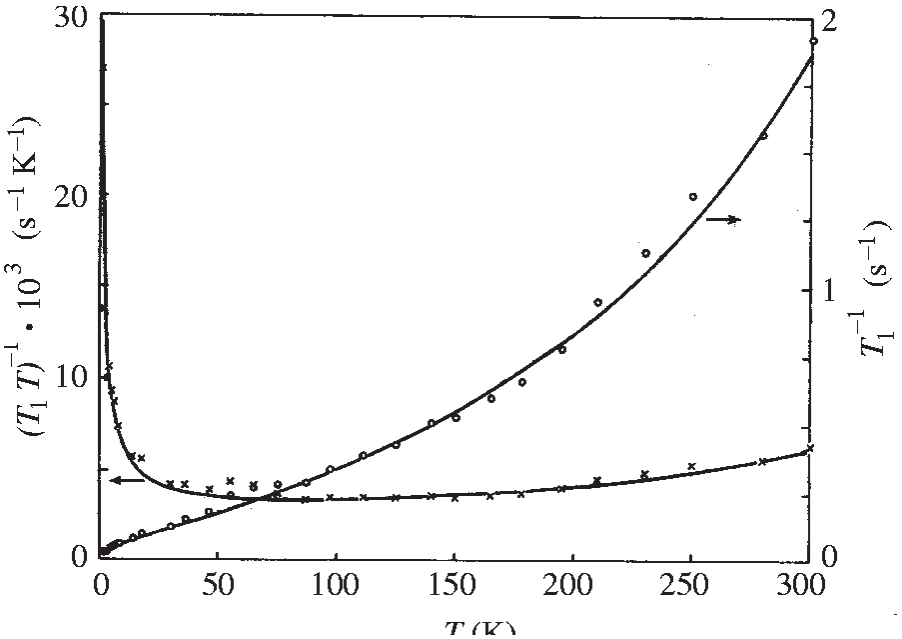

Figure 3.2: The NMR relaxation rate in TTF[Ni(dmit)$_2$]$_2$ as a function of temperature. The continuous line is the Tomonaga-Luttinger liquid theory prediction. After [111].

$K_\rho < 1/4$. Other signatures of a one-dimensional physics in organic conductors are the behavior of Nuclear Magnetic Resonance (NMR) relaxation rate[108] and the conductivity along the chains[109, 110]. In NMR, the relaxation rate T_1 is given by:

$$\frac{1}{T_1} = \lim_{\omega \to 0} \int \frac{dq}{2\pi} \frac{k_B T}{\omega} \mathrm{Im}\chi^{+-}(q,\omega), \tag{3.2}$$

where χ^{+-} is the response function:

$$\chi^{+-}(q,\omega) = i \int dx \int_0^{+\infty} \langle [S^+(x,t), S^-(0,0)] \rangle e^{i[qx-(\omega+i0)t]}. \tag{3.3}$$

Using Eqs.(1.112), one finds that the $2k_F$ component of the spin-density gives a contribution $\propto T^{K_\rho}$ which is dominant for $K_\rho < 1$. In the organic conductor TTF[Ni(dmit)$_2$]$_2$, such a power-law behavior has been observed for 1K $< T <$ 300K.[111] In the Fabre salts, the charge degree of freedom localize, leading to an effective $K_\rho = 0$ in the absence of long range ordering [108]. Concerning optical conductivity, the frequency dependent conductivity can be derived from the sine-Gordon Hamiltonian describing the charge excitations and the expression of the charge current $j = \sqrt{2}\partial_t \phi_\rho / \pi$.[112, 113] For high frequency, perturbation theory gives an ac conductivity $\sigma(\omega) \sim \omega^{4n^2K_\rho - 5}$ and a d. c. resistivity $\rho(T) \sim T^{4n^2K_\rho - 3}$ with $n = 1$ in the case of a half-filled umklapp, and $n = 2$ in the case of a quarter filled umklapp. By comparing measurements at high frequency with the prediction from perturbation theory, one can extract an exponent K_ρ.[109, 110] The results are compatible with an exponent $K_\rho = 0.22$ and $n = 2$.

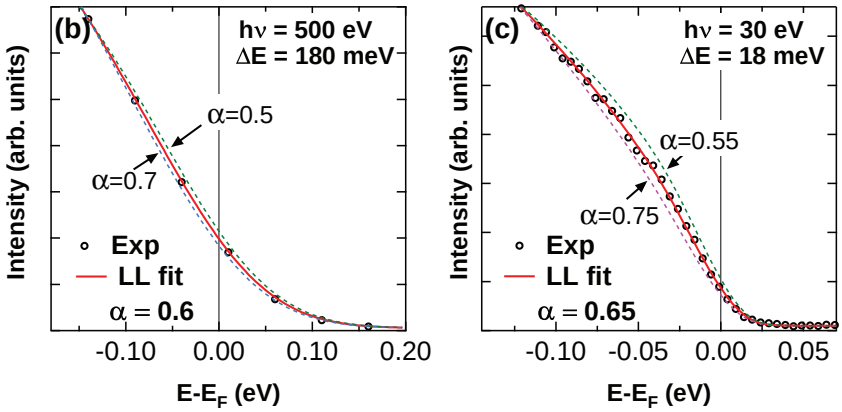

Figure 3.3: The momentum integrated spectrum in $Li_{0.9}Mo_6O_{17}$ fitted to a Luttinger liquid theory. (b) corresponds to photons of high energy and (c) to photons of low energy. The energy independence shows that the measured spectrum does not vary with the penetration of the photons in the material, and therefore corresponds to bulk states. After [116]

Measurements of dc conductivity in the direction transverse to the chains also yield a power-law dependence compatible with an exponent $K_\rho = 0.22$.[110]

3.1.3 Inorganic one-dimensional conductors

The Li purple bronze, $Li_{0.9}Mo_6O_{17}$ possesses two quasi-one dimensional bands that are crossing the Fermi energy. Photoemission studies suggest a Luttinger liquid state [114, 115, 116] The integrated photoemission spectra follow a scaling form: $I(E) = T^\alpha B[(E - E_F)/T]$ with $\alpha = 0.6$[116] This is the form that would be predicted by TLL theory with $\alpha = (K_\rho + K_\rho^{-1} - 2)/4$ and this would be in agreement with $K_\rho = 0.25$. Such behavior was confirmed by Scanning Tunneling Spectroscopy measurements[117]. However, when considering the spectral function $A(k, \omega)$, the situation is less clear. Second, the position of the spinon edges follows scaling, but not the one of the holon peaks. Second, the spectral function does not follow the scaling $A(k, \omega) = T^{\alpha-1}\bar{A}(k/T, \omega/T)$ that would be expected from TLL theory but instead scales as $T^\alpha \bar{A}(k/T, \omega/T)$.[114]

To conclude that section, although some evidence for TLL properties exist in quasi-1D conductors, interchain couplings cannot be neglected. In order to find stronger evidence of TLL properties, one has to turn to artificial structures such as nanotubes or nanowires which can be studied in isolation. Another possibility is to turn to systems made of weakly coupled spin chains. In such systems, isolated chains only carry a single-component Luttinger liquid, which is less complicated to characterize. A third route is to consider ultracold atomic gases, trapped in a quasi-one dimensional geometry. Below the degeneracy temperature, these systems can be expected to exhibit TLL features. Moreover, by working with bosons instead of fermions, one can obtain a single-component TLL.

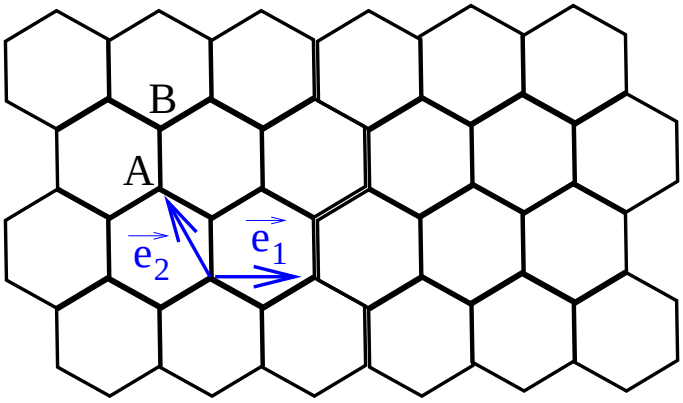

Figure 3.4: The two-dimensional honeycomb lattice, with the inequivalent A and B sites. $\mathbf{e}_{1,2}$ are the basis vectors of the translation group that leaves the honeycomb lattice invariant.

3.2 Carbon nanotubes

Carbon nanotubes[118] have a 1D structure, made of a graphene sheet rolled into a cylinder. For nanotubes of not too small radius, the overlap of the p^z orbitals is not too strongly modified by the curvature of the nanotube, and the band structure can be understood from that of a two-dimensional nearest-neighbor tight-binding model on a honeycomb lattice as represented on Fig. 3.4. The Hamiltonian reads:

$$H = -t \sum_{\langle i,j \rangle} (c^\dagger_{i,A,\sigma} c_{j,B,\sigma} + \text{H.c.}) \tag{3.4}$$

giving a dispersion $E_\pm(\mathbf{k}) = \pm t\sqrt{1 + 2\cos(k_x/2)\cos(\sqrt{3}k_y/2) + 4\cos^2(k_x/2)}$. There are two non-equivalent points $\mathbf{K}, -\mathbf{K}$ in reciprocal space for which $E_\pm(k)$ is vanishing. However, since the graphene sheet is rolled into a cylinder, not all wavevectors are allowed. If the position $\mathbf{R}_i$ and the position $\mathbf{R}_i + n\mathbf{e}_1 + m\mathbf{e}_2$ are identified, the wavevector $\mathbf{k}$ will have to satisfy the condition $\mathbf{k} \cdot (n\mathbf{e}_1 + m\mathbf{e}_2) \in 2\pi\mathbb{Z}$. Such a condition constrains the allowed wavevectors to remain on parallel lines. If these lines intersect the points $\mathbf{K}$ and $-\mathbf{K}$ the nanotube will be metallic, otherwise it will be semiconducting. The condition to have a metallic nanotube is that $(n + m) \in 3\mathbb{Z}$. In armchair nanotubes, with $n = 2m$ this condition is always satisfied. In zigzag nanotubes, with $m = 0$, the condition is satisfied when $n \in 3\mathbb{Z}$.

In the above picture, interactions have been completely neglected. Wen interactions are taken into account, conducting carbon nanotubes are expected to show TLL features[119, 120, 121]. The advantage of carbon nanotubes over organic conductors for the observation of TLL physics is that it is possible to probe a single nanotube and avoid interchain coupling effects. Evidence for TLL behavior comes from tunneling conductivity measurements[122], photoemission[123], STM[124] and NMR[125] experiments. Theoretical consideration of tunneling from a Fermi liquid into a Luttinger liquid lead to the prediction[126] that the tunnel

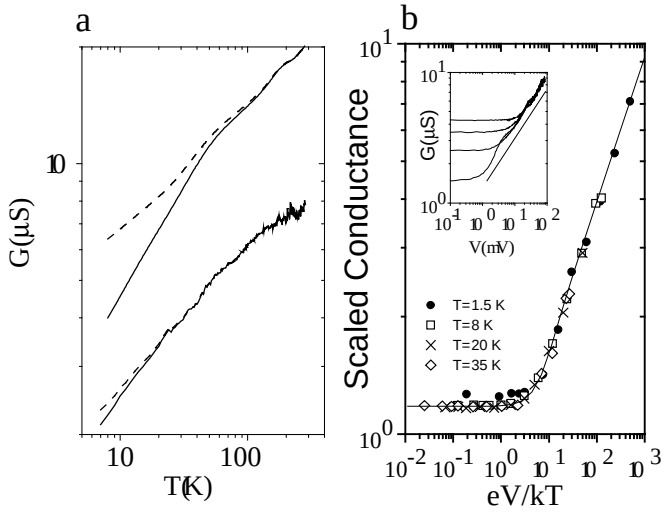

Figure 3.5: Tunnel conductance in carbon nanotubes. (a) plot of the tunnel conductance as a function of temperature on a logarithmic scale. (b) Plot of the conductance scaled according to (3.5) as a function of eV/k_BT for different values of temperature. The collapse is an indication of Tomonaga-Luttinger liquid behavior. After Bockrath et al. [122]

current behaves as:

$$I = I_0 T^{1+\alpha} \sinh\left(\frac{V}{2T}\right) \left|\Gamma\left(1+\frac{\alpha}{2}+i\frac{V}{2\pi T}\right)\right|^2, \tag{3.5}$$

where I_0 is a non-universal prefactor, and $\alpha = (K_\rho + 1/K_\rho - 2)/8$ for tunneling in the bulk of the nanotube, $\alpha = (1/K_\rho - 1)/4$ for tunneling at the tip of the nanotube. Eq.(3.5) show that the tunneling current satisfies scaling as a function of V/T. Such scaling has been observed in experiments on metallic carbon nanotubes[122]. The results are compatible with $K_\rho = 0.2$.

ARPES measurements have also been performed on carbon nanotubes[123]. The results are also compatible with a TLL state with an exponent $K_\rho = 0.28$. figure 3.6.

STM measurements of carbon nanotubes[124] on a gold surface are also compatible with a Luttinger liquid state but with $K_\rho = 0.55$. The difference with the measurements performed on insulating substrates could be explained by a better screening of Coulomb interaction in the nanotube by the metallic substrate.

3.3 spin-1/2 chains

In spin-1/2 chains, measurements of magnetic susceptibility in Sr_2CuO_3 have shown[127] that for low temperature, the susceptibility exhibited logarithmic corrections as predicted by (2.19). In the spin-1/2 chain material $KCuF_3$, the dynamical structure factor has been measured by neutron scattering.[129, 130, 131] From Eq.(1.56), the magnetic structure factor of a Luttinger liquid can be predicted. For temperature sufficiently high, to avoid three-dimensional effects, the TLL behavior has been obtained.

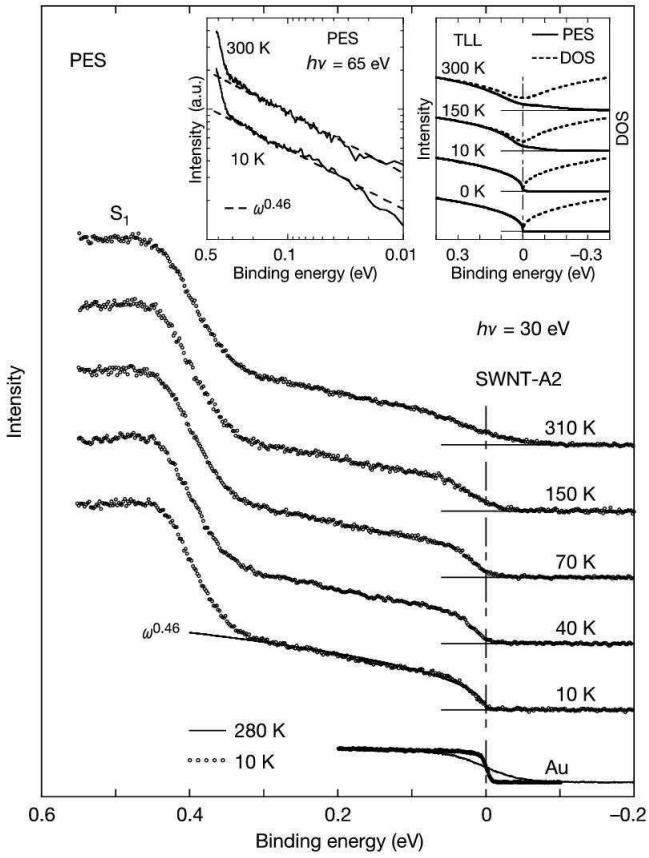

Figure 3.6: Photoemission spectroscopy measurements on Carbon nanotubes bundles with energy $h\nu$ =30 meV and energy resolution of 13 meV. The solid line $\omega^{0.46}$ represents the spectral function $A(\omega) \sim \omega^{(K_\rho+1/K_\rho-2)/4}$ broadened by the instrumental resolution. Left inset: photoemission spectra with energy $h\nu$ =65 meV and resolution 15 meV on logarithmic scale. Right panel: After Ishii et al.[123].

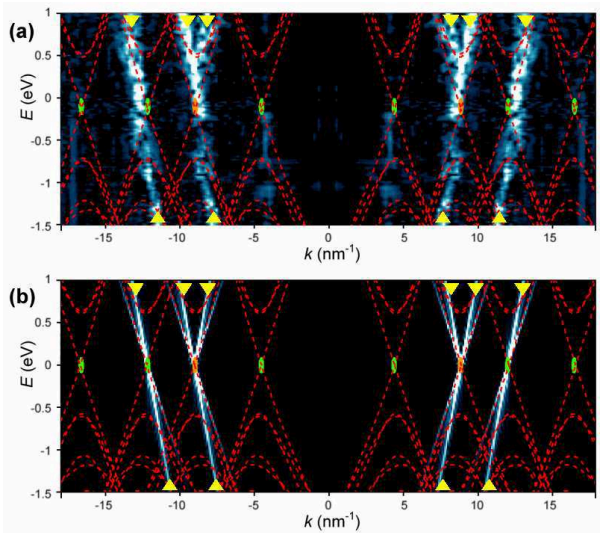

Figure 3.7: Oscillations of the local density of states in a Carbon nanotube. After [124]

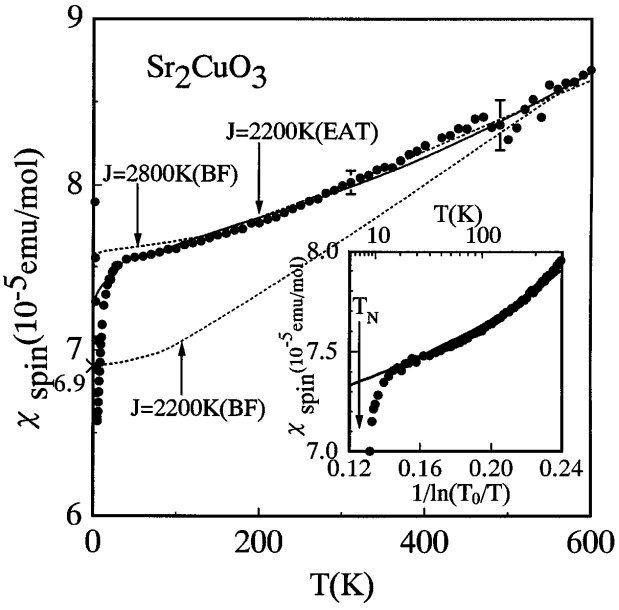

Figure 3.8: The magnetic susceptibility in Sr_2CuO_3 for temperatures below 600 K compared with the Bonner-Fisher approximation[128] for $J = 2200$ K and $J = 2800$ K (dotted lines) and the Eggert-Affleck-Takahashi theory[70] (solid line). Inset: magnetic susceptibility versus $1/\ln(T_0/T)$ dots: experiment, solid line: theory. After [127].

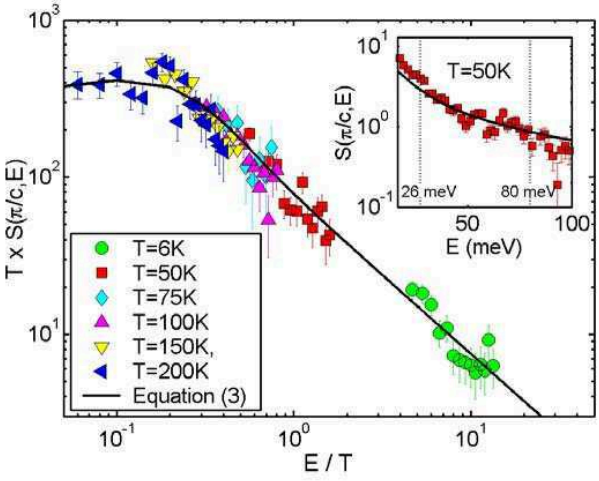

Figure 3.9: Structure factor at $k = \pi/c$ in the spin-1/2 chain material $KCuF_3$. The solid line is the Luttinger liquid theory prediction. After [132]

Copper pyrazine dinitrate is a good realization of a spin-1/2 chain with exchange constant $J \simeq 0.91meV$. It remains disordered for $T > 0.1$ K, indicating that the interchain coupling is less than $10^{-4}J$. It has been possible to measure the behavior of the magnetization and the specific heat under applied field[133] and compare with the predictions of the Bethe Ansatz for the spin-1/2 chain. Moreover, neutron scattering measurements have also confirmed[133, 134] that the dynamical structure factor was in good agreement with a spin-1/2 chain model.

3.4 Cold atomic gases

Using optical and/or magnetic cooling and trapping technologies, it is possible to obtain gases of bosonic or fermionic atoms at temperature well below the degeneracy temperature. In optical traps, the trapping potential can be engineered to create quasi-one dimensional structures[135, 136, 137], and interactions can be modulated by a magnetic field using Feshbach resonances.[138, 139] One-dimensional gases of hard core bosons have been realized experimentally with optical trapping.[140, 141, 142] The thermodynamic measurements[141] such as the temperature and the size of the cloud as a function of interaction are in agreement with the Lieb-Liniger theory[29] as shown on Figs. 3.10 and 3.11. By superimposing a periodic lattice[140] in the longitudinal direction, it is possible to further increase the effective mass an enhance the effect of interactions. The momentum distribution is also in agreement with the prediction of a model of hard core bosons in a harmonic potential as shown on Fig. 3.12.

Using magnetic trapping, it is possible to trap atoms in the vicinity of a thin wire, and realize a quasi-one dimensional system.[143] In such systems, Feshbach resonances cannot be used for modulating interaction strength, nevertheless it has been possible to check that the Lieb-Liniger equation of state gave a good description of the thermodynamics of a trapped one-dimensional

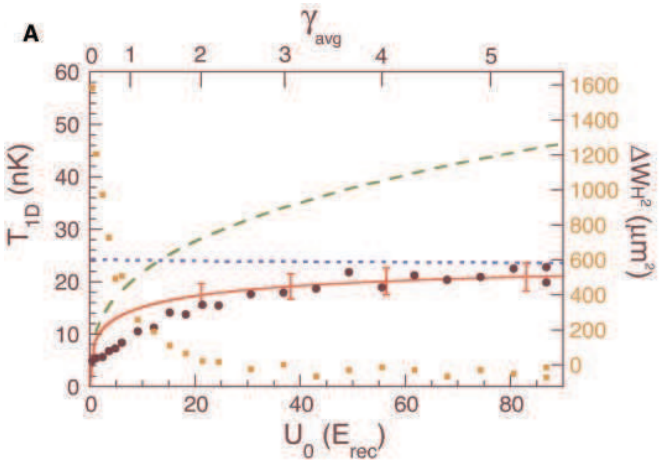

Figure 3.10: The one-dimensional temperature of a trapped gas as a function of transverse confinement U_0 measured in units of the recoil energy E_{rec}. For $U_0 \geq 20E_{\text{rec}}$, the system can be considered one dimensional with negligible intertube interaction. The circles represent experimental data. The solid line is the exact Lieb-Liniger gas theory, with error bars to account for uncertainty in the determination of experimental parameters. The short dashed line represent the hard core boson theoretical result. The long dashed line the mean field theory. After [141]

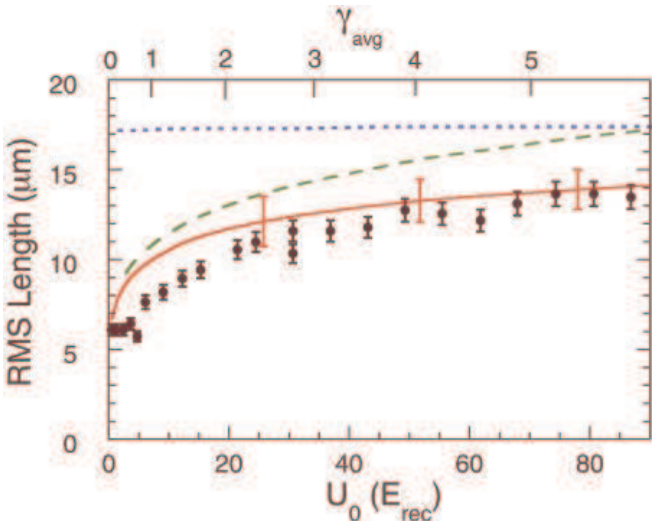

Figure 3.11: The RMS length of a trapped gas as a function of transverse confinement U_0. The solid line is the Lieb-Liniger theory, with error bars coming from uncertainty on experimental parameters. The short dashed line is the hard core boson result, and the long dashed line the mean field theory. After [141]

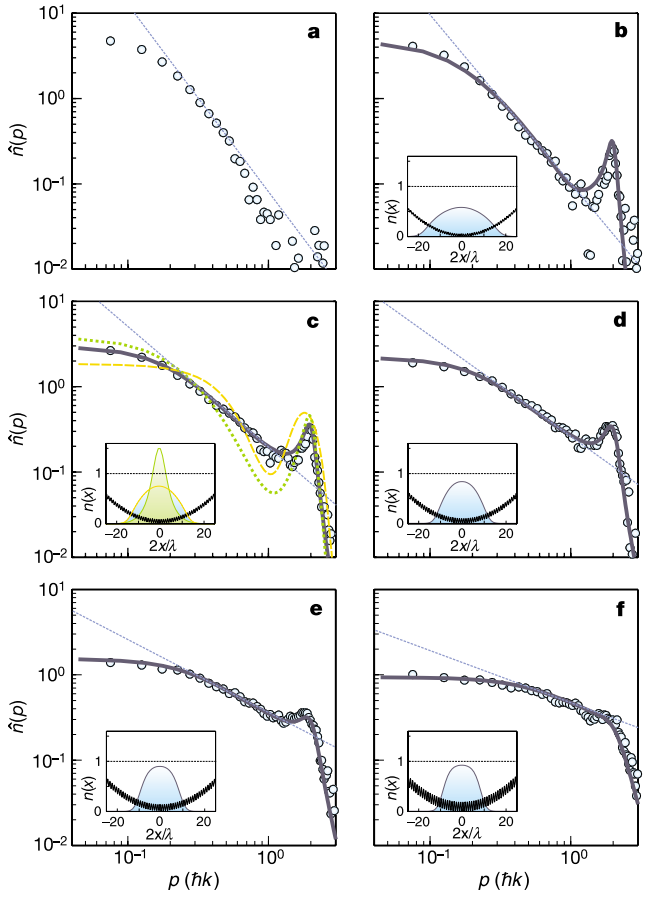

Figure 3.12: The momentum distribution in an array of trapped atomic gases in double logarithmic scale. The circles are experimental data, the thick solid line is the theoretical result for a gas of hard core bosons in a harmonic potential. The thin solid line materializes the $n(p) \sim p^{\alpha}$ behavior of the momentum distribution. From (b) to (f), the axial lattice depth $V_{\rm ax}/E_{\rm rec}$, the temperature T/J, the exponent α of $n(p) \sim p^{-\alpha}$ and the interaction parameter $\gamma = U/J$ are: (b) 4.6, 0.5,1.9, 5.5 (c) 7.4,0.7,1.4,13.7 (d) 9.3, 0.9, 1.2, 23.6 (e) 12, 1.3,0.8,47.6 (f) 18.5, 3.9, 0.6, 204.5. For (a) there is no superimposed periodic potential in the longitudinal direction, and $\alpha = 2.2$ and $\gamma = 0.5$. After [140]

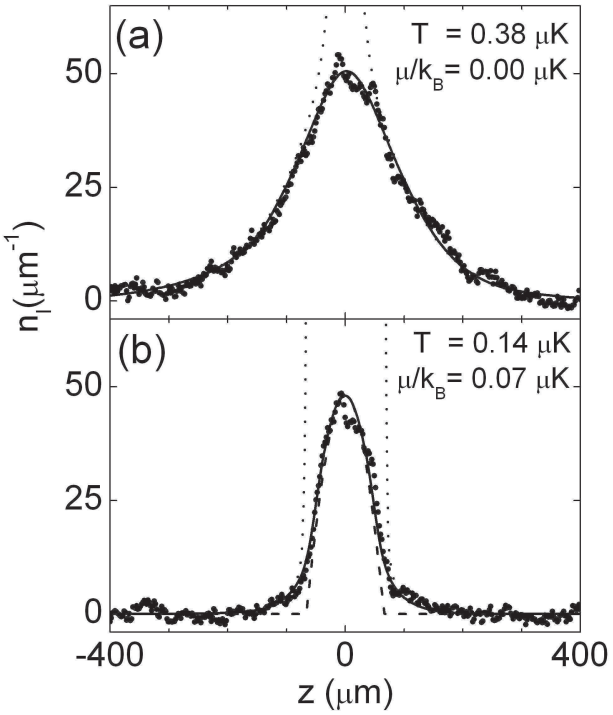

Figure 3.13: The density profile of an on-chip Bose gas. The continuous lines are computed from the Thermodynamic Bethe Ansatz applied to the Lieb-Liniger gas, while the dotted lines correspond to an ideal Bose gas. The dashed line in (b) corresponds to a quasi-condensate having the same peak density as the experimental data. The transverse confinement frequency $\omega_\perp = 158$nK. After [144]

gas.[144] More precisely, assuming that bosons in the ground state of the radial trapping form a Lieb-Liniger gas, whose density profile can be obtained from the Thermodynamic Bethe Ansatz, while the bosons in the excited states of the radial trapping are forming an ideal gas, and adding together the densities of each component, it is possible to fit accurately the density profile of the 1D boson gas trapped on a chip, as can be seen on the Figure 3.13.

In [145], the effect of a periodic potential on a one-dimensional Bose gas was measured. In the presence of a commensurate potential, $V(x) = V_0 \cos(2\pi\rho_0 x)$, from Eq. (1.87), the low energy excitations are described by the sine-Gordon model[107]. For $K < 2$, the cosine term is irrelevant, and the Tomonaga-Luttinger liquid state is stable in the presence of a weak potential. As the strength of the potential is increased, a BKT phase transition to the gapful Mott state is observed. The measurements in [145] are in agreement with the formation of a Mott state when the commensurate periodic potential exceeds a critical value that depends on interaction strength. For $K < 2$ which corresponds to a Lieb-Liniger parameter $\gamma > 3.5$, a small lattice potential immediately opens a gap as represented on Fig. 3.14.

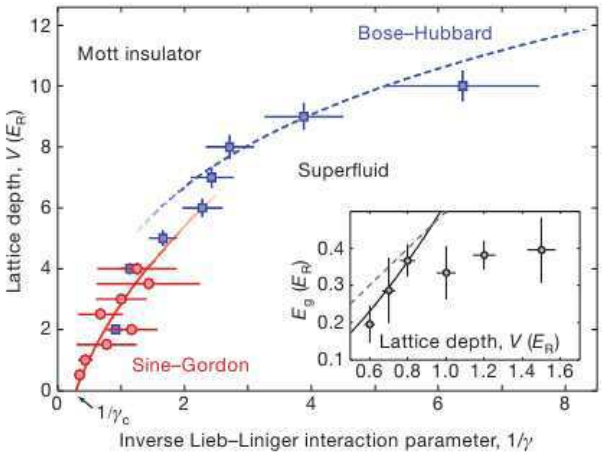

Figure 3.14: The phase diagram of a Bose gas under a periodic potential in the plane of lattice depth V_0 and inverse Lieb-Liniger parameter. The solid line is the prediction from the sine-Gordon theory, while the dashed line is from the Bose-Hubbard model[146]. For strong interaction and weak lattice depth, the sine-Gordon model describes the phase transition. The inset shows the behavior of the gap as a function of the lattice depth. The solid line is the prediction from the sine-Gordon model (2.54), and the dashed line the result for free fermions. After [145]

Part II

Quantum magnetism

Chapter 4

the two-leg ladder

The present chapter is based on the articles[147, 148, 149, 150, 151].

The two-leg ladder model (see Fig. 4.1) is a system made of a pair of exchange coupled antiferromagnetic spin chains, with Hamiltonian:

$$
\begin{aligned}
H &= H_1 + H_2 + H_{interchain} && (4.1)\\
H_p &= \sum_n J(S^x_{n,p}S^x_{n+1,p} + S^y_{n,p}S^y_{n+1,p}) + J_z S^z_{n,p}S^z_{n+1,p} && (4.2)\\
H_{interchain} &= \sum_n J_\perp(S^x_{n,1}S^x_{i,2} + S^y_{n,1}S^y_{n,2}) + J^z_\perp S^z_{n,1}S^z_{n,2} && (4.3)\\
&\quad + \sum_n J'_\perp(S^x_{n,1}S^x_{n+1,2} + S^y_{n,1}S^y_{n+1,2}) + J'^z_\perp S^z_{n,1}S^z_{n+1,2} && (4.4)\\
&\quad + \sum_n J"_\perp(S^x_{n,1}S^x_{n-1,2} + S^y_{n,1}S^y_{n-1,2}) + J''^z_\perp S^z_{n,1}S^z_{n-1,2} && (4.5)
\end{aligned}
$$

The ladder model is known to possess a spin gap[152]. This is most easily understood in the limit of $J'_\perp = J"_\perp = 0$, $J_\perp \gg J > 0$. In that limit, the ground state is given by a spin singlet on each rung, and excited states are formed by a band of triplet excitations with dispersion $J_\perp - J\cos k$. In the limit of $J'_\perp = J"_\perp = 0$ and $J_\perp \to -\infty$, the ladder model becomes equivalent to an antiferromagnetic spin-1 chain which is also known to possess a spin gap[153]. Using bosonization, it is possible to show that in the limit of $|J_\perp|, |J'_\perp|, |J"_\perp| \ll J$, a spin gap is formed[154, 155, 156]

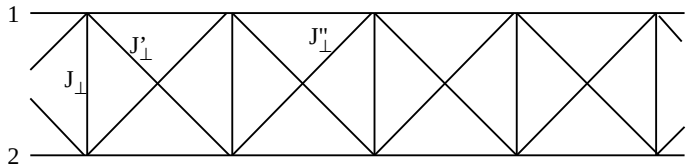

Figure 4.1: The interchain exchange interactions in the two-leg ladder. The couplings $J_\perp$ are along the vertical, while $J'_\perp$ and $J"_\perp$ are along the diagonals.

4.1 Bosonization

4.1.1 General case

Starting from the boson representation of the single chain, and using Eqs. (1.66)–(1.67) one obtains[154, 155, 156] the following bosonized representation of the two-leg ladder model:

$$H_p = \int \frac{dx}{2\pi}\left[u_p K_p(\pi\Pi_p)^2 + \frac{u_p}{K_p}(\partial_x\phi_p)^2\right] - \frac{2\Delta_p}{(2\pi\alpha)^2}\int dx\cos 4\phi_p \tag{4.6}$$

$$\begin{aligned} H_{interchain} &= \int\left[\frac{2g_1}{(2\pi a)^2}\cos(\theta_1-\theta_2) + \frac{2g_2}{(2\pi a)^2}\cos 2(\phi_1-\phi_2) + \frac{2g_3}{(2\pi a)^2}\cos 2(\phi_1+\phi_2)\right]dx \\ &\quad + J_\perp^z a\int dx\frac{\partial_x\phi_1\partial_x\phi_2}{\pi^2} \end{aligned} \tag{4.7}$$

Near the XY symmetric point, the coupling constants are given by:

$$\begin{aligned} g_1 &= \pi(J_\perp - J'_\perp - J"_\perp)a \\ g_2 &= (J_\perp^z - J_\perp'^z - J_\perp''^z)a \\ g_3 &= (J_\perp^z - J_\perp'^z - J_\perp''^z)a \end{aligned} \tag{4.8}$$

More generally, the amplitudes are renormalized by interactions. It is convenient to rewrite the Hamiltonian in terms of the fields:

$$\phi_a = \frac{\phi_1-\phi_2}{\sqrt{2}}, \phi_s = \frac{\phi_1+\phi_2}{\sqrt{2}} \tag{4.9}$$

which yields:

$$\begin{aligned} H &= H_s + H_a \\ H_a &= \int\frac{dx}{2\pi}\left[u_a K_a(\pi\Pi_a)^2 + \frac{u_a}{K_a}(\partial_x\phi_a)^2\right] \\ &\quad + \frac{2g_3}{(2\pi\alpha)^2}\int dx\cos(\sqrt{8}\phi_a) + \frac{2g_1}{(2\pi\alpha)^2}\int dx\cos(\sqrt{2}\theta_a) \\ H_s &= \int\frac{dx}{2\pi}\left[u_s K_s(\pi\Pi_s)^2 + \frac{u_s}{K_s}(\partial_x\phi_s)^2\right] \\ &+ \frac{2g_2}{(2\pi\alpha)^2}\int dx\cos(\sqrt{8}\phi_s) \end{aligned} \tag{4.10}$$

Where:

$$\begin{aligned} u_s &= u\left(1+\frac{KJ_\perp^z a}{2\pi u}\right), K_s = K\left(1-\frac{KJ_\perp^z a}{2\pi u}\right) \\ u_a &= u\left(1-\frac{KJ_\perp^z a}{2\pi u}\right), K_a = K\left(1+\frac{KJ_\perp^z a}{2\pi u}\right) \end{aligned} \tag{4.11}$$

It is worthwhile to note that the Hamiltonian 4.10 was obtained previously in a bosonization study of the spin-1 chain[23], in which the spin-1 operators were represented as a symmetric combination of spins-1/2. That result hints that spin-1 chains and two-leg ladders should present similar physical properties at low energy.

The phase diagram can be obtained from the self-consistent harmonic approximation[154] or the renormalization group[156]. For $K_s < 1$, the field ϕ_s becomes long range ordered, and the Hamiltonian H_s has a gap in its excitation spectrum. In the Hamiltonian H_a as discussed in [155, 156] at least one of the operators is relevant so that the Hamiltonian is always gapped. Two phases are possible, one with ϕ_a long range ordered, and the other with θ_a long range ordered. The different regimes are represented on the tables4.1 and 4.2 . The phases are named according to the terminology of the paper by H. J. Schulz[157]. In the phase called $XY1$ the correlations of $S_1^+ - \mathrm{sign}(J_\perp)S_2^+$ are quasi-long range ordered. In the phase called $XY2$, the correlations of $S_1^z - \mathrm{sign}(J_\perp^z)S_2^z$ are long range ordered. In the singlet phase and the Haldane gap phase, all the local operators have only short range order correlations. It is possible however to construct a non-local order parameter[158] for these phases analogous to the VBS order parameter[159, 160, 161] of the spin-1 chain. We will consider first the case of $J_\perp - J'_\perp - J"_\perp < 0$, where the Haldane gap phase is expected. The VBS order parameter $\mathcal{C}$ is a nonlocal order parameter defined for a spin-1 chain as:

$$\mathcal{C} = \lim_{|k-j|\to\infty} \langle S_k^z \exp(i\pi \sum_{k<n<j} S_n^z) S_j^z \rangle \tag{4.12}$$

In the Haldane gap phase, all the spin-spin correlation functions decay exponentially but $\mathcal{C} \neq 0$. A non-zero VBS order parameter indicates that if all the sites where $S_n^z = 0$ are removed from a spin-1 antiferromagnetic chain the remaining ("squeezed") chain has antiferromagnetic order. For our ladder system, the VBS order parameter takes the form[162, 147]:

$$O_{\mathrm{odd}} = \lim_{|k-j|\to\infty} \langle (S_{k,1}^z + S_{k,2}^z) \exp\left[i\pi \sum_{k<n<j} (S_{n,1} + S_{n,2}^z) \right] (S_{j,1}^z + S_{j,2}^z) \rangle \tag{4.13}$$

To derive a representation of the string operator, we first use the identity: $\exp(i\pi(S_1^z + S_2^z)) = -\exp(i\pi(S_1^z - S_2^z))$, yielding:

$$\prod_{k<n<j} \exp(i\pi(S_1^z + S_2^z)) = (-)^{j-k-1} \exp(\sum_{k<n<j} i\pi(S_1^z - S_2^z)), \tag{4.14}$$

which is straightforwardly bosonized in the form $(-)^{k-j} \cos\sqrt{2}(\phi_a(ka) - \phi_a(ja))$. Using the bosonized expression of $S_1^z + S_2^z = S^z$, the VBS order parameter is obtained in the form:

$$O_{\mathrm{odd}} \propto \lim_{|x-y|\to\infty} \langle \cos\sqrt{2}\phi_s(x) \cos\sqrt{2}\phi_s(y) \rangle = (\langle \cos\sqrt{2}\phi_s \rangle)^2 \tag{4.15}$$

Since in the Haldane gap phase, $\langle \phi_s \rangle = 0$ (see table 4.1) the VBS order parameter is non-zero. Turning to the case of $J_\perp - J'_\perp - J"_\perp > 0$, we have to consider another VBS-like order

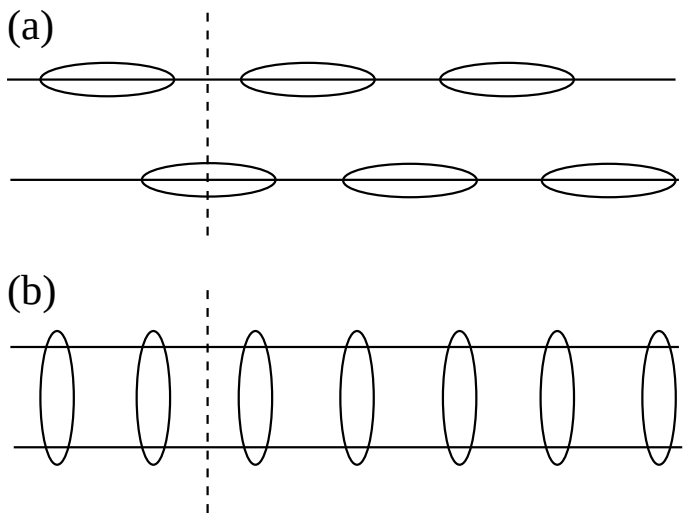

Figure 4.2: A schematic view of (a) the AKLT picture of the Haldane gap phase, and (b) the singlet phase of the two leg ladder. In the Haldane gap phase (a), the dashed line encounters one singlet, while in the singlet phase it does not encounter any singlet.

parameter:

$$O_{\text{even}} = \lim_{|i-j|\to\infty} \langle (S^z_{i,1} - S^z_{i,2}) \exp\left[i\pi \sum_{i<n<j} (S_{n,1} + S^z_{n,2}) \right] (S^z_{j,1} - S^z_{j,2}) \rangle, \tag{4.16}$$

which we can express as:

$$O_{\text{even}} \propto \lim_{|x-y|\to\infty} \langle \sin\sqrt{2}\phi_s(x) \sin\sqrt{2}\phi_s(y) \rangle = (\langle \sin\sqrt{2}\phi_s \rangle)^2 \tag{4.17}$$

In the singlet phase, $\langle \phi_s \rangle = \pi/\sqrt{8}$ (see table 4.2) the even VBS order parameter is non-zero. The two order parameters are mutually exclusive indicating that the singlet phase and the Haldane gap phase are distinct. The difference between the two phases is topological. In the AKLT picture[163, 164], a spin-1 is represented as a symmetric combination of two spins 1/2, and in the Haldane gap phase, the spins 1/2 are paired as singlets along the chain direction (see figure 4.2 (a)). By contrast, in the singlet phase the spins 1/2 are paired along the rung direction figure 4.2 (a)). These two valence-bond crystal states are therefore associated to two topologically non-equivalent dimer coverings of the two leg ladder. In the Haldane gap phase, a vertical line will encounter an odd number of dimers, while in the singlet phase a vertical line will encounter an even number of dimers.

4.1.2 Isotropic case

In the isotropic case, it is possible to make a more detailed analysis of the Hamiltonian 4.10. Indeed, the isotropic case corresponds to $K_1 = K_2 = 1/2$ with the terms $\cos 4\phi_{1,2}$ marginally irrelevant. If, in a first approximation (which becomes exact when $J_\perp + J'_\perp + J"_\perp = 0$), we neglect

	I	II	III	IV
K_s K_a	< 1 $< 1/2$	< 1 $> 1/2$	> 1 $< 1/2$	> 1 $> 1/2$
ϕ_s	$\langle\phi_s\rangle = 0$	$\langle\phi_s\rangle = 0$	critical	critical
θ_a, ϕ_a	$\langle\phi_a\rangle = 0$	$\langle\theta_a\rangle = 0$	$\langle\phi_a\rangle = 0$	$\langle\theta_a\rangle = 0$
phase	Ising AF	Haldane gap	$XY2$	$XY1$
Order parameter	$\cos(\sqrt{2}\phi_s)\cos(\sqrt{2}\phi_a)$	VBS-like	$e^{\imath\sqrt{2}\theta_s}$	$e^{\imath\frac{\theta_s}{\sqrt{2}}}\cos(\frac{\theta_a}{\sqrt{2}})$

Table 4.1: The four sectors of the phase diagram of a two leg ladder with ferromagnetic rung coupling

	I	II	III	IV
K_s K_a	< 1 $< 1/2$	< 1 $> 1/2$	> 1 $< 1/2$	> 1 $> 1/2$
ϕ_s	$\langle\phi_s\rangle = \frac{\pi}{\sqrt{8}}$	$\langle\phi_s\rangle = \frac{\pi}{\sqrt{8}}$	critical	critical
θ_a, ϕ_a	$\langle\phi_a\rangle = \frac{\pi}{\sqrt{8}}$	$\langle\theta_a\rangle = \frac{\pi}{\sqrt{2}}$	$\langle\phi_a\rangle = \frac{\pi}{\sqrt{8}}$	$\langle\theta_a\rangle = \frac{\pi}{\sqrt{2}}$
phase	Ising AF	singlet	$XY2$	$XY1$
Order parameter	$\sin(\sqrt{2}\phi_s)\sin(\sqrt{2}\phi_a)$	VBS-like	$e^{\imath\sqrt{2}\theta_s}$	$e^{\imath\frac{\theta_s}{\sqrt{2}}}\sin(\frac{\theta_a}{\sqrt{2}})$

Table 4.2: The four sectors of the phase diagram of a 2 leg ladder with antiferromagnetic rung coupling.

all the marginal operators in the Hamiltonian 4.10 we can make the rescaling $\phi_a \to \phi_a/\sqrt{2}$, $\theta_a \to \sqrt{2}\theta_a$ and fermionize the resulting Hamiltonian[162]. It is convenient to rewrite the Hamiltonian using a Majorana fermion representation:[1]

$$H = -i\frac{u}{2}\sum_{\substack{a=0\\r=\pm}}^{2}\int dx r\zeta_{r,a}\partial_x\zeta_{r,a} \tag{4.18}$$

$$+im\int dx\left(\sum_{a=1}^{3}\zeta_{a,+}\zeta_{a,-} - 3\zeta_{0,+}\zeta_{0,-}\right), \tag{4.19}$$

showing that the spectrum consists of a triplet of Majorana fermions of mass m and a singlet Majorana fermion of mass $-3m$. Moreover, using the relation between massive Majorana fermions and the Ising model, a representation of the spin-operators can be derived.[162] If one writes: $\mathbf{S}_{n,p} = \mathbf{J}_p(x) + (-)^n\mathbf{n}(x)$, then one has:

$$M_x = n_1^x + n_2^x = \lambda\sigma_1\mu_2\sigma_3\sigma_0 \tag{4.20}$$
$$M_y = n_1^y + n_2^y = \lambda\mu_1\sigma_2\sigma_3\sigma_0 \tag{4.21}$$
$$M_z = n_1^z + n_2^z = \lambda\sigma_1\sigma_2\mu_3\sigma_0 \tag{4.22}$$
$$m_x = n_1^x - n_2^x = \lambda\mu_1\sigma_2\mu_3\mu_0 \tag{4.23}$$
$$m_y = n_1^y - n_2^y = \lambda\sigma_1\mu_2\mu_3\mu_0 \tag{4.24}$$
$$m_z = n_1^z - n_2^z = \lambda\mu_1\mu_2\sigma_3\mu_0 \tag{4.25}$$

Using the results of[74], this allows the calculation of zero temperature correlation functions in terms of Painlevé III functions. The results of such computations are in good agreement with numerical work[166]. The uniform component of the magnetization can be directly expressed in terms of the Majorana fermion operators as:

$$J_1^x + J_2^x = \frac{i}{2}(\zeta_{+,2}\zeta_{+,3} + \zeta_{-,2}\zeta_{-,3}) \tag{4.26}$$
$$J_1^y + J_2^y = \frac{i}{2}(\zeta_{+,3}\zeta_{+,1} + \zeta_{-,3}\zeta_{-,1}) \tag{4.27}$$
$$J_1^y + J_2^y = \frac{i}{2}(\zeta_{+,1}\zeta_{+,2} + \zeta_{-,1}\zeta_{-,3}) \tag{4.28}$$
$$J_1^x - J_2^x = \frac{i}{2}(\zeta_{+,0}\zeta_{+,1} + \zeta_{-,0}\zeta_{-,1}) \tag{4.29}$$
$$J_1^y - J_2^y = \frac{i}{2}(\zeta_{+,0}\zeta_{+,2} + \zeta_{-,0}\zeta_{-,2}) \tag{4.30}$$
$$J_1^z - J_2^z = \frac{i}{2}(\zeta_{+,0}\zeta_{+,3} + \zeta_{-,0}\zeta_{-,3}) \tag{4.31}$$

[1] This technique is also applicable in the presence of biquadratic spin-spin interaction[165].

4.2 Semi-infinite ladder

In the case of the semi-infinite spin-1 chain, it has been shown, by considering the topological term in the path integral representation,[167] that in the Haldane gap phase, spin-1/2 edge states would be obtained. A simple picture of this result can be obtained by considering the AKLT ground state: cutting the chain anywhere will necessarily cut a dimer a leave one free spin-1/2. The same question can be asked in the case of the two-leg ladder, i. e. whether a semi-infinite ladder will present edge states. In fact, the edge states are only obtained[149] when the ladder is in the Haldane gap state with $O_{\text{odd}} \neq 0$. To discuss that result, we first need to consider the case of a spin-1/2 chain with open boundary conditions.[168, 169]

4.2.1 Open boundary conditions in a spin-1/2 chain

Let us first consider the spin-1/2 chain with open boundary conditions in the XY limit. The Hamiltonian reads:

$$H = J\sum_{n=1}^{+\infty}(S_n^+ S_{n+1}^- + S_n^- S_{n+1}^+), \tag{4.32}$$

and becomes, after the Jordan-Wigner transformation (1.57):

$$J = -J\sum_{n=1}^{+\infty}(c_n^\dagger c_{n+1} + c_{n+1}^\dagger c_n), \tag{4.33}$$

giving the eigenvalue equations:

$$\begin{aligned} Ec_n &= -J(c_{n+1} + c_{n-1}), (n \geq 2) && (4.34)\\ Ec_1 &= -Jc_2, && (4.35) \end{aligned}$$

These equations can be reduced to a single equation by introducing a fictitious site 0 such that $c_0 = 0$. The Hamiltonian (4.33) is then diagonalized by introducing:

$$\begin{aligned} c_n &= \sqrt{\frac{2}{N}}\sum_{k>0} c_k \sin(kn), && (4.36)\\ H &= \sum_{k>0}\epsilon(k)c_k^\dagger c_k. && (4.37) \end{aligned}$$

Taking the continuum limit of that Hamiltonian, we find:

$$\begin{aligned} \frac{c_n}{\sqrt{a}} &= e^{i\frac{\pi}{2}n}\psi_+(na) - e^{-i\frac{\pi}{2}n}\psi_+(-na), && (4.38)\\ H &= -iv\int_{-\infty}^{\infty} dx\psi_+^\dagger \partial_x \psi_+ && (4.39) \end{aligned}$$

We notice that we can bring that representation to the same form as in the case of the infinite system simply by introducing $\psi_-(x) = -\psi_+(-x)$. In terms of the bosonized representation, the latter condition is simply $\phi_+(x) + \phi_-(-x) = \pi$. Using the equation of motions of the chiral fields, $\phi_r(x,t) = \phi_r(x - rut, 0) = \phi_r(0, t - rx/u)$ that condition can be rewritten as $\phi(0,t) = \pi/2\,\forall t$. So we see that the bosonized representation of a semi-infinite XY spin chain is obtained simply by imposing a boundary condition $\phi(0,t) = \pi/2$. Such boundary condition can be viewed as the condition that $\sin 2\phi(0,t) = 0$ i. e. that the staggered component of the magnetization (1.67) vanishes. Simultaneously, the staggered dimerization operator (1.68) takes at the edge of the chain its maximal value. In the interacting case, the boundary condition is preserved, and the general XXZ spin-1/2 chain bosonized Hamiltonian is:

$$H = \int_0^\infty \frac{dx}{2\pi}\left[uK(\pi\Pi)^2 + \frac{u}{K}(\partial_x\phi)^2\right] - \frac{2\Delta}{(2\pi\alpha)^2}\int dx\cos 4\phi \tag{4.40}$$

$$\phi(0) = \pi/2 \tag{4.41}$$

Indeed, with the boundary condition $\phi(0) = \pi/2$, we ensure that the staggered component of the magnetization vanishes on the edge, irrespective of interaction. By defining $\phi(x) = \pi/2 + \sqrt{K}\tilde{\phi}$ and $\theta(x) = \tilde{theta}(x)/\sqrt{K}$, we can transform the Hamiltonian (4.40) into a non-interacting Hamiltonian. We then find that the boundary condition $\tilde{\phi}(0,t) = 0$ is solved by introducing the chiral field $\tilde{\phi}_+(x,t) = \tilde{\phi}_+(x - ut, 0)$ and writing:

$$\tilde{\phi}(x,t) = \frac{1}{2}(\tilde{\phi}_+(x-ut) - \tilde{\phi}_+(-x-ut)); \tilde{\theta}(x,t) = -\frac{1}{2}(\tilde{\phi}_+(x-ut) + \tilde{\phi}_+(-x-ut)), \tag{4.42}$$

so that:

$$\phi(x,t) = \frac{\pi}{2} + \frac{\sqrt{K}}{2}(\tilde{\phi}_+(x-ut) - \tilde{\phi}_+(-x-ut)) \tag{4.43}$$

$$\theta(x,t) = -\frac{1}{2\sqrt{K}}(\tilde{\phi}_+(x-ut) + \tilde{\phi}_+(-x-ut)) \tag{4.44}$$

With Eq. (4.43), we find that in a semi-infinite chain, $\langle e^{i\lambda\theta(x)+\mu\phi(x)}\rangle = 0$ and $\langle e^{i\lambda\phi(x)}\rangle = e^{i\lambda\frac{\pi}{2}}[\alpha/(2x)]^{\lambda^2 K/4}$. In the absence of an external magnetic field, this leads to $\langle S_n^{x,y,z}\rangle = 0$. When a magnetic field is applied along the z direction, $k_F \neq \pi/2$ and Friedel oscillations of the magnetization appear. In the case of a spin-1/2 chain, we can turn the boundary condition $\phi(0) = \pi/2$ into the simpler boundary condition $\phi(0) = 0$ provided that we change the sign of $\sin 2\phi$ and $\cos 2\phi$ in Eqs.(1.66)– (1.68).

4.2.2 Two-leg ladder with open boundary conditions

We are now considering a semi-infinite ladder model with open boundary conditions. We can still apply bosonization, but the Hamiltonian (4.10) is now restricted to $x > 0$ with boundary conditions $\phi_s(0) = 0$ and $\phi_a(0) = 0$. The ladder can still be fermionized, but a relation now exists between the right moving and the left moving fields[149]:

$$\zeta_{+,n}(0) = \zeta_{-,n}(0), \tag{4.45}$$

for $0 \leq n \leq 3$. To find the eigenstates of the fermionized Hamiltonian, it is sufficient to consider for each n the 1D Dirac equation:

$$(-iu\sigma_3\partial_x + m_n\sigma_2)\Psi_n(x) = E\Psi_n(x), \tag{4.46}$$

where $\Psi(x)$ is a two-component column vector,

$$\Psi_n(x) = \begin{pmatrix} \zeta_{n,+} \\ \zeta_{n,-} \end{pmatrix}. \tag{4.47}$$

The general solution taking into account the boundary condition (4.45) reads:

$$\Psi_n(x,t) = \frac{1}{\sqrt{2L}} \sum_{k>0} \left\{ a_k \begin{pmatrix} \cos(kx+\theta_k) + i\sin(kx) \\ \cos(kx+\theta_k) - i\sin(kx) \end{pmatrix} e^{-i\epsilon_k t} + H.c. \right\} + \sqrt{\frac{m_n}{u}} \begin{pmatrix} 1 \\ 1 \end{pmatrix} e^{-m_n x/u}\, \theta(m_n)\, \eta_n, \tag{4.48}$$

where $\epsilon(k) = \sqrt{(uk)^2 + m^2}$, a_k is a fermion annihilation operator, $e^{i\theta_k} = (uk + im)/\epsilon(k)$, and η is a Majorana fermion operator. The Majorana fermion is present only when $m_n > 0$. As a result, in the case of a ladder with $J_\perp - J'_\perp - J''_\perp < 0$, a triplet of Majorana fermion bound states is formed near the edge, while in the opposite case, a singlet Majorana fermion bound state is formed.

In the case where a triplet of Majorana fermions is formed, since from (4.26) the uniform magnetization is:

$$\mathcal{M}_c = \int_0^\infty dx(J_{+,c} + J_{-,c}) = i\frac{\epsilon_{abc}}{2} \int dx(\zeta_{+,a}\zeta_{+,b} + \zeta_{-,a}\zeta_{-,b}), \tag{4.49}$$

after integration, a contribution to the magnetization:

$$\mathcal{M}_c = \frac{i}{2}\epsilon_{abc}\eta_a\eta_b, \tag{4.50}$$

where η_a are the Majorana fermion operators associated with the bound state. Eq. (4.50) is precisely the representation of a spin-1/2 in terms of Majorana fermion operators[170]. The presence of a spin-1/2 excitation at the edge in a ladder with ferromagnetic coupling can be understood from the limit of infinite ferromagnetic rung coupling where the ladder becomes a spin-1 chain. It is known that the spin-1 chain in the Haldane gap phase with open boundary condition possesses spin-1/2 edge modes[167]. Those edge modes can be understood from the AKLT picture[163, 164]. In that picture, each spin-1 is decomposed into two spins 1/2. The spins 1/2 are then paired with their nearest neighbors in singlets so that one of the spins is paired with a spin on the left, and the other with a spin on the right, thus leaving an infinite chain translationally invariant. It is clear in that picture that cutting the spin 1 chain anywhere, will leave a free spin-1/2 edge state.

The Majorana fermion representation also allows the calculation of the staggered magnetization and the staggered dimerization in the semi-infinite two-leg ladder. Indeed, as we have seen in Sec. 2.2.2, massive Majorana fermions on an infinite line are related with the one-dimensional

quantum Ising chain and the two-dimensional classical Ising model. In the case of a semi-infinite line, the equivalence persists, but the boundary conditions on the Majorana fermions translate into boundary conditions on the Ising degrees of freedom. Fortunately, the latter conditions are quite simple. When the Majorana fermions obey the boundary condition $\zeta_+(0) = \zeta_-(0)$, the spins σ satisfy the free boundary condition, whereas when the Majorana fermions obey $\zeta_+(0) = -\zeta_-(0)$, the spins satisfy the fixed boundary conditions $\sigma(0) = 1$.[171, 172, 173] Since under a duality transformation the order (σ) and the disorder (μ) parameter are exchanged, free boundary conditions for the spin σ translate into fixed boundary conditions for μ and vice-versa. In the Ising language, the semi-infinite ladder is therefore equivalent to four decoupled semi-infinite Ising models with free boundary conditions. A positive mass for the Majorana fermions corresponds to a two-dimensional Ising model below its critical temperature. With free boundary conditions, the localized Majorana fermion mode corresponds to a domain wall bound to the edge in the Ising model. When the mass is negative, the Ising model is above the critical temperature, and no domain wall is attached to the edge. Using the results from [171, 172, 173, 174, 175], we obtain the following expression for the staggered magnetization:

$$\langle n_+^z(x)\rangle \sim \left(\frac{m_t^3|m_s|a^4}{v_t^3 v_s}\right)^{1/8} e^{-m_t x/v_t} H^2\left(\frac{m_t x}{v_t}\right) G\left(\frac{m_t x}{v_t}\right) G\left(\frac{|m_s|x}{v_s}\right), \tag{4.51}$$

where the functions G and H can be expressed terms of a solution to the Painlevé III differential equation:

$$\frac{1}{\eta}\frac{d^2\eta}{d\theta^2} = \left(\frac{1}{\eta}\frac{d\eta}{d\theta}\right)^2 - \frac{1}{\theta\eta}\frac{d\eta}{d\theta} + \eta^2 - \frac{1}{\eta^2}. \tag{4.52}$$

with boundary conditions on η :

$$\begin{aligned} \eta(\theta) &\sim -\theta\left[\ln\frac{\theta}{4} + \gamma_E\right](\theta \to 0) \\ \eta(\theta) &\sim 1 - \frac{K_0(2\theta)}{2\pi}(\theta \to \infty), \end{aligned} \tag{4.53}$$

γ_E being the Euler's constant. The functions G and H are defined by:

$$\begin{aligned} G(y) &= \eta^{-1/4}(y)\exp\left[\int_y^\infty d\theta\left\{\frac{\theta}{8}\eta^{-2}(\theta)\left((1-\eta^2(\theta))^2 - \left(\frac{d\eta}{d\theta}\right)^2\right) - \frac{1}{2}(1-\eta(\theta))\right\}\right] \\ H(y) &= \eta^{1/4}(y)\exp\left[\int_y^\infty d\theta\left\{\frac{\theta}{8}\eta^{-2}(\theta)\left((1-\eta^2(\theta))^2 - \left(\frac{d\eta}{d\theta}\right)^2\right) - \frac{1}{2}(\eta^{-1}(\theta)-1)\right\}\right] \end{aligned} \tag{4.54}$$

There is an apparent paradox in having a non vanishing staggered magnetization in the absence of an external magnetic field since this violates the $SU(2)$ invariance of the model. Actually, the Eq. (4.51) is only valid when $S^z_{tot.} = 0$. Such a state is only invariant under rotations around the z-axis, and can sustain a staggered magnetization, as has been observed in DMRG calculations[176, 177]. A staggered dimerization is also present. Using the bosonized

expression (1.68), and the mapping to the Ising spins, we find that the staggered dimerization is $\epsilon_+ \sim \mu_1\mu_2\mu_3\mu_0$. The expectation value is then:

$$\langle \epsilon_+ (x) \rangle \sim \left(\frac{m_t^3 |m_s| a^4}{v_t^3 v_s} \right)^{1/8} e^{-3m_t x/v_t} G^3 \left(\frac{m_t x}{v_t} \right) G \left(\frac{|m_s| x}{v_s} \right). \tag{4.55}$$

for ferromagnetic rung interaction, and:

$$\langle \epsilon_+ (x) \rangle \sim \left(\frac{|m_t|^3 m_s a^4}{v_t^3 v_s} \right)^{1/8} e^{-m_s x/v_t} G^3 \left(\frac{|m_t| x}{v_t} \right) G \left(\frac{m_s x}{v_s} \right), \tag{4.56}$$

for antiferromagnetic rung interaction.

We can also obtain the staggered magnetization profile when the edge spin is polarized by an external magnetic field. We find in the ferromagnetic rung case:

$$\langle n_+^x (x) \rangle \sim e^{-|m_t| x/v_t} G^3 \left(\frac{|m_t| x}{v_t} \right) G \left(\frac{m_s x}{v_s} \right), \tag{4.57}$$

and in the antiferromagnetic rung case:

$$\langle n_+^x (x) \rangle \sim e^{-2m_t x/v_t - |m_s| x/v_s} G^3 \left(\frac{m_t x}{v_t} \right) G \left(\frac{|m_s| x}{v_s} \right), \tag{4.58}$$

4.3 Ladders under a magnetic field

Until now, we have restricted ourselves to ladders in zero external magnetic field. In the presence of an applied field, one must add a term:

$$H_{field} = -\frac{h}{\pi} \int dx \partial_x (\phi_1 + \phi_2) \tag{4.59}$$

$$= -\frac{h\sqrt{2}}{\pi} \int dx \partial_x \phi_s. \tag{4.60}$$

When H_s is gapped in zero magnetic field, that term induces a commensurate-incommensurate transition[178, 179]. For $h > h_c$, the Hamiltonian $H_s + H_{field}$ has a Luttinger liquid ground state with gapless spectrum[180, 181, 182]. The Singlet or Haldane phase are turned into the $XY1$ phase, while the Ising antiferromagnetic phase are turned into the $XY2$ phase. The transition is most easily understood in the SU(2) invariant limit. Indeed, in that case, we can fermionize $H_s + H_{field}$ in the form;

$$H = \int dx \left[-iu_s(\psi_+^\dagger \partial_x \psi_+ - \psi_-^\dagger \partial_x \psi_-)dx + i\Delta_s \int (\psi_+^\dagger \psi_- - \psi_-^\dagger \psi_+) - h(\psi_+^\dagger \psi_+ + \psi_-^\dagger \psi_-) \right] \tag{4.61}$$

and the energy of excitations is simply $E_\pm(k) = \pm\sqrt{(u_s k)^2 + \Delta_s^2} - h_s$. When $|h_s| < |\Delta_s|$, there are no zero energy excitations, and the system remains gapped. When $|h_s| > |\Delta_s|$, a fermion or

hole Fermi surface is formed with a Fermi momentum $k_F = \sqrt{h_s^2 - \Delta_s^2}/u_s$. This implies that the ladder is becoming magnetized, with a magnetization proportional to k_F. Moreover, we can derive a bosonized description of the fermions, which leads to a Hamiltonian of the form (1.27) for the ϕ_s modes,

$$H = \int \frac{dx}{2\pi} \left[u_s^*(h) K_s^*(h) (\pi \Pi_s)^2 + \frac{u_s^*(h)}{K_s^*(h)} (\partial_x \phi_s)^2 \right] \tag{4.62}$$

Since the fermions are non-interacting, we have $K_s^* = 1$ and $u_s^*(h) = u_s \sqrt{1 - (\Delta_s/h)^2}$ in Eq.(4.59). Away from the non-interacting point $K_s = 1$, it has been shown[183] that when h goes to the critical field h_c the Tomonaga-Luttinger exponent K_s goes to 1. For the general sine-Gordon model, the velocity and exponent were derived in[184]. Right at the critical field, the dispersion of the excitations is quadratic, and the system is at a $z = 2$ quantum critical point[185]. The spin-spin correlation functions in the magnetized phase have been derived explicitly in [181, 182].

Such a transition can be observed in organic two-leg ladders such as BPCB.[186] In such a system however, the rung coupling is larger than the leg coupling, and the weak coupling bosonization analysis is not justified. However, in the limit of $J_\perp \gg J$, an effective XXZ spin chain model can be derived to describe the low energy physics of the model.[187, 188] In the derivation, one first neglects J and considers simply the eigenstates of a simple dimer. They are formed of a singlet of energy $-3J_\perp/4$ and a triplet with energies $J_\perp/4 + h, J_\perp, J_\perp - h$. For $h = J_\perp$, the singlet and the triplet with both spins polarized along the magnetic field (i. e. $S^z = 1$) exchange stability. Thus, one can choose a low-energy subspace formed of two states, the singlet and the $S^z = 1$ triplet on each rung, and apply perturbation theory to derive the effective Hamiltonian. The two states can be represented with a pseudospin τ^z with $\tau^z = -1/2$ in the singlet state and $\tau^z = 1/2$ in the triplet state so that $S^z = 1/2 + \tau^z$. The effective spin chain Hamiltonian reads:

$$H = -J \sum_n (\tau_n^x \tau_{n+1}^x + \tau_n^y \tau_{n+1}^y + \frac{1}{2} \tau_n^z \tau_{n+1}^z) - (h - J_\perp) \sum_n \tau_n^z, \tag{4.63}$$

and the local magnetization in the plane orthogonal to the magnetic field can be written as:

$$S_{n,p}^+ = \frac{(-1)^p \tau_n^+}{\sqrt{2}} \tag{4.64}$$

In the partially magnetized phase, the spin chain described by the Hamiltonian (4.63) is in a Tomonaga-Luttinger liquid state. With the representation (1.69), we can interpret the triplets as hard core boson particles, and the singlet as a particle vacuum. In that picture, the magnetized ladder can be viewed as a Tomonaga-Luttinger liquid of hard-core bosons. Using the Bethe Ansatz solution of the XXZ chain, (4.63) the velocity and Tomonaga-Luttinger exponents have been derived[182]. Moreover, when the magnetization is at half the saturation value, $\tau_n^z = 0$ and the amplitudes in Eqs. (1.95) are given by (1.97). In the intermediate case of BPCB, where $J_\parallel = 3.55$ K and $J_\perp = 12.6$ K, a numerical approach is necessary. The method used in [151] is the Density Matrix Renormalization Group (DMRG).[189, 190] In its simplest version,

this method allows to find the ground state of a two leg ladder with open boundary conditions and obtain equal time correlation functions. Since the low-energy physics is described by a Tomonaga-Luttinger liquid model with a known representation of spin the operators, it is possible to calculate the Friedel oscillations of the spin as a function of the Tomonaga-Luttinger exponent[191, 192, 193] By fitting the Friedel oscillations, the Tomonaga-Luttinger exponent can be extracted. The velocity is extracted from the magnetic susceptibility.

In the BPCB compound, the ladders are not strictly isolated. There is an interladder exchange J_x which is smaller than the leg and rung exchanges. For sufficiently low temperature, the existence of this interladder exchange destabilizes the Tomonaga-Luttinger liquid. The spins then develop a long-range antiferromagnetic ordering on the ladders, and satisfy the constraints imposed by the interladder exchange. The long range ordering is of the easy plane type, with the spins lying in the plane orthogonal to the applied field. In a bosonization description, the effective model that describes the coupled ladders takes the form:

$$H = \sum_m \int \frac{dx}{2\pi} \left[u^*(h) K^*(h) (\pi \Pi_m)^2 + \frac{u^*(h)}{K^*(h)} (\partial_x \phi_m)^2 \right] - J' \sum_{\langle m,m' \rangle} A_0^x(h) \int dx \cos(\theta_m - \theta_{m'}) \quad (4.65)$$

where m is the ladder index, J' is the interladder exchange, and $A_0^x(h)$ is an amplitude as in Eq. (1.95). The Hamiltonian (4.65) can be treated in mean field theory.[194] The mean field is:

$$h_{MF} = z J' A_0^x(h) \langle \cos \theta_m \rangle_{H_{MF}}, \quad (4.66)$$

where z is the number of nearest neighbors of a given ladder, and the mean-field Hamiltonian used to determine h_{MF} selfconsistently reads:

$$H_{MF} = \int \frac{dx}{2\pi} \left[u^*(h) K^*(h) (\pi \Pi)^2 + \frac{u^*(h)}{K^*(h)} (\partial_x \phi)^2 - h_{MF} \int dx \cos \theta \right]. \quad (4.67)$$

such a Hamiltonian can be brought to the form (2.1) by a duality transformation and a rescaling. Using perturbation theory, it is possible to derive the critical temperature. Indeed, (4.66) can be rewritten as:

$$h_{MF} = z J' A_0^x(h) \langle T_\tau e^{h_{MF} \int dx \int_0^\beta d\tau \cos \theta(x,\tau)} \cos \theta(0,0) \rangle. \quad (4.68)$$

Expanding to first order in h_{MF} we find that the self-consistency condition is going to be satisfied at a temperature β_c such that:

$$1 = z J' A_0^x(h) \int dx \int_0^{\beta_c} d\tau \langle T_\tau \cos \theta(x,\tau) \cos \theta(0,0) \rangle. \quad (4.69)$$

Using Eq. (1.56), we obtain the critical temperature.

$$T_c = \frac{u}{2\pi} \left[\sin\left(\frac{\pi}{4K}\right) B^2 \left(\frac{1}{8K}, 1 - \frac{1}{4K} \right) \cdot \frac{z J' A_0^x(h)}{2u} \right]^{\frac{2K}{4K-1}}. \quad (4.70)$$

It is possible to go further and obtain also the order parameter for zero temperature using the results of [79]

$$m_x = F(K) \cdot \sqrt{A_0^x} \left(\frac{\pi z J' A_0^x}{2u} \right)^{\frac{1}{8K-2}}, \tag{4.71}$$

where

$$F(K) = \left\{ \frac{\frac{\pi^2}{\sin(\frac{\pi}{8K-1})} \cdot \frac{8K}{8K-1} \left[\frac{\Gamma(1-\frac{1}{8K})}{\Gamma(\frac{1}{8K})} \right]^{\frac{8K}{8K-1}}}{\Gamma\left(\frac{4K}{8K-1}\right)^2 \Gamma\left(\frac{16K-3}{16K-2}\right)^2} \right\}^{\frac{8K-1}{8K-2}}.$$

The parameters $u(h), K(h), A_0(h)$ can be obtained from DMRG calculations[151, 195, 196, 197]. A comparison of the experimental transition temperature and zero temperature magnetization with the theoretical result is shown on Figs. 4.3 (c)-(d). For the critical temperature, the fitting parameter is $J' = 20$ mK. With that fitting parameter, the amplitude of the order parameter can be obtained. After adjusting for an overall scale, the staggered magnetization obtained in NMR can be compared with the theoretical prediction. Neutron scattering allows to measure precisely the amplitude of the order parameter, without adjustable overall amplitude.

4.4 Ladders with Dzyaloshinskii-Moriya interaction

Besides the Heisenberg exchange interaction, localized spin systems can also present the Dzyaloshinskii-Moriya interaction[198, 199]. This interaction originates in relativistic effects that give rise to spin orbit interactions. In a tight binding formulation, the spin-orbit interaction takes the form of a spin-dependent hopping integral:

$$H = -\sum_{i,j} T_{ij;\alpha\beta} c^\dagger_{i,\alpha} c_{j,\beta}, \tag{4.72}$$

$$T_{ij;\alpha\beta} = t^0_{ij} \delta_{\alpha\beta} + \mathbf{t}_{ij} \cdot \sigma_{\alpha\beta} \tag{4.73}$$

When this hopping integral is inserted in the Hubbard model[200, 201, 202] and second order perturbation theory is used to eliminate the doubly occupied sites, it gives rise, besides the Heisenberg exchange term, to a spin-spin interaction of the form:

$$\sum_{ij} \mathbf{D}_{ij} \cdot (\mathbf{S}_i \times \mathbf{S}_j) + A^{\alpha\beta}_{ij} S^\alpha_i S^\beta_j, \tag{4.74}$$

where $\mathbf{D}_{ij}$ is the Dzyaloshinskii-Moriya (DM) vector and $A^{\alpha\beta}_{ij}$ is the Kaplan-Shekhtman-Entin-Wolfmann-Aharony (KSEA) tensor. A necessary condition for the presence of a DM interaction is the absence of an inversion center in the middle of the bond ij. When the on-site interactions possess the full $SU(2)$ symmetry, the KSEA tensor and the Dzyaloshinskii-Moriya vector are not independent from each other.[200, 201, 202] The interaction (4.74) can be rewritten in the form:

$$\sum_{ij} D S^\alpha_i \mathcal{R}^{\alpha\beta}_{ij} S^\beta_j, \tag{4.75}$$

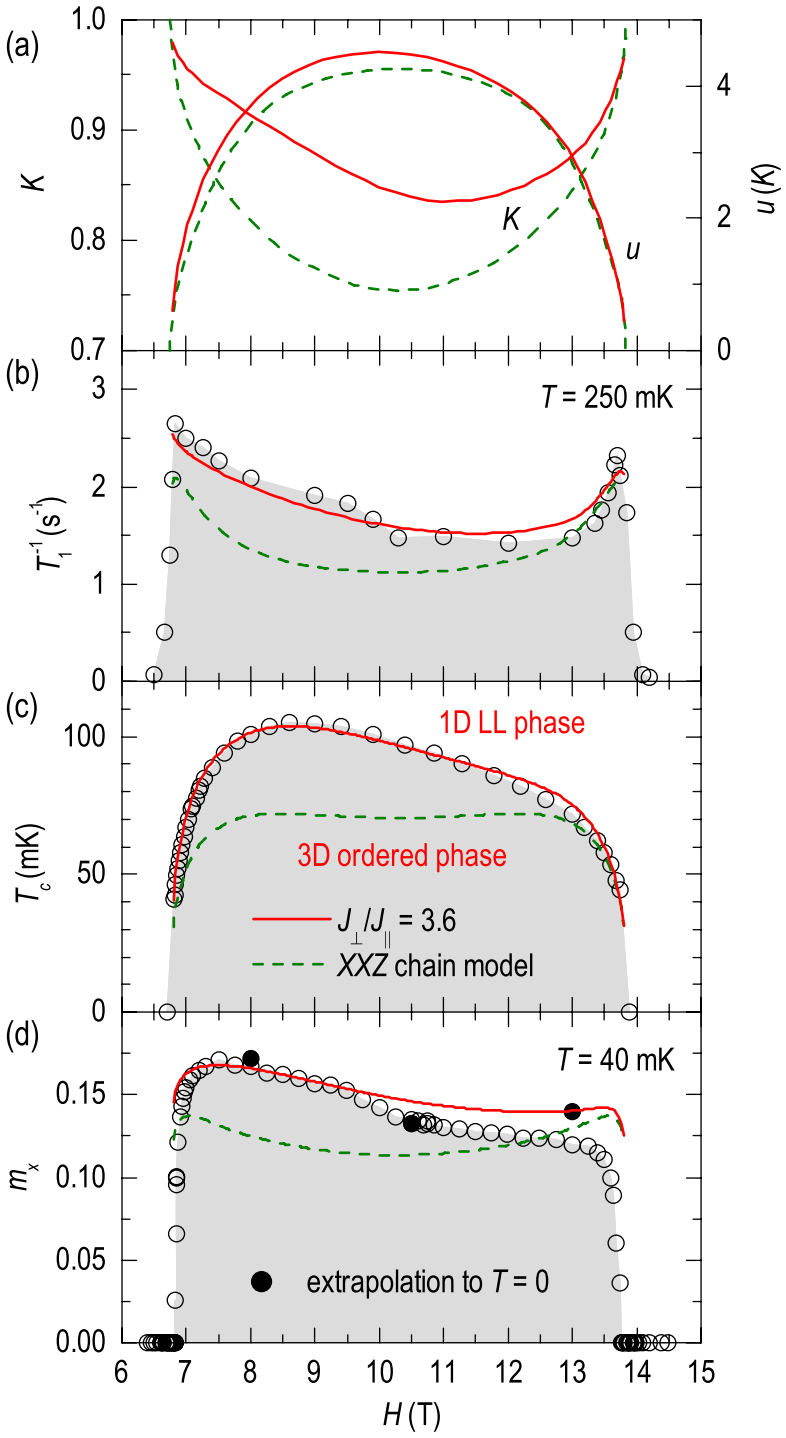

Figure 4.3: (a) the velocity u and Tomonaga-Luttinger exponent K derived from the strong coupling model (green dashed line) and from DMRG (red solid line). (b-d) Comparison of NMR measurements on BPCB with the ladder mean field theory. (b) the NMR relaxation rate T_1 versus magnetic field. (c) the Néel ordering temperature versus magnetic field. (d) the staggered magnetization versus magnetic field. The green dashed line is the result from the effective XXZ spin chain model at strong coupling, the solid red line is obtained from the DMRG extracted Tomonaga-Luttinger liquid parameters.

Material	References
Copper benzoate	[203]
$PMCu(NO_3)_2H_2O_{2_n}$ (copper pyrimidine dinitrate)	[207, 208, 209]
Yb_4As_3	[210, 211]
$CuCl_2.2$(dimethylsulfoxide)	[212]
$BaCu_2Ge_2O_7$	[213]
$CuSe_2O_5$	[214]
$KCuGaF_6$	[215, 216]

Table 4.3: Spin-1/2 chain compounds with staggered Dzyaloshinskii-Moriya interactions.

where $\mathcal{R}_{ij} \in \mathrm{SO}(3)$ is a rotation matrix. In such case, the DM+KSEA interactions are imposing a fixed angle between the spins which differs from π and can give rise to frustration. More precisely, if we consider a local rotation SO(3) of the spins, $S_i^\alpha = \mathcal{P}_i^{\alpha\beta}\tilde{S}_i^\beta$, the DM+KSEA interaction will become $\tilde{S}_i^\alpha \tilde{\mathcal{R}}_{ij}^{\alpha\beta}\tilde{S}_j^\beta$, with $\tilde{\mathcal{R}}_{ij} = \mathcal{P}_i^{-1}\mathcal{R}_{ij}\mathcal{P}_j$. In order to reduce the DM+KSEA interaction to an ordinary Heisenberg exchange coupling, we must have: $\mathcal{R}_{ij} = P_i\mathcal{P}_j^{-1}$. A consequence of that constraint is that the ordered product of the $\mathcal{R}$ matrices on any closed loop must be identity. When that condition cannot be satisfied, the DM+KSEA interactions are giving rise to frustration.

Staggered Dzyaloshinskii-Moriya interactions in spin-1/2 chains[203, 204, 205] are known to give rise to the formation of spin gaps $\Delta \propto B^{2/3}$ under an external magnetic field B. Besides the original copper benzoate material, other examples of spin-chain systems where Dzyaloshinskii-Moriya interactions give rise to spin gaps under field are listed in table 4.3. In the case of uniform Dzyaloshinskii-Moriya interactions, it has been shown[206] that the uniform interactions can be removed by a local gauge transformation, leaving only incommensurate spin-spin correlations.

4.4.1 Uniform Dzyaloshinskii-Moriya interaction

In the present section, we consider the effect of a uniform Dzyaloshinskii-Moriya interaction. For a uniform interaction along the chains, a similar gauge transformation to the case of the isolated chain[206] can be applied.[148] When both chains are equivalent, this results in an incommensurate modulation of the exponentially decaying spin-spin correlations of the two-leg ladder. With a Dzyaloshinskii-Moriya vector along the rungs of a ladder,

$$H_{DM+KSEA} = \sum_i \mathbf{D}\cdot(\mathbf{S}_{1,i}\times\mathbf{S}_{2,i}) + S_{1,i}^\alpha A^{\alpha\beta} S_{2,i}^\beta \tag{4.76}$$

If we use the quantization axis $\hat{z}$ for the spins such that $\mathbf{D} = D\hat{z}$, the anisotropy tensor reduces to $A_{zz} = A$ and all other components become zero. Using the gauge transformation:

$$S_{i,1}^+ = e^{-i\alpha}\tilde{S}_{i,1}^+; \quad S_{i,2}^+ = e^{i\alpha}\tilde{S}_{i,2}^+ \tag{4.77}$$

where $2\alpha = \arctan(D/J_\perp)$, we bring the ladder Hamiltonian to the form:

$$H = \sum_i \left[J_\parallel \sum_{p=1}^{2} \tilde{\mathbf{S}}_{p,i}\tilde{\mathbf{S}}_{p,i+1} + \tilde{J}_\perp(\tilde{S}_{i,1}^x\tilde{S}_{i,2}^x + \tilde{S}_{i,1}^y\tilde{S}_{i,2}^y) + (J_\perp + A)\tilde{S}_{i,1}^z\tilde{S}_{i,2}^z \right] \tag{4.78}$$

where $\tilde{J}_\perp = \sqrt{J_\perp^2 + D^2}\text{sign}(J_\perp)$. As a result, the determination of the spectrum of a two-leg ladder with uniform Dzyaloshinskii-Moriya interaction reduces to an anisotropic version of (4.10). Following the approach of [162] the spin-spin correlations are obtained as:

$$\langle T_\tau M_x(x,\tau) M_x(0,0)\rangle \sim \frac{A_\infty^4 \sin^2\alpha}{\sqrt{2\pi m r/u}} e^{-mr/u} \tag{4.79}$$

$$\langle T_\tau m_x(x,\tau) m_x(0,0)\rangle \sim \frac{A_\infty^4 \cos^2\alpha}{\sqrt{2\pi m r/u}} e^{-mr/u} \tag{4.80}$$

$$\langle T_\tau M_z(x,\tau) M_z(0,0)\rangle \sim A_\infty^4 \left(\frac{u}{2\pi (m^2 m_4)^{1/3} r}\right)^{3/2} e^{-(2m+m_4)r/u} \tag{4.81}$$

$$\langle T_\tau m_z(x,\tau) m_z(0,0)\rangle \sim \frac{A_\infty^4}{\sqrt{2\pi m_3 r/u}} e^{-mr/u} \tag{4.82}$$

$$\tag{4.83}$$

where $M_\alpha(x) = n_1^\alpha(x) + n_2^\alpha(x)$ and $m_\alpha = n_1^\alpha(x) - n_2^\alpha(x)$. In general, the in-plane and out of plane correlation functions have a different correlation length in contrast to the case of a ladder with isotropic interactions. When the KSEA interaction satisfies the condition for SU(2) symmetry, in-plane and out-of plane correlations have the same correlation length. The ratio between the M_x and m_x correlation indicates the angle of rotation.

The behavior of the two-leg ladder with uniform Dzyaloshinskii-Moriya interaction under an external field is more interesting. The Hamiltonian reads:

$$H = \sum_{k>0} {}^t\vec{\zeta}(-k)\mathcal{H}(k)\vec{\zeta}(k) \tag{4.84}$$

where:

$$\vec{\zeta}(k) = \begin{pmatrix} \xi_R^2(k) \\ \xi_L^2(k) \\ \xi_R^3(k) \\ \xi_L^3(k) \\ \xi_R^4(k) \\ \xi_L^4(k) \end{pmatrix} = \frac{1}{\sqrt{L}} \int_0^L dx \vec{\zeta}(x) e^{-ikx}, \tag{4.85}$$

and:

$$\mathcal{H}(k) = \begin{pmatrix} uk & im & ih\cos\alpha & 0 & ih\sin\alpha & 0 \\ -im & -uk & 0 & ih\cos\alpha & 0 & ih\sin\alpha \\ -ih\cos\alpha & 0 & uk & im_3 & 0 & 0 \\ 0 & -ih\cos\alpha & -im_3 & -uk & 0 & 0 \\ -ih\sin\alpha & 0 & 0 & 0 & uk & im_4 \\ 0 & -ih\sin\alpha & 0 & 0 & -im_4 & -uk \end{pmatrix}. \tag{4.86}$$

Diagonalizing the matrix $\mathcal{H}$ gives the spectrum under field. A typical plot is shown on Fig. 4.4. Contrarily to the isotropic case, the gap never closes under field. The commensurate-incommensurate transition is replaced by a simple crossover. A similar situation is obtained in spin-1 chains with anisotropic interactions[217].

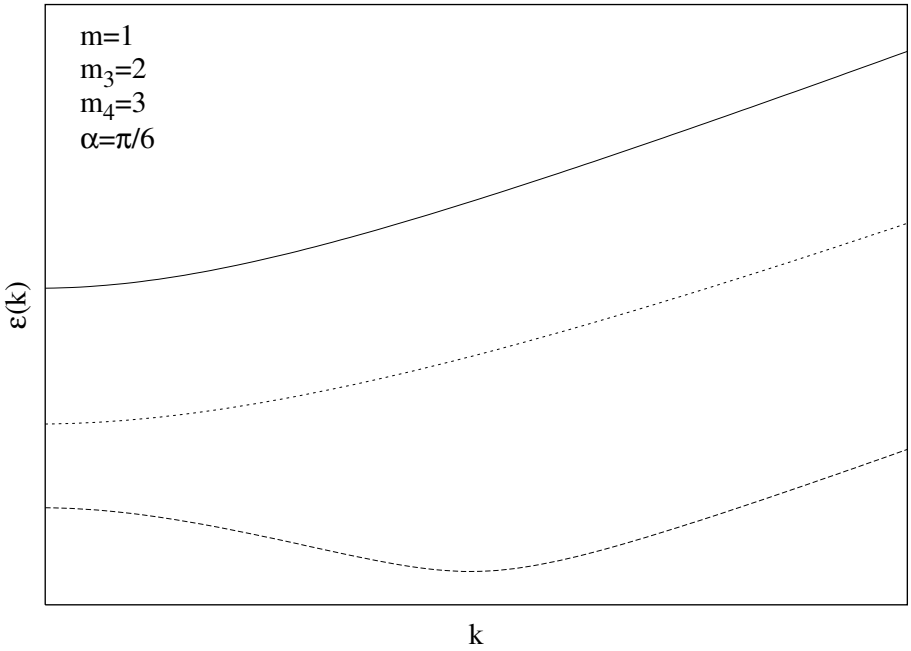

Figure 4.4: The spectrum of a two-leg ladder with uniform Dzyaloshinskii-Moriya interaction under a uniform magnetic field. The model does not have SU(2) symmetry, and it is seen that the spin gap never closes.

4.4.2 Staggered Dzyaloshinskii-Moriya interaction

In the material CuHpCl, [218, 219, 220], the magnetic interactions can be described with a two-leg ladder model having a staggered DM interaction along the rungs.

The staggered DM interaction is:

$$H_{DM} = \sum_n (-)^n \mathbf{D} \cdot (\mathbf{S}_{n,1} \times \mathbf{S}_{n,2}) \tag{4.87}$$

with $\mathbf{D} = D\hat{y}$. In CuHpCl, $J_\perp = 13$K, $J_\parallel = 0.2J_\perp$ and $D = 0.05J_\perp$.[218] In the presence of the staggered DM interaction, the Luttinger liquid phase obtained under applied field is replaced by a gapped phase.[219] It has been shown that the model with staggered DM interaction gave a better fitting of the magnetization[219] and the magnetic specific heat under applied field[220].

We will first discuss the weak coupling form of the interaction (4.87). We will consider the case of a magnetic field along the z direction. The bosonized form interaction is:

$$H_{DM} = D \int dx \left[\frac{1}{\pi\sqrt{2\pi a}} (\partial_x \phi_2 \cos\theta_1 - \partial_x \phi_1 \cos\theta_2) - \frac{1}{\pi a \sqrt{2\pi a}} (\cos\theta_1 - \cos\theta_2) \cos 2\phi_1 \cos 2\phi_2 \right] \tag{4.88}$$

In the magnetized phase, since $\langle \partial_x \phi_{1,2} \rangle = -\pi m$, where m is the magnetization, the Eq. (4.88) , gives a term $mD(\cos\theta_1 - \cos\theta_2)$ in the Hamiltonian. Since $\langle \theta_a \rangle = \pi/\sqrt{2}$, this term further reduces to $mD\langle \sin\theta_a/\sqrt{2}\rangle \sin(\theta_s/\sqrt{2})$. A spin gap : $\Delta_{DM} \sim J_\parallel (J_\perp/J_\parallel)^{\frac{2K_a}{4K_a-1}}$, thus opens in the magnetized phase for $K_a > 1/4$.

In the strong coupling limit, we can use the mapping [221, 188] to an XXZ spin chain, and obtain an effective interaction:

$$H_{DM} = \frac{D}{\sqrt{2}} \sum_n (-1)^n \tau_n^x. \tag{4.89}$$

A bosonized form of that Hamiltonian can be derived:

$$H = \int \frac{dx}{2\pi} \left[uK(\pi\Pi)^2 + \frac{u}{K}(\partial_x \phi)^2 \right] + \frac{\lambda D}{a\sqrt{2}} \int dx \cos\theta, \tag{4.90}$$

The model (4.90) possesses for $K > 1/4$ breathers with masses:

$$M_n = 2M_0 \sin\left(\frac{\pi}{2} \frac{n}{8K-1} \right), \tag{4.91}$$

In order to observe those breather excitations, it is not possible to rely on ESR measurements as ESR absorption intensity is proportional to an autocorrelation function of $(S_1^x + S_2^x)$, but this operator becomes zero in the strong coupling model. However, Raman scattering can be used to probe the breather modes. In the Fleury-Loudon approximation[222], valid for frequencies of incoming radiation much smaller than the Mott gap of the material[223], the Raman operator takes the form:

$$H_R = \sum_{i,j} J_{ij} (\hat{e}_O \cdot \hat{n}_{ij})(\hat{e}_I \cdot \hat{n}_{ij}) \mathbf{S}_i \cdot \mathbf{S}_j, \tag{4.92}$$

where $\hat{n}_{ij}$ is the unit vector connecting the sites i and j,$\hat{e}_I$ the polarization vector of the incoming radiation, $\hat{e}_O$ is the polarization vector of the outgoing radiation. In full generality, the amplitude J_{ij} depends on the geometry [224] but, as in most studies [225], we take it constant *i.e.* $J_{ij} = \gamma$.

For simplicity, here we restrict ourselves to simple geometrical setups, e.g. to the XX, YY and X'Y' geometries corresponding to $\hat{e}_I$ and $\hat{e}_O$, both along the chains direction, both perpendicular to the chains and at 45-degrees from the crystal axes (X'=X+Y, Y'=X-Y), respectively. The corresponding Raman operators can then be written as,

$$\hat{O}_R^{XX} = \gamma \sum_n (\mathbf{S}_{n,1} \cdot \mathbf{S}_{n+1,1} + \mathbf{S}_{n,2} \cdot \mathbf{S}_{n+1,2}), \tag{4.93}$$

$$\hat{O}_R^{YY} = \gamma \sum_n \mathbf{S}_{n,1} \cdot \mathbf{S}_{n,2}, \tag{4.94}$$

$$\hat{O}_R^{X'Y'} = \frac{1}{2}(\hat{O}_R^{XX} - \hat{O}_R^{YY}). \tag{4.95}$$

Going to the continuum limit, it is convenient to introduce a density for the Raman operator, $O_R^{\alpha\beta}(x)$ so that $\hat{O}_R^{alpha\beta} = \int O_R^{\alpha\beta}(x)dx$. Using the density of Raman operator, and the standard definition of Raman scattering intensity, we finally find that:

$$I_{R,\parallel}(\omega) = \sum_n |\langle n, \mathbf{P}_n = 0 | O_R^{XX}(0) | 0 \rangle|^2 \delta(\omega - E_n) \tag{4.96}$$

where $|0\rangle$ is the ground state (GS) of the system and $|n, \mathbf{P}_n\rangle$ is the $n-$th excited state with $\mathbf{P}_n$ its total momentum. Since the Raman operator is a sum over all sites, Raman scattering is conserving photon momenta. This explains why only the states with zero momenta (i.e. having the same momentum as the ground state) contribute to the sum (4.96).

In the following, we compute the Raman intensity for frequencies smaller than $2J_\perp$ using the strong coupling theory. We consider first the case of a field parallel to the legs in Sec. 4.4.2, and then the case of a field parallel to the rungs in Sec. 4.4.2.

Electric field along the legs

In the strong coupling limit, we can rewrite the Raman operator (4.93) as,

$$\begin{aligned} \hat{O}_R^{XX} &= \frac{\gamma}{2}\sum_n (\tau_n^+\tau_{n+1}^- + \tau_{n+1}^+\tau_n^- \\ &+ (\tau_n^z + 1/2)(\tau_{n+1}^z + 1/2)), \end{aligned} \tag{4.97}$$

yielding the expression:

$$\hat{O}_R^{XX} = \gamma \frac{H - H_{DM} + (h - J_\perp - J_\parallel/2)\sum \tau_n^z}{J_\parallel} + \text{const.}, \tag{4.98}$$

where H is the full strong coupling effective spin chain Hamiltonian. In the computation of the Raman scattering intensity time independent terms do not contribute. Therefore, we can consider the effective Raman operator:

$$\hat{O}_R^{XX} = \gamma(h_0 \sum_n \tau_n^z - H_{DM})/J_\parallel, \tag{4.99}$$

where $h_0 = h - J_\perp - J_\parallel/2$.

In the continuum limit, we have the following bosonized expression for the density O_R^{XX} in the Raman operator.

$$O_R^{XX}(x) = \frac{\gamma}{J_\parallel}\left(\frac{\lambda D}{a\sqrt{2}}\cos\theta(x) - \frac{h_0}{\pi}\partial_x\phi\right) \tag{4.100}$$

Using the symmetries of the operators in Eq. (4.100), it is possible to further simplify the expression of the Raman intensity. The sine-Gordon Hamiltonian (4.90) is invariant under the simultaneous transformations $\theta \to -\theta$ and $\phi \to -\phi$, and its eigenstates can be classified according to their parity under this transformation. The operator $\cos\theta$ is even under such transformation, while the operator $\partial_x\phi$ is odd. Therefore, the non-vanishing matrix elements of $\cos\theta$ are between the ground state and even states, whereas those of $\partial_x\phi$ are between the ground state and the odd states. Thus :

$$I_{R,\parallel}(\omega) = I_{R,\parallel}^{(o)}(\omega) + I_{R,\parallel}^{(e)}(\omega), \tag{4.101}$$

where:

$$I^{(o)}_{R,\|}(\omega) = \left(\frac{\gamma h_0}{\pi J_\|}\right)^2 \sum_{|n\rangle odd} |\langle n|\partial_x\phi|0\rangle|^2 \delta(\omega - E_n) \quad (4.102)$$

$$I^{(e)}_{R,\|}(\omega) = \left(\frac{\lambda\gamma D}{aJ_\|\sqrt{2}}\right)^2 \sum_{|n\rangle even} |\langle n|\cos\theta|0\rangle|^2 \delta(\omega - E_n)$$

The intensity $I^{(e)}_{R,\|}(\omega)$ has been computed previously in Ref. [93] in the context of spin chains with staggered Dzyaloshinskii-Moriya interactions. From the results of Ref. [93], $I^{(e)}_{R,\|}(\omega)$ contains delta-function peaks at the frequencies of even breathers, and thresholds at frequencies equal to twice the soliton frequency, and to frequencies equal to the sum of the masses of two breathers of identical parity. The lowest threshold is therefore obtained at the frequency $\omega = 2M_1$. Since that threshold is below the energies of the breathers of mass M_2 and M_4, peaks are obtained in the continuum. Of course, in a more realistic model, the conservation laws that make the sine Gordon model integrable are absent, and the peaks become resonances whose width is determined by the coupling with the two-breathers continuum. If the deviations of the lattice model from the continuum sine-Gordon model become too important (for instance when the gap is so large that the continuum limit is not justified), the resonances may not even exist.

Similarly, the intensity $I^{(o)}_{R,\|}(\omega)$, can be related to the electrical conductivity of a one dimensional Mott insulator [90, 91] using the equation of motion $\partial_t\theta = \frac{u}{K}\partial_x\phi$, In [91], it was shown that if the sine-Gordon model describing the low energy charge excitations of the Mott insulator possesses breathers in its spectrum, the conductivity of the Mott insulator has delta peaks at the breather frequencies. In the Raman scattering context, this implies that $I^{(o)}_{R,\|}(\omega)$ has delta function peaks at the frequencies of the odd breathers. Moreover, there are thresholds at frequencies equal to twice the soliton mass and to the sum of two breather masses of different parities. The first threshold in $I^{(o)}_{R,\|}(\omega)$ is thus at the frequency $\omega = M_1 + M_2$.

Combining the two contributions, all breather modes contribute a peak in the Raman intensity. Moreover, the Raman intensity exhibits thresholds for all frequencies equal to the sum of two breather masses or to twice the soliton mass. A qualitative sketch of the Raman intensity is visible on the figure 4.5.

In the special case of $h_{\text{eff}} = 0$, the intensity $I^{(o)}_{R,\|}$ is vanishing and only the even breathers contribute to the Raman spectrum.

The weight of the delta peaks has been computed from the Form factor expansion using the pole structure (2.93) of the two-particle form factors.[226, 91] In the case of $K = 3/4$, which corresponds to a magnetization equal to half the saturation magnetization in the strong coupling limit (4.90), the sine-Gordon model (4.90) has 4 breathers. The weight of the peak associated with the first breather is obtained numerically as $0.345C_1$. For the peak associated with the third breather the weight is only $0.0116C_1$ i.e. about 3% of the weight of the first breather. Similarly, the weight of the second breather, we is $0.0367C_2$ and the weight of the fourth breather is $0.0058C_2$ i. e. about 16% of the intensity associated of the second breather. Note that the ratio C_2/C_1 depends not only on the Luttinger parameter but also on the ratio $D/J_\|$.

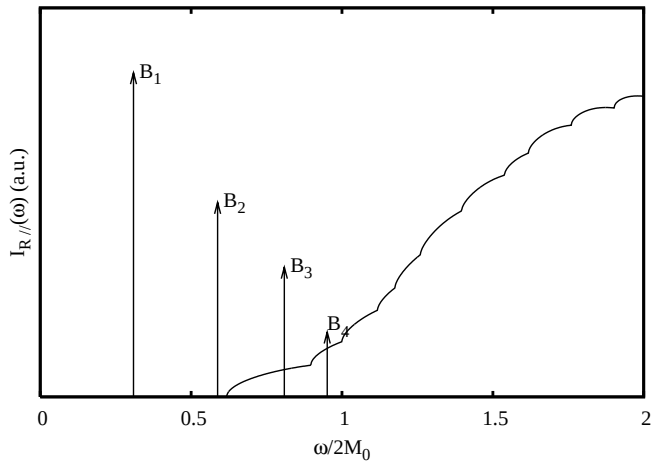

Figure 4.5: A sketch of the Raman intensity for polarization parallel to the legs (XX). The arrows represent the position of the the breathers δ–peaks. The intensity in the peak, proportional to its height is decreasing with the breather index. The continuum starts at a frequency equal to twice the mass of the lightest breather. Above the threshold, resonances are expected instead of δ-functions (beyond a SG analysis).

Electric field along the rungs

In the case of an electric field parallel to the rungs, the Raman operator (4.94) can be rewritten, in the strong coupling limit, as:

$$\hat{O}_R^{YY} = \gamma \sum_n \left(\tau_n^z - \frac{1}{4} \right) . \tag{4.103}$$

In the absence of the Dzyaloshinskii-Moriya interaction, this term is proportional to the total magnetization, which leads to a vanishing Raman intensity for $\omega \neq 0$. When $D \neq 0$, the total magnetization is not anymore a good quantum number, and a non-zero Raman intensity exists for energies small compared to $J_\perp$. Using bosonization, we can express the Raman intensity as:

$$I_{R,\perp}(\omega) = \frac{K^2\gamma^2}{\pi^2 u^2} \sum_n E_n^2 |\langle 0|\theta|n\rangle|^2 \delta(P_n)\delta(\omega - E_n) \tag{4.104}$$

Since $I_{R,\perp}(\omega) \propto I_{R,\|}^{(o)}(\omega)$ it only contains contributions from odd states. Moreover, the continuum starts at the frequency $M_1 + M_2$ which is larger than in the case of a polarization along the legs. The behavior of $I_{R,\perp}(\omega)$ is sketched on Fig. 4.6. Again, as we noted in Sec. 4.4.2, the breather B_3 has a higher energy than the lowest two-B_1 breather excitation. So the breather B_3 may be unstable in a more realistic model, and may appear as a broad resonance or be completely absent.

In the case of $X'Y'$ polarization, the resulting Raman operator is a linear combination of O_R^{XX} and O_R^{YY}, and the resulting intensity is qualitatively similar to $I_{R,\|}$ shown on Fig. 4.5.

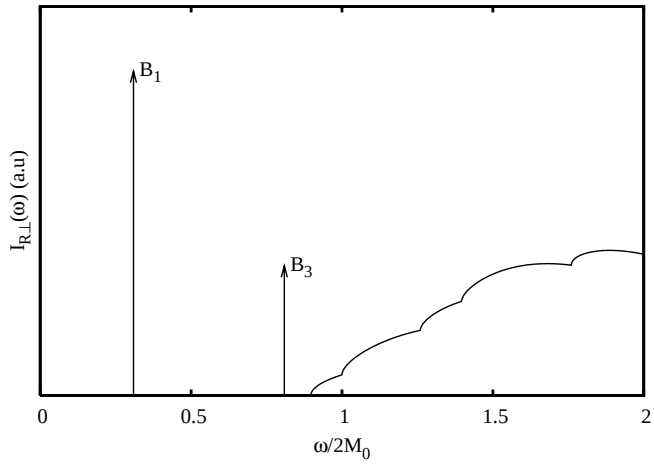

Figure 4.6: A sketch of the Raman intensity for polarization parallel to the rungs (YY). The arrows represent the position of the the breathers δ–peaks. The intensity in the peak, proportional to its height is decreasing with the breather index. In contrast to the case of polarization along the legs, only odd breathers contribute to the Raman intensity. The continuum starts at a frequency equal to the sum of the masses of the lightest odd and even breathers, which is higher than in the case of polarization along the legs.

Chapter 5

the spin-Peierls transition

The present chapter is based on the article[227]

It is well known that one-dimensional metals on a deformable lattice are unstable[228]: a deformation of the lattice of wavevector $2k_F$ creates a periodic potential that opens a gap at the Fermi level turning the one-dimensional metal into a band insulator. In a mean-field theory, the gap can be shown to possess a BCS-like expression. Since we have seen that a XY spin-1/2 chain could be mapped to one dimensional spinless fermions on a lattice, an XY spin-1/2 chain will exhibit the same instability, with a lattice modulation of wavevector π/a (where a is the lattice spacing) in zero external field.[229, 230, 231] This instability is called the spin-Peierls instability. In the case of the XXZ chain, the Hamiltonian takes the form:

$$H = J\sum_n (1+\lambda(u_{n+1}-u_n))(S^x_n S^x_{n+1} + S^y_n S^y_{n+1} + \Delta S^z_n S^z_{n+1}) + H_{phonons}, \tag{5.1}$$

where u_n is the displacement of the n-th site, g is a spin-phonon coupling constant, $\Delta = J_z/J$ is the anisotropy. In the spin-Peierls phase, $\langle u_n\rangle = (-)^n u$. The presence of $J_z \neq 0$, the spin-phonon is renormalized by J_z. A mean-field theory taking into account such renormalization was developed in 1979.[232] The bosonized theory takes the form:

$$H = \int \frac{dx}{2\pi}\left[uK(\pi\Pi)^2 + \frac{u}{K}(\partial_x\phi)^2\right] - \frac{2g\delta}{(2\pi\alpha)^2}\cos\sqrt{2}\phi + \frac{k}{2}\delta^2, \tag{5.2}$$

where the dimensionless dimerization parameter $\delta = 2\lambda u$ and k depends on the elastic constants of the lattice. The amplitude g is coming from the bosonized form of the dimerization operator (1.68) and is a non-universal parameter, not known in general. The notation in (5.2) is chosen so that the case with $SU(2)$ symmetry corresponds to $K = 1$ while the case $\Delta = 0$ corresponds to $K = 2$.

For $\delta \neq 0$, the cost in elastic energy is $k\delta^2/2$, while the energy gained from the opening of a spin gap is obtained from scaling as: $\sim \delta\delta^{K/(4-K)} = \delta^{4/(4-K)}$. The case $K = 2$ is the marginal case (where the energy gain actually contains a logarithmic factor). For $K > 2$ (*i. e.* $J_z < 0$), the energy gained from the opening of the spin gap is insufficient to compensate the cost in elastic energy, while for $K < 2$ (*i. e.* $J_z < 0$) the energy gained makes it always

Material	$T_{SP}(K)$	References
$TTFCuS_4C_4(CF_3)_4$ (TTFCuBDT)	12	[234, 235]
$TTFAuS_4C_4(CF_3)_4$ (TTFAuBDT)	2.1	[235]
MEM-$(TCNQ)_2$	17.7	[236]
$(TMTTF)_2PF_6$	$\simeq 15$	[237, 238, 239]
$(BCPTTF)_2PF_6$	36	[240]
$CuGeO_3$	14	[241]
TiOCl	67	[242]

Table 5.1: Quasi-one dimensional spin-1/2 antiferromagnets with a spin-Peierls transition

favorable to open a gap. This corresponds to antiferromagnetic interactions in the XXZ chain, and in particular this includes the case of $J_z = J$ for which $K = 1$. Spin-Peierls transitions have been observed in various organic and inorganic materials. A non-exhaustive list can be found in table 5.1. A review of experiments can be found in[233].

5.1 Mean-field theory

In [243, 227], we have further elaborated the mean-field theory[232] of the spin-Peierls state using the exact results on the quantum sine-Gordon model to develop a more quantitative description of the low temperature dimerized phase. Since we are restricting ourselves to the isotropic case, we have $K = 1$ in Eq.(5.2). By comparing with numerical calculations[243] the approximate expression of the amplitude λ in Eq.(5.2) can be found. We have [see Eq.(1.68), noting that we have rescaled the field ϕ] :

$$\frac{1}{\alpha}\mathbf{S}_n \cdot \mathbf{S}_{n+1} = \text{uniform} + (-)^n \frac{3}{\pi^2 \alpha}\left(\frac{\pi}{2}\right)^{1/4} \cos 2\phi. \tag{5.3}$$

To obtain (5.3), we have fitted the results of numerical calculations of the spin-gap in a dimerized chain[244, 245] to the sine-Gordon expression (2.54) in the isotropic limit $K = 1/2$. The results agree with numerical work for a dimerization $\delta \geq 0.03$ within 10%. Our expression for the gap is $\Delta = 1.723 J \delta^{2/3}$. More recently, Takayoshi and Sato have published numerical values of the dimer amplitude in XXZ spin chains[246] that would permit to tackle the spin-Peierls transition in the anisotropic case.

As a result of (5.4), the amplitude g in Eq.(5.2) reads:

$$g = 6J\left(\frac{\pi}{2}\right)^{1/4} \alpha, \tag{5.4}$$

Then, using that amplitude, and neglecting logarithmic corrections, minimizing with respect to δ the ground state energy, we obtain the ground state dimerization as a function of the spin-phonon coupling constant:

$$\delta = \left(\frac{2}{3\sqrt{3}}\right)^{3/2} \left(\frac{\Gamma(1/6)}{\Gamma(2/3)}\right)^3 \left[\frac{\Gamma(3/4)}{\Gamma(1/4)}\frac{3}{\pi^2}\left(\frac{\pi}{2}\right)^{1/4}\right]^2 \left(\frac{J}{\bar{K}}\right)^{3/2} \simeq 0.219 \left(\frac{J}{\bar{K}}\right)^{3/2}$$

$$\Delta = \frac{2\sqrt{\pi}}{3\sqrt{3}}\left(\frac{\Gamma(1/6)}{\Gamma(2/3)}\right)^3\left[\frac{\Gamma(3/4)}{\Gamma(1/4)}\frac{3}{\pi^2}\left(\frac{\pi}{2}\right)^{1/4}\right]^2\frac{J^2}{\bar{K}} \simeq 0.627\frac{J^2}{\bar{K}}, \tag{5.5}$$

where $\bar{K} = k\alpha$.

Using high-temperature perturbation theory as in 4.3, we obtain the approximate expression of the free energy:

$$\begin{aligned} F_s(T,\delta) &= -\frac{\pi}{6u}T^2 - \frac{a}{4}\left(\frac{2g\delta}{(2\pi a)^2}\right)^2\frac{\pi^2}{\Gamma(3/4)^4 T} \\ &= -\frac{\pi}{6u}T^2 - \frac{9J^2\delta^2}{4\pi^2\Gamma(\frac{3}{4})^4 aT}\left(\frac{\pi}{2}\right)^{1/2}, \end{aligned} \tag{5.6}$$

from which we deduce:

$$T_{SP} = \frac{9}{2\pi^2\Gamma(3/4)^4}\left(\frac{\pi}{2}\right)^{1/2}\frac{J^2}{\bar{K}} = 0.25342\frac{J^2}{\bar{K}} \tag{5.7}$$

Compared with the original mean-field theory[232], the exponents are of course recovered, but the amplitudes are also determined. Moreover, for $0 < T < T_{SP}$, it is possible to use the results of [86, 87, 88] to calculate at any temperature the Free energy of the sine-Gordon model. Using δ as a parameter, we can minimize the sum of the sine Gordon free energy and the elastic energy. This allows us to obtain the temperature dependence of δ. In turn, knowing that quantity allows the quantitative determination of the free energy.

The sine-Gordon model with $K = 1/2$ and $\cos 2\phi$ is mapped to the form (2.1) by the rescaling $\phi \to \sqrt{2}\phi$ and $K \to K/2$. Using the Eq.(2.56) with $K = 1/4$ we note that there are two breathers, a light one of mass $M_1 = M$ and a heavy one of mass $M_2 = M\sqrt{3}$. The light breather has the same mass as the solitons, and possesses a spin $S^z = 0$ while the soliton and antisoliton possess the spins $S^z = \pm 1$. Together, they form a massive spin triplet[81, 82] with the heavy breather forming a spin singlet. The sine-Gordon model is at a reflectionless point, and as a consequence of the $SU(2)$ symmetry, there are only three different S-matrix amplitudes corresponding to triplet-triplet collisions (S_{11}), singlet-triplet collisions (S_{12}) and singlet-singlet collisions (S_{22}).

Knowing the masses of the excitations, we can thus use (2.76) to determine the free energy a for given dimerization.

We have obtained the following equations[227]:

$$F_s(T,\delta) = -\frac{T}{2\pi u}\int_{-\infty}^{\infty} d\theta \Delta\cosh\theta\left[3\ln(1+e^{-\epsilon_1(\theta)/T}) + \sqrt{3}\ln(1+e^{-\epsilon_2(\theta)/T})\right] - \frac{u}{a^2}\tan\frac{\pi}{6}\frac{M^2}{4} \tag{5.8}$$

where the pseudoenergies are solutions of the integral equations:

$$\begin{aligned} \epsilon_1(\theta) &= \Delta\cosh\theta + \frac{3T}{2\pi}\int_{-\infty}^{\infty} d\theta' K_{11}(\theta-\theta')\ln(1+e^{-\epsilon_1(\theta')/T}) + \frac{T}{2\pi}\int_{-\infty}^{\infty} d\theta' K_{12}(\theta-\theta')\ln(1+e^{-\epsilon_2(\theta')/T}), \\ \epsilon_2(\theta) &= \Delta\sqrt{3}\cosh\theta + \frac{3T}{2\pi}\int_{-\infty}^{\infty} d\theta' K_{12}(\theta-\theta')\ln(1+e^{-\epsilon_1(\theta')/T}) + \frac{T}{2\pi}\int_{-\infty}^{\infty} d\theta' K_{22}(\theta-\theta')\ln(1+e^{-\epsilon_2(\theta')/T}) \end{aligned} \tag{5.9}$$

BCS/Peierls	spin-Peierls
$\frac{\Delta(0)}{k_B T_c} = 1.76$	$\frac{\Delta(0)}{K_B T_{SP}} = 2.47$
$\frac{\Delta C_v}{C_v(T_c+0)} = 1.43$	$\frac{\Delta C_v}{C_v(T_{SP}+0)} = 2.1$

Table 5.2: The universal ratios in the BCS mean-field theory and in the mean-field theory of the spin-Peierls transition.

The pseudoenergies $\epsilon_{1,2}$ have a transparent physical interpretation[85]: $\epsilon_1(\theta)$ represents the dressed energy of the solitons and of the light breather (which have identical masses at the $\beta^2 = 2\pi$ point), whereas the pseudoenergy $\epsilon_2(\theta)$ represents the dressed energy of the heavy breather. The integral kernels, deduced from the expressions of the S-matrix (2.60)– (2.65) are given by:

$$\begin{aligned} K_{11}(\theta) &= \frac{2\sin\frac{\pi}{3}\cosh\theta}{\sinh^2\theta + \sin^2\frac{\pi}{3}}, \\ K_{12}(\theta) &= \frac{2\sin\frac{\pi}{6}\cosh\theta}{\sinh^2\theta + \sin^2\frac{\pi}{6}} + \frac{2\cosh\theta\sin\frac{\pi}{2}}{\sin^2\frac{\pi}{2} + \sinh^2\theta}, \\ K_{22}(\theta) &= 3K_{11}(\theta). \end{aligned} \tag{5.10}$$

We use a simple numerical procedure to solve (5.9) for various values of the dimerization δ at a fixed temperature T. This provides us with the variational free energy energy for an entire range of δ at fixed temperature. We then identify the value of δ which minimizes that variational free energy. Repeating that process for various values of the temperature T permits us to obtain $\delta(T)$. The dimerization follows a law of corresponding states: $\delta(T) = (T_{SP}/J)^{3/2} f(T/T_{SP})$. These results for $\delta(T)$ are then used to obtain thermodynamic quantities, which also satisfy a law of corresponding states. On Fig. 5.1, the mean field dimerization $\delta(T)$ is plotted as a function of the reduced temperature T/T_{SP}. On Figs. 5.2 and 5.3 the the gap and the specific heat are represented as functions of the reduced temperature T/T_{SP} In the vicinity of T_{SP}, the gap vanishes as $\Delta \propto (T_{SP} - T)^{1/3}$ and the specific heat jumps at T_{SP} as expected for a second order transition. In the case of the usual Peierls transition, the specific heat jump and the zero temperature gap are related to the transition temperature by the same ratios as in the BCS theory of s-wave superconductivity[247]. The law of corresponding states that result from our mean-field theory of the spin-Peierls transition implies that similar universal rations will obtain. However, those ratios are strongly renormalized. The ratios are compared in the table 5.2

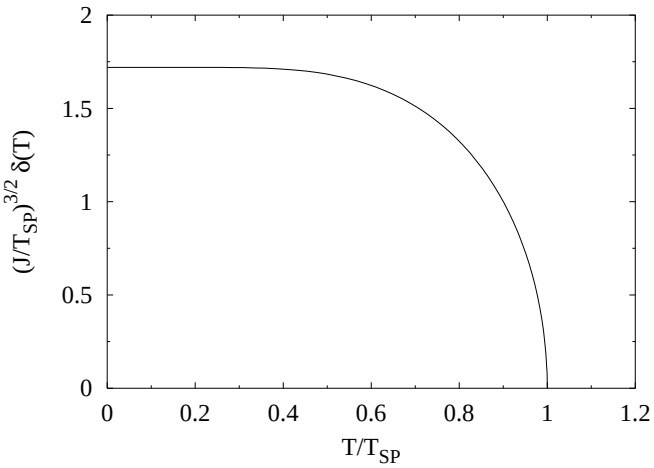

Figure 5.1: The dimensionless scaling function $\bar{\delta}$ describing the law of corresponding states followed by the spin-Peierls dimerization. The zero temperature value is reached for $T < 0.4T_{SP}$. For $T \to T_{SP}$ the scaling function $\bar{\delta} \sim (1 - T/T_{SP})^{1/2}$.

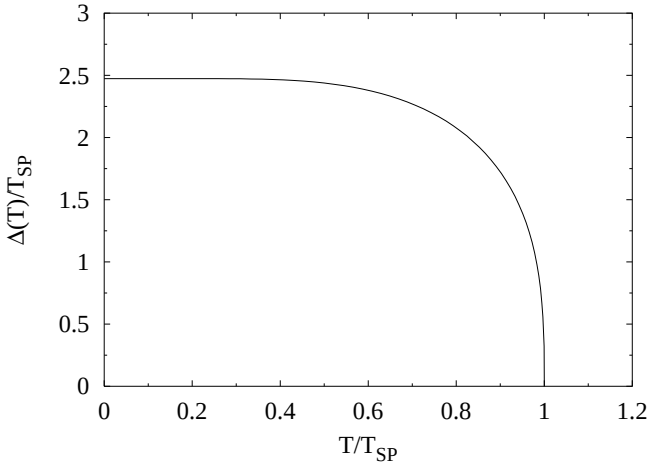

Figure 5.2: The dimensionless scaling function $\bar{\Delta}$ describing the law of corresponding states followed by the spin-Peierls gap. The universal ratio 2.47 is reached for $T < 0.4T_{SP}$. For $T \to T_{SP}$ the scaling function $\bar{\Delta} \sim (1 - T/T_{SP})^{1/3}$.

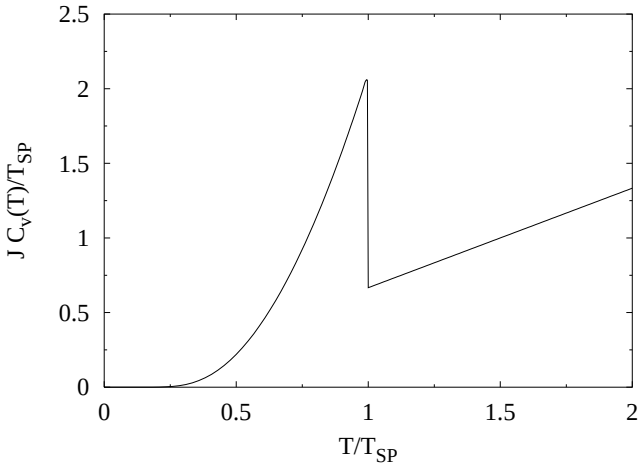

Figure 5.3: The specific heat of the spin-Peierls problem in the mean field approximation.

Part III

Interacting bosons

Chapter 6

Dipolar bosons

The present chapter is based on the articles[248, 249, 250, 251].

6.1 qualitative considerations

In trapped gases, the atoms are neutral, and their interactions are of the Van der Waals type. A phenomenological description of the interaction is obtained by using a contact interaction which reproduces the scattering cross section,

$$V(\mathbf{r}) = \frac{4\pi a}{m}\delta(\mathbf{r}). \tag{6.1}$$

In the case of gases trapped in a quasi-one dimensional geometry, the transverse degrees of freedom are frozen, and the interaction becomes a one-dimensional δ interaction. One obtains the Lieb-Liniger model[29] which is integrable. Experiments with trapped gases has been sucessfully interpreted within that framework[144, 142, 140]. Recently, atomic gases carrying a permanent magnetic dipolar moment have been trapped[252, 253] If those gases are polarized by an applied magnetic field, a dipole-dipole interaction

$$V_{dip.}(\mathbf{r}) = \frac{\mu_0}{4\pi}\frac{\mathbf{m}_1\cdot\mathbf{m}_2 - 3(\mathbf{m}_1\cdot\hat{\mathbf{r}})(\mathbf{m}_1\cdot\hat{\mathbf{r}})}{|\mathbf{r}|^3}, \tag{6.2}$$

where $\mathbf{m}$ is the magnetic moment of an atom, and $\hat{\mathbf{r}} = \mathbf{r}/|\mathbf{r}|$ is present. Moreover, molecules with permanent electric dipoles have been also trapped (but not cooled to degeneracy) and in these systems electric dipole forces are also present. When the dipoles are polarized in a direction orthogonal to the axis, the forces are repulsive, and vary as C/r^3.

In one-dimension, dipolar interactions are short range forces, with $\int_a^\infty |V_{dip.}(r)|dr < \infty$, where a is a short distance cutoff. The Mermin-Wagner-Hohenberg theorem ensures that they cannot induce a crystalline order[16, 17, 18] and a Tomonaga-Luttinger liquid is still expected. However, for short distances, in one dimension, the dipolar forces are strongly repulsive. Indeed, if we consider a two-body Schrödinger equation,

$$H = -\frac{1}{2m}\partial_x^2\psi + \frac{C}{|x|^3}\psi = E\psi, \tag{6.3}$$

where x is the relative coordinate, a semiclassical WKB approximation gives a wavefunction $\psi(x)$ varying as:

$$\psi(x) \sim \frac{1}{\sqrt{mC}} e^{-2\sqrt{\frac{mC}{|x|}}}, \tag{6.4}$$

and vanishing when the particles are coming in contact. As a result, in a dilute gas of dipolar particles, where three-body interactions are infrequent, one expects that the many-body wavefunction vanishes anytime two particles are at the same point. Such a condition is also satisfied in a fermionic gas. However, the wavefunction of a fermion gas is antisymmetric under permutation of particles, while the wavefunction of a Bose gas is symmetric under particle permutation. This difference can be corrected by multiplying the fermion wavefunction by a factor:

$$\prod_{i<j} \text{sign}(x_i - x_j) = \text{sign}\left[\prod_{i<j} (x_i - x_j)\right], \tag{6.5}$$

indeed, the expression in the right hand-side of (6.5) is the sign of a Vandermonde determinant (the columns of which are successive powers of the coordinates of the particles) which is changing sign under permutation of the particle coordinates. Multiplying the factor (6.5) by a fermionic wavefunction gives a function that does not change sign under permutation of particles but vanishes every time two particles are at the same point. This process in in fact[254] a first quantized version of the Jordan-Wigner transformation (1.57). Since in a dilute dipolar gas interactions beyond two body can be neglected, one can take as the fermionic wavefunction a Slater determinant of plane waves. This leads us to expect that the dilute gas of bosonic particles has the same thermodynamics as a free fermionic gas, with an energy per unit length varying as $e(n_0) \propto n_0^3$. In the opposite limit of high density, if we were dealing with a classical gas, the repulsion between the particles would give us a one dimensional crystal. In such a crystal, the energy per unit length would be:

$$e(n_0) = C\zeta(3) n_0^4, \tag{6.6}$$

where n_0 is the number of particles per unit length, and would dominate the kinetic energy from zero point motion, $\propto n_0^3$. Since the system is in the Tomonaga-Luttinger liquid state, we can use (6.6) to estimate the particle velocity and Tomonaga-Luttinger exponent. By Galilean invariance (1.80),

$$uK = \frac{\pi n_0}{M}, \tag{6.7}$$

and by the compressibility relation (1.76), giving

$$K = \frac{\pi}{\sqrt{12\zeta(3) M n_0}}. \tag{6.8}$$

From these qualitative considerations, we expect that for low density $K \to 1$ and for high density $K \to 0$. This is to be contrasted with the behavior of the Luttinger exponent in the Lieb-Liniger gas, where $K \to +\infty$ for high density, and $K \to 1$ for low density. The dipolar is covering a range of Tomonaga-Luttinger exponent complementary to that of the Lieb-Liniger gas.

6.2 Determination of the Luttinger exponent

In order to determine the exponents quantitatively, one must turn to numerical methods. The Reptation Quantum Monte-Carlo method [255] were done by S. De Palo in Trieste.

In order to extract the Tomonaga-Luttinger exponent from the numerical simulation, we have use the following approach. In a finite size system with periodic boundary conditions, we can use the Haldane expansion (1.87) and the correlation function:

$$\langle e^{2im\phi(x)}e^{-2im\phi(0)}\rangle = \left[\frac{(1-e^{-\frac{2\pi a_0}{L}})^2}{\left(1-e^{-\frac{2\pi a_0}{L}}e^{\frac{2i\pi x}{L}}\right)\left(1-e^{-\frac{2\pi a_0}{L}}e^{-\frac{2i\pi x}{L}}\right)}\right]^{m^2K}, \tag{6.9}$$

we can obtain an expression of the static structure factor:

$$S(q) = \int e^{iqx}\langle n(x)n(0)\rangle, \tag{6.10}$$

in the form:

$$S(q) = \sum_{m\neq 0} A_m^2 n_0^2 \Sigma_m(q \pm 2\pi m n_0) + S_0(q), \tag{6.11}$$

where:

$$\Sigma_m(q) = L(1-e^{-\frac{2\pi a_0}{L}})^{2m^2K}\frac{\Gamma(m^2K+\frac{|q|L}{2\pi})}{\Gamma(m^2K)\Gamma(1+\frac{|q|L}{2\pi})}{}_2F_1\left(m^2K, m^2K+\frac{|q|L}{2\pi}; 1+\frac{|q|L}{2\pi}; e^{\frac{-4\pi\alpha}{L}}\right), \tag{6.12}$$

and:

$$S_0(Q) = \frac{KQ}{2\pi}. \tag{6.13}$$

When $2m^2K < 1$, the expression (6.12) can be simplified to the form:

$$\Sigma_m(q) = L(1-e^{-\frac{2\pi\alpha}{L}})^{2m^2K}\sin(\pi m^2K)B\left(1-2m^2K, m^2K+\frac{|q|L}{2\pi}\right), \tag{6.14}$$

so that $\Sigma_m(0) \sim L^{1-2m^2K} \to +\infty$ as $L \to +\infty$, while for $2m^2K > 1$, $\Sigma_m(q)$ behaves as:

$$\Sigma_m(q) \to 2\pi a_0 2^{1-2m^2K}\frac{\Gamma(2m^2K-1)}{\Gamma(m^2K)^2}. \tag{6.15}$$

We fit $S(q)$ for $q \ll 2\pi n_0$ to a straight line, and obtain the exponent K from the slope. The result is represented on the Fig.6.1. For low density, we obtain $K \simeq 1$ as expected from the previous heuristic arguments. At high density, the exponent behaves as $(nr_0)^{-1/2}$. Knowing the exponent, we can check the TLL behavior by comparing for $2m^2K < 1$ the behavior of $S(q)/S(2\pi m n_0)$ for q in the vicinity of $2\pi m n_0$ with the predictions of Eq. (6.12). The result of such comparison is shown on the Fig.6.2. [248, 249, 250, 251]

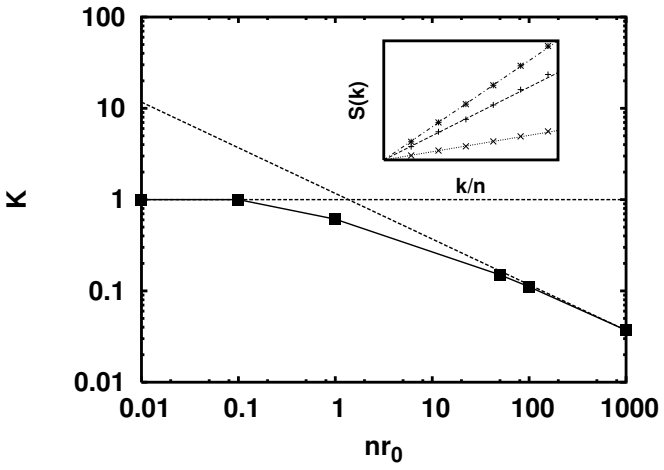

Figure 6.1: The Tomonaga-Luttinger exponent of the one-dimensional gas of dipoles as a function of density. The squares are the numerically computed exponent, the dotted line is the hard-core boson exponent, the dashed line the high density limit. In the inset, the structure factor for different values of the density has been represented. The linear slope at the origin directly gives the Tomonaga-Luttinger exponent. From [248]

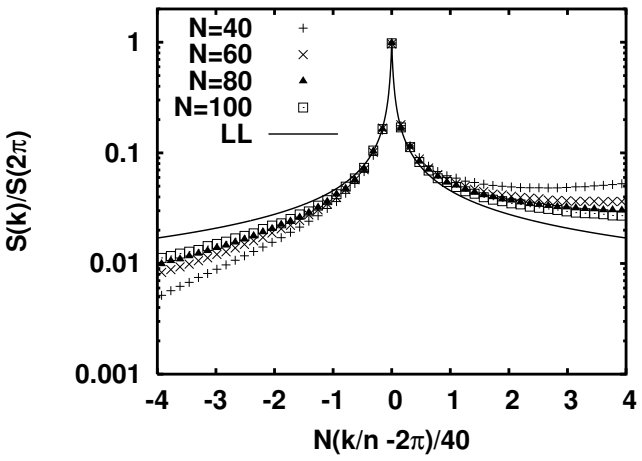

Figure 6.2: Scaling of the structure factor in the vicinity of the peak $k = 2\pi\rho_0$ at fixed density and for an increasing system size. The solid line is the prediction from the Tomonaga-Luttinger liquid theory. From [248]

Chapter 7

Bosonic ladders under field

The present chapter is based on the article [256].

We consider two one-dimensional bosonic chains coupled by interchain repulsion and interchain hopping. Those systems can be realized either by coupling Josephson junctions or by coupling two one-dimensional trapped atomic gases. The Hamiltonian of coupled Josephson junctions reads[257, 258, 259]

$$\begin{aligned} H &= -\sum_{n,p}\left[J_{\parallel}\cos(\theta_{n,p}-\theta_{n+1,p})+\frac{e^2}{2C}N_{n,p}^2-eV_gN_{n,p}\right] \\ &\quad -\sum_{n}\left[J_{\perp}\cos(\theta_{n,1}-\cos\theta_{n,2})+\frac{e^2}{C_{\perp}}N_{n,1}N_{n,2}\right], \end{aligned} \tag{7.1}$$

where $J_{\parallel}, J_{\perp}$ are the longitudinal and transverse Josephson couplings, C is the capacity to the ground, and V_g is the gate voltage. From the Eqs. (1.93) and (1.87), it is easily seen that those systems have the same Hamiltonian (4.10) as two-leg spin ladders. The phase diagram of the spin ladders translate directly into a phase diagram for the boson ladders. However, in Josephson ladders, the Cooper pairs are charged, and are sensitive to an applied external magnetic field. To consider the effect of an external magnetic field, we must first remark that (7.1) is not gauge invariant. Indeed, under a gauge transformation of the vector potential $A \to A + \nabla\chi$, the Cooper pair creation operator transforms as:

$$e^{i\theta_{n,p}} \to e^{i\theta_{n,p}+2e\chi_{n,p}}, \tag{7.2}$$

so that in order to obtain a gauge invariant expression we have to make the Peierls substitution:

$$e^{i(\theta_n-\theta_m)} \to e^{i(\theta_n-\theta_m)-2e\int_n^m A dr}, \tag{7.3}$$

We can choose a gauge with the vector potential $\mathbf{A} = -By\mathbf{e}_x$ along the chains. In that gauge, the longitudinal Josephson couplings become:

$$J_{\parallel}\cos\left(\theta_{n,p}-\theta_{n+1,p}-eB(p-1/2)ba\right), \tag{7.4}$$

where a is the length of a junction along the chain, and b is the length of a rung junction and the transverse couplings are unchanged. In the case of coupled one-dimensional gases, it is possible

to create artificial gauge fields that simulate the effect of a uniform magnetic field.[260, 261, 262] After bosonization, the Hamiltonian becomes[263]

$$\begin{aligned} H &= H_s + H_a \\ H_a &= \int \frac{dx}{2\pi}\left[u_a K_a(\pi\Pi_a - e^* A_a)^2 + \frac{u_a}{K_a}(\partial_x\phi_a)^2\right] - \frac{J_\perp}{\pi a}\int dx\cos(\sqrt{2}\theta_a) \\ &\quad + \frac{2Va}{(2\pi a)^2}\int dx\cos\sqrt{8}\phi_a, \end{aligned} \tag{7.5}$$

with $V \sim e^2/C_\perp$ and the currents are:

$$j_a = uKe^*\sqrt{2}(\Pi_\nu - \frac{e^*}{\pi}A_\nu) \tag{7.6}$$

$$j_\perp = \frac{e^* J_\perp}{\pi a}\sin(\sqrt{2}\theta_a) \tag{7.7}$$

The Hamiltonian (7.5) also describes a two-leg spin ladder having different uniform Dzyaloshinskii-Moriya interactions on the two legs.

With a weak external field, the Hamiltonian H_a remains gapped with $\langle j_a\rangle = -uK\frac{(e^*)^2\Phi}{\pi a}$ and $\langle j_\perp\rangle = 0$. There is only a current circulating along the edge of the system, with no current in the bulk of the ladder. That low field phase can be identified with a Meissner phase[258]. Under a stronger field, a commensurate-incommensurate transition as discussed in Sec.4.3 can be obtained. There are however two differences with the case of the ladder in applied field. The obvious first one is that now the field θ_a is coupled to the applied magnetic field instead of the field ϕ_s. The second, and more important difference, is that the field $\cos\sqrt{8}\phi_a$ is also present in H_a. Since at the transition $K_a^* = 1/2$, that field is relevant, the commensurate-incommensurate transition is avoided[264] and the system remains gapped across the transition. In the magnetized phase, the system is showing power-law density wave correlations with exponential decay of the bosonic correlation functions $\langle e^{i\theta_{n,p}}e^{-i\theta_{m,p}}\rangle$.

For sufficiently large field, we can have $K_a^*(h) > 1$ and $\cos\sqrt{8}\phi_a$ again irrelevant. The spectrum of H_a is then gapless and both density wave and bosonic correlations decay as power-laws. The gapful regime and the gapless regime are separated by a Kosterlitz-Thouless phase transition.

In the presence of a stronger flux, close to a rational number p/q of quantum of flux per plaquette $e^*\Phi = 2\pi\frac{p}{q} + \delta\Phi$, with the denominator q not too large and $\delta\Phi \ll 2\pi\frac{p}{q}$, the gauge with the vector potential along the legs of the ladder is not convenient for perturbative bosonization as it would give an very large field. The most convenient gauge choice is instead $A_\perp(n) = n(2\pi e^* p)/q$ and $A_a = (\delta\Phi)/(a\sqrt{2})$. With such a gauge choice, the interchain Josephson coupling is of the form:

$$J_\perp\sum_n \cos(\theta_{n,1} - \theta_{n,2} - A_\perp(n)), \tag{7.8}$$

which is in general an oscillating term and gives a vanishing contribution to the Hamiltonian in bosonization. However, perturbation theory to order q will give a term:

$$(J_\perp)^q/J_\parallel^{q-1}\sum_n \cos q(\theta_{n,1} - \theta_{n,2}), \tag{7.9}$$

which is not oscillating since $qA_\perp(n)$ is an integer multiple of 2π. After bosonization, we obtain a Hamiltonian of the form:

$$\begin{aligned} H_a &= \int \frac{dx}{2\pi}\left[u_a K_a(\pi\Pi_a - e^* A_a)^2 + \frac{u_a}{K_a}(\partial_x\phi_a)^2\right] - \frac{J_\perp^q}{\pi J_\parallel^{q-1} a}\int dx\cos(q\sqrt{2}\theta_a) \\ &+ \frac{2Va}{(2\pi a)^2}\int dx\cos\sqrt{8}\phi_a, \end{aligned} \tag{7.10}$$

which, when $4K_a > q^2$ can present a gapful phase for small $\delta\Phi$ and a gapless phase for larger $\delta\Phi$. We note that for $q \geq 2$, the $\cos\sqrt{8}\phi_a$ term is irrelevant, and will not modify the commensurate incommensurate transition in contrast to the zero-flux case. In the gapful phase, the gapped excitations are vortices carrying a fractional flux $2\pi/q$. The gauge transformation makes the transverse current $j_\perp = J_\perp \sin(\sqrt{2}\theta_a - A_\perp(n))$ a spatially modulated quantity. In the gapful phase, $\langle j_\perp\rangle(x)$ becomes a periodic function of x, while the longitudinal current $\langle j_\parallel\rangle = 0$. Returning to the original gauge, this indicates that $\theta_{n,1} - \theta_{n,2}$ is growing linearly with n *i. e.* that a commensurate vortex lattice is formed. When $\delta\Phi$ is such that the system is in the incommensurate phase, $\langle j_\perp(x)\rangle = 0$ while $\langle j_\parallel\rangle \propto \delta\Phi$. That phase can be seen as a Luttinger liquid of vortices (carrying the fractional flux $2\pi/q$). This leads us to conjecture the following form of the vortex density:

$$\rho_V(x) = \frac{1}{\pi\sqrt{2}}\partial_x\theta_a + \sum_{m=-\infty}^{m=\infty}\frac{C_m}{\pi a}\, e^{im[2\pi\bar{\rho}_V x + \sqrt{2}(\theta_a - \langle\theta_a\rangle)]} \tag{7.11}$$

When the density of vortices is p/q, the potential energy term (7.9) can be interpreted as the coupling of the vortex density to a pinning potential of period q lattice spacings.

In the classical case [265], a vortex lattice phase is obtained each time the flux per plaquette in a rational multiple of the quantum of flux, leading to a devil's staircase structure in the behavior of the magnetization. Here, the quantum fluctuations wipe out the large fractions for which $q^2 > 4K_a$, so only some plateaux remain as shown on Fig. 7.1.

It is also possible to use the fermionization approach to calculate the behavior of the current in the ladder in the vicinity of the commensurate-incommensurate transition for $q > 1$. We find that the current behaves as:

$$\langle j_a\rangle = \frac{u(e^*)^2}{2\pi a}(\sqrt{\Phi^2 - \Phi_c^2}\,\theta(\Phi^2 - \Phi_c^2) - \Phi) \tag{7.12}$$

For $\Phi < \Phi_c$, the current is linear in flux, producing a one-dimensional analog of the Meissner effect. When $\Phi > \Phi_c$, vortices appear in the ladder, and the applied flux is only partially screened.

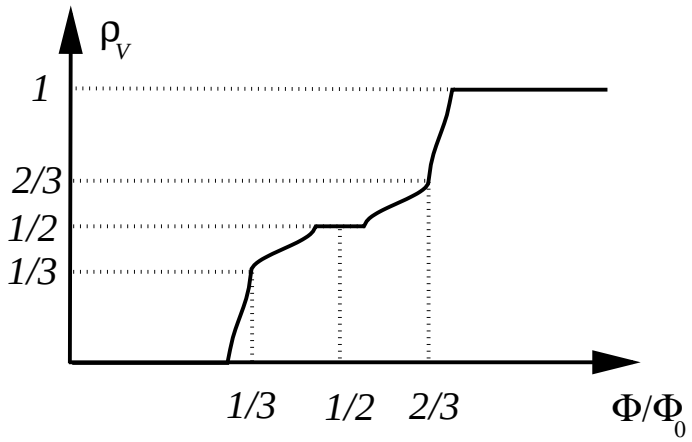

Figure 7.1: Sketch of the staircase in the magnetization of the bosonic or Josephson ladder. On the figure, $K_a = 4$, so that only the plateaus obtained for $p/q = 0, 1/3, 1/2, 2/3, 1$ survive to the quantum fluctuations. Note that the width of the $1/3$ and $2/3$ plateaus is already extremely reduced compared with the width of the $1/2$ plateau.

Chapter 8

Disordered bosons

The present chapter is based on the articles [266, 267].

8.1 The Aubry-André transition

The Aubry-André transition was predicted in tight-binding chains with an on-site quasiperiodic potential.[268] The Aubry-André Hamiltonian reads:

$$H = -t\sum_n (a_n^\dagger a_{n+1} + a_{n+1}^\dagger a_n) + \Delta \sum_n \cos(2\pi Q n) a_n^\dagger a_n, \tag{8.1}$$

where Q is an irrational number so that the potential in (8.1) is not periodic. Going to Fourier space,

$$a_n = \frac{1}{\sqrt{N}} \sum_n \hat{a}_k e^{ikn}, \tag{8.2}$$

we rewrite the Hamiltonian (8.1) as:

$$H = \sum_k \left[-2t\cos(k)\hat{a}_k^\dagger \hat{a}_k + \frac{\Delta e^{i\phi}}{2}\hat{a}_k^\dagger \hat{a}_{k-2\pi Q} + \frac{\Delta e^{-i\phi}}{2}\hat{a}_k^\dagger \hat{a}_{k+2\pi Q} \right] \tag{8.3}$$

We note that the Hamiltonian (8.3) is of a form similar to (8.1), the sites being the momentas $2\pi nQ$, the kinetic energy $-2t\cos(2\pi nQ)$ being the on-site energy, and the hopping being $\Delta/2$.Here, the irrationality of Q plays a crucial role. The set of numbers $nQ+m$ with $n, m \in \mathbb{Z}$ is dense in the set of real numbers allowing us to approximate any momentum k as $2\pi nQ$ for some n. The mapping of the Hamiltonian (8.1) on the Hamiltonian (8.3) is a duality transformation, that exchanges Δ with $2t$. For small $\Delta/(2t)$, the eigenstates of (8.1) are extended in real space, and the eigenstates of (8.3) are localized. Vice-versa, for large $\Delta/(2t)$, the eigenstates of (8.1) are localized, while those of (8.3) are extended. Thus, a transition from extended to localized eigenstates is expected in the Aubry-André model at the self-dual point $\Delta = 2t$. Under that hypothesis, the localization length in the phase $\Delta > 2t$ can be obtained from the

Herbert-Jones-Thouless formula[269, 270]. According to that relation, in a one-dimensional non-interacting system, the inverse localization length $\ell_{\rm loc.}(E)$ is related to the density of states ${}_rho(E)$ by the relation:

$$\frac{1}{\ell_{\rm loc.(}E)} = \int dE' \rho(E') \ln|E - E'|, \tag{8.4}$$

Since duality implies that $t\rho(E,\Delta) = \Delta\rho(E,2t)/2$, we obtain from (8.4) that

$$\frac{1}{\ell_{\rm loc.}(E,\Delta)} = \frac{1}{\ell_{\rm loc.}(E,2t)} + 2\ln\left(\frac{\Delta}{2t}\right), \tag{8.5}$$

and since for $\Delta > 2t$ the states must be localized, the localization length is $2\ln[\Delta/(2t)]$. The localization length is diverging at the metal-insulator transition.

Recently, experiments on cold atomic gases have observed the Aubry-André transition.[271]. A trapped gas was left to expand in a quasiperiodic potential created by lasers of different wavelengths. A Feshbach resonance was used to tune the repulsive interaction on the bosons to zero. It was observed that when the strength of the secondary lattice exceeded a critical value, the expansion of the gas stopped.

8.2 Effect of interaction

An interesting question is the effect of interaction on the Aubry-André transition of bosons. That problem can be investigated in the framework of the Bose-Hubbard-Aubry-André model with Hamiltonian:

$$H = -t\sum_n (b_n^\dagger b_{n+1} + b_{n+1}^\dagger b_n) + \Delta\sum_n \cos(2\pi Q n) b_n^\dagger b_n + U\sum_n (b_n^\dagger b_n)^2 \tag{8.6}$$

A simple case is the limit of the hard core bosons $U/t \to \infty$, where we can map the problem onto non-interacting fermions. Then, it is obvious that the Aubry-André transition remains at $\Delta = 2t$. Below the transition, the Fermion wavefunctions are extended, and we thus expect the hard core Bose gas to remain in the TLL state. Above the transition, we expect the bosons to become localized. However, the compressibility remains finite, so we should have a Bose glass phase. In the case of a finite but nonzero U/t, and for $\Delta \ll t$, two cases are possible. First, when the density ρ_0 is such that Q/ρ_0 is not an integer, the potential is incommensurate, and for $\Delta \ll t$, the TLL state is stable. A phase transition to the Bose Glass state can be obtained only when $\Delta/t = O(1)$. Second, when $Q = m\rho_0$, where m is integer, the system is described by a sine-Gordon model. When the cosine term is relevant (i. e. for $K < 1/(2m^2)$ or for large enough Δ), a gap opens, and the Luttinger liquid is replaced by an incommensurate density wave[272]. Otherwise, the TLL state remains stable. A more detailed study of the problem can be done using the DMRG technique. To distinguish the TLL from the Bose glass state, one needs to obtain the stiffness which is nonzero only in the former phase.

In the TLL phase, the momentum distribution $n(k) \sim |k|^{1/(2K)-1}$ for $kL \gg 1$. In the hard core boson limit,[272] $K = 1$ everywhere in the TLL phase. Moreover, because of the

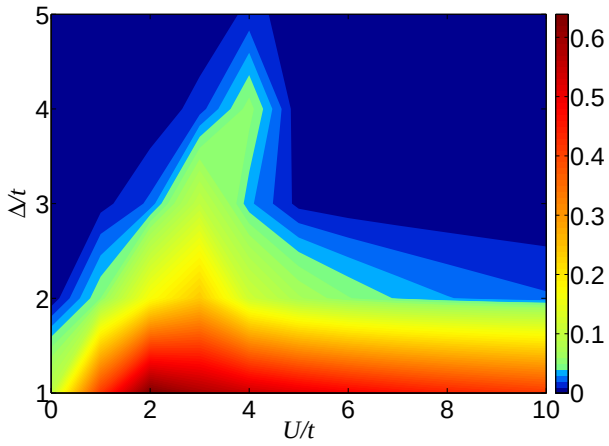

Figure 8.1: Intensity plot of the Kohn stiffness for the Bose-Hubbard-Aubry-André model at half-filling versus U/t and Δ/t. The regions with small Kohn stiffness correspond to a Bose Glass, the regions with large Kohn stiffness to a Tomonaga-Luttinger liquid. The boundary $\Delta/t = 2$ between the localized phase and the TLL is recovered in the two limits $U/t \to 0$ and $U/t \to +\infty$.

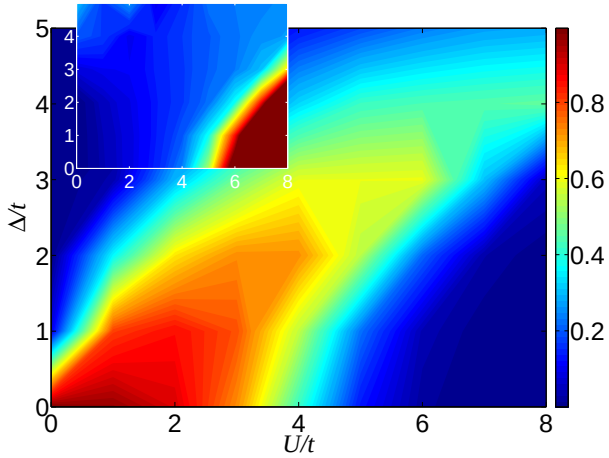

Figure 8.2: Phase diagram of the Bose-Hubbard-Aubry-André model at filling of one boson per site. Main panel: Intensity plot of the Kohn stiffness versus U/t and Δ/t. The regions with small Kohn stiffness correspond to a Bose Glass or a Bosonic Mott insulator, the regions with large Kohn stiffness to a Tomonaga-Luttinger liquid. Inset: Intensity plot of the inverse compressibility. The region of low compressibility is a Mott insulator.

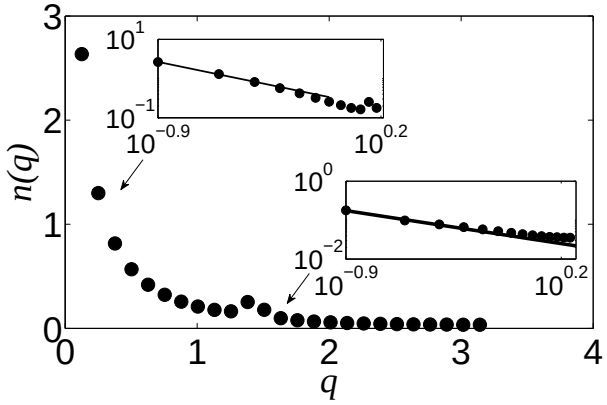

Figure 8.3: The momentum distribution function in the TLL phase with $U = 2t$, $\Delta = U/2$. Both peaks at $q = 0$ and $q = 2\pi Q$ correspond to a power law decay with an exponent $1/(2K) - 1 = -0.85$.

presence of the incommensurate potential, the peak in the vicinity of $k = 0$ possesses satellites at $k = 2\pi Q$ as shown on Fig. 8.3.

Bibliography

[1] L. D. Landau, Sov. Phys. JETP **3**, 920 (1957).

[2] L. D. Landau, Sov. Phys. JETP **5**, 101 (1957).

[3] L. D. Landau, Sov. Phys. JETP **8**, 70 (1958).

[4] P. Nozieres, *Theory of Interacting Fermi Systems*, Benjamin, New York, 1961.

[5] A. A. Abrikosov, L. P. Gorkov, and I. E. Dzyaloshinski, *Methods of Quantum Field Theory in Statistical Physics*, Dover, New York, 1963.

[6] J. Sólyom, Adv. Phys. **28**, 209 (1979).

[7] V. J. Emery, Theory of the one-dimensional electron gas, in *Highly conducting one-dimensional solids*, edited by J. T. Devreese, R. P. Evrard, and V. E. van Doren, page 247, New York and London, 1979, Plenum Press.

[8] S. Tomonaga, Prog. Theor. Phys. **5**, 544 (1950).

[9] J. M. Luttinger, J. Math. Phys. **4**, 1154 (1963).

[10] F. D. M. Haldane, J. Phys. C **14**, 2585 (1981).

[11] L. D. Landau and E. M. Lifshitz, *Theory of Elasticity*, Pergamon Press, New York, 1959.

[12] D. C. Mattis and E. H. Lieb, J. Math. Phys. **6**, 304 (1965).

[13] A. Luther and I. Peschel, Phys. Rev. B **9**, 2911 (1974).

[14] D. Orgad, Phil. Mag. B **81**, 377 (2001).

[15] A. E. Mattson, S. Eggert, and H. Johannesson, Phys. Rev. B **56**, 15615 (1997).

[16] N. D. Mermin and H. Wagner, Phys. Rev. Lett. **17**, 1133 (1967).

[17] N. D. Mermin, Phys. Rev. **176**, 250 (1968).

[18] P. C. Hohenberg, Phys. Rev. **158**, 383 (1967).

[19] M. Abramowitz and I. Stegun, *Handbook of mathematical functions*, Dover, New York, 1972.

[20] G. D. Mahan, *Many Particle Physics*, Plenum, New York, 1981.

[21] R. Shankar, Int. J. Mod. Phys. B **4**, 2371 (1990).

[22] H. J. Schulz and C. Bourbonnais, Phys. Rev. B **27**, 5856 (1983).

[23] H. J. Schulz, Phys. Rev. B **34**, 6372 (1986).

[24] P. Jordan and E. Wigner, Z. Phys. **47**, 631 (1928).

[25] J. M. Ziman, *Principles of the Theory of Solids*, Cambridge University Press, Cambridge, 1972.

[26] I. Affleck, Field theory methods and quantum critical phenomena, in *Fields, Strings and Critical Phenomena*, edited by E. Brezin and J. Zinn-Justin, page 563, Amsterdam, 1988, Elsevier Science.

[27] T. Holstein and H. Primakoff, Phys. Rev. **58**, 1098 (1940).

[28] M. Girardeau, J. Math. Phys. **1**, 516 (1960).

[29] E. H. Lieb and W. Liniger, Phys. Rev. **130**, 1605 (1963).

[30] A. Luther and I. Peschel, Phys. Rev. B **12**, 3908 (1975).

[31] F. D. M. Haldane, Phys. Rev. Lett. **45**, 1358 (1980).

[32] C. Itzykson and J.-M. Drouffe, *Statistical Field Theory*, volume 2, Cambridge University Press, Cambridge, UK, 1991.

[33] K. Nomura, The end of c=1 cft, cond-mat/9605070, 1996.

[34] D. C. Cabra and J. E. Drut, J. Phys.: Condens. Matter **15**, 1445 (2003).

[35] V. L. Berezinskii, Sov. Phys. JETP **32**, 493 (1971).

[36] J. M. Kosterlitz and D. J. Thouless, J. Phys. C **6**, 1181 (1973).

[37] M. A. Cazalilla, J. Phys. B **37**, S1 (2004).

[38] T. D. Kühner and H. Monien, Phys. Rev. B **58**, R14741 (1998).

[39] F. D. M. Haldane, Phys. Rev. Lett. **47**, 1840 (1981).

[40] S. Lukyanov and V. Terras, Nucl. Phys. B **654**, 323 (2003), hep-th/0206093.

[41] T. Giamarchi and H. J. Schulz, Phys. Rev. B **39**, 4620 (1989).

[42] J. von Delft and H. Schoeller, Ann. Phys. (Leipzig) **7**, 225 (1998).

[43] H. Kruis, I. McCulloch, Z. Nussinov, and J. Zaanen, Europhys. Lett. **65**, 512 (2004).

[44] H. V. Kruis, I. P. McCulloch, Z. Nussinov, and J. Zaanen, Phys. Rev. B **70**, 075109 (2004).

[45] H. J. Schulz, Phys. Rev. Lett. **64**, 2831 (1990).

[46] F. Mila and X. Zotos, Europhys. Lett. **24**, 133 (1993).

[47] H. Frahm and V. E. Korepin, Phys. Rev. B **42**, 10553 (1990).

[48] H. Frahm and V. E. Korepin, Phys. Rev. B **43**, 5663 (1991).

[49] K. Penc, K. Hallberg, F. Mila, and H. Shiba, Phys. Rev. Lett. **77**, 1390 (1996).

[50] G. A. Fiete, Rev. Mod. Phys. **79**, 801 (2007).

[51] K. A. Matveev, A. Furusaki, and L. I. Glazman, Phys. Rev. B **76**, 155440 (2007).

[52] A. Iucci, G. A. Fiete, and T. Giamarchi, Phys. Rev. B **75**, 205116 (2007).

[53] A. Erdélyi, W. Magnus, F. Oberhettinger, and F. G. Tricomi, *Higher transcendental functions*, volume 1, McGraw-Hill, NY, 1953.

[54] M. Le Bellac, *Quantum and Statistical Field Theory*, Oxford University Press, Oxford, UK, 1992.

[55] A. O. Gogolin, A. A. Nersesyan, and A. M. Tsvelik, *Bosonization and Strongly Correlated Systems*, Cambridge University Press, Cambridge, 1999.

[56] E. Orignac, M. Tsuchiizu, and Y. Suzumura, Phys. Rev. B **84**, 165128 (2011), arXiv:1107.3497.

[57] E. Orignac, M. Tsuchiizu, and Y. Suzumura, Spectral functions in a two-velocities tomonaga-luttinger liquid, 2012, to be published in J. Phys. Conf. Series, proceedings of SCES 2011 08/29 to 09/03/2011 Cambridge, UK.

[58] V. Meden and K. Schönhammer, Phys. Rev. B **46**, 15753 (1992).

[59] J. Voit, Phys. Rev. B **47**, 6740 (1993).

[60] N. Nakamura and Y. Suzumura, Prog. Theor. Phys. **98**, 29 (1997).

[61] K. Kugel and D. Khomskii, Usp. Fiz. Nauk **136**, 621 (1982).

[62] K. A. Muttalib and V. J. Emery, Phys. Rev. Lett. **57**, 1370 (1986).

[63] T. Hikihara, A. Furusaki, and K. A. Matveev, Phys. Rev. B **72**, 035301 (2005).

[64] E. Orignac, M. Tsuchiizu, and Y. Suzumura, Phys. Rev. A **81**, 053626 (2010).

[65] E. Orignac and R. Citro, Response functions in multicomponent luttinger liquids, arXiv:1209.3874, 2012.

[66] F. D. M. Haldane, Phys. Rev. B **25**, 4925 (1982), *ibid.* **26**, 5257(E) (1982).

[67] R. Rajaraman, *Solitons and Instantons: An Introduction to solitons and Instantons in Quantum Field Theory*, North Holland, Amsterdam, 1982.

[68] J. Cardy, *Scaling and Renormalization in Statistical Physics*, Cambridge University Press, Cambridge, 1996.

[69] S. Eggert, Phys. Rev. B **54**, R9612 (1996).

[70] S. Eggert, I. Affleck, and M. Takahashi, Phys. Rev. Lett. **73**, 332 (1994).

[71] A. Luther and V. J. Emery, Phys. Rev. Lett. **33**, 589 (1974).

[72] J. B. Zuber and C. Itzykson, Phys. Rev. D **15**, 2875 (1977).

[73] B. Schroer and T. T. Truong, Nucl. Phys. B **144**, 80 (1978).

[74] T. Wu, B. McCoy, C. Tracy, and E. Barouch, Phys. Rev. B **13**, 1976 (1976).

[75] E. Ince, *Ordinary Differential Equations*, Dover, New York, 1956.

[76] H. Bergknoff and H. B. Thacker, Phys. Rev. D **19**, 3666 (1979).

[77] H. A. Thacker, Rev. Mod. Phys. **53**, 253 (1981).

[78] A. B. Zamolodchikov, Int. Review of Modern Physics A **10**, 1125 (1995).

[79] S. Lukyanov and A. B. Zamolodchikov, Nucl. Phys. B **493**, 571 (1997).

[80] R. F. Dashen, B. Hasslacher, and A. Neveu, Phys. Rev. D **11**, 3424 (1975).

[81] I. Affleck, Nucl. Phys. B **265**, 448 (1986).

[82] G. S. Uhrig and H. J. Schulz, Phys. Rev. B **54**, R9624 (1996).

[83] P. Dorey, Exact s-matrices, hep-th/9810026, 1998.

[84] G. Mussardo, Phys. Rep. **218**, 215 (1992).

[85] H. Saleur, Lectures on non perturbative field theory and quantum impurity problems, in *Topological aspects of low dimensional systems*, edited by A. Comtet, T. Jolicoeur, S. Ouvry, and F. David, volume 69 of *Les Houches Summer School*, page 475, Berlin, 1998, Springer.

[86] M. Fowler and X. Zotos, Phys. Rev. B **24**, 2634 (1981).

[87] M. Fowler and X. Zotos, Phys. Rev. B **25**, 5806 (1982).

[88] M. D. Johnson, N.-N. Chen, and M. Fowler, Phys. Rev. B **34**, 7851 (1986).

[89] E. Jeckelmann, F. Gebhard, and F. H. L. Essler, Phys. Rev. Lett. **85**, 3910 (2000).

[90] D. Controzzi, F. H. L. Essler, and A. M. Tsvelik, Dynamical properties of one-dimensional mott insulators, in *New Theoretical approaches to strongly correlated systems*, edited by A. M. Tsvelik, volume 23 of *NATO Science Series II. Mathematics, Physics and Chemistry*, page 25, Dordrecht, 2001, Kluwer Academic Publishers.

[91] F. H. L. Essler, F. Gebhard, and E. Jeckelmann, Phys. Rev. B **64**, 125119 (2001).

[92] F. H. L. Essler, A. M. Tsvelik, and G. Delfino, Phys. Rev. B **56**, 11001 (1997).

[93] F. H. L. Essler and A. M. Tsvelik, Phys. Rev. B **57**, 10592 (1998).

[94] F. H. L. Essler, Phys. Rev. B **59**, 14376 (1999).

[95] F. H. L. Essler, A. Furusaki, and T. Hikihara, Phys. Rev. B **68**, 64410 (2003).

[96] F. H. L. Essler and A. M. Tsvelik, Phys. Rev. Lett. **88**, 96403 (2002).

[97] M. Karowski and P. Wiesz, Nucl. Phys. B **139**, 455 (1978).

[98] V. I. Smirnov, *A course of higher mathematics*, volume IV-1, Pergamon Press, New York, 1964.

[99] H. Saleur, Lectures on non perturbative field theory and quantum impurity problems: Part ii, in *New Theoretical Approaches to Strongly Correlated systems*, edited by A. M. Tsvelik, volume 23 of *NATO SCIENCE SERIES: II: Mathematics, Physics and Chemistry*, chapter 3, page 47, Kluwer Academic Publishers, Dordrecht, 2001.

[100] F. A. Smirnov, *Form Factors in Completely Integrable Models of Quantum Field Theory*, World Scientific, Singapore, 1992.

[101] C. Bourbonnais and L. G. Caron, Int. J. Mod. Phys. B **5**, 1033 (1991).

[102] S. Brazovskii and V. Yakovenko, **46**, L111 (1985).

[103] V. M. Yakovenko, JETP Lett. **56**, 510 (1992).

[104] D. Boies, C. Bourbonnais, and A.-M. S. Tremblay, Phys. Rev. Lett. **74**, 968 (1995).

[105] J. P. Pouget et al., Phys. Rev. Lett. **37**, 437 (1976).

[106] M. Sing et al., Phys. Rev. B **68**, 125111 (2003).

[107] T. Giamarchi, Physica B **230-232**, 975 (1997).

[108] P. Wzietek et al., J. Phys. I (France) **3**, 171 (1993).

[109] A. Schwartz et al., Phys. Rev. B **58**, 1261 (1998).

[110] M. Dressel, K. Petukhov, B. Salameh, P. Zornoza, and T. Giamarchi, Phys. Rev. B **71**, 75104 (2005).

[111] C. Bourbonnais et al., Europhys. Lett. **6**, 177 (1988).

[112] T. Giamarchi, Phys. Rev. B **44**, 2905 (1991).

[113] T. Giamarchi and A. J. Millis, Phys. Rev. B **46**, 9325 (1992).

[114] L. Dudy et al., Photoemission spectroscopy and the unusually robust one dimensional physics of lithium purple bronze, arXiv:1206.0798v1, 2012.

[115] F. Wang et al., Phys. Rev. Lett. **96**, 196403 (2006).

[116] F. Wang et al., Phys. Rev. B **74**, 113107 (2006).

[117] J. Hager et al., Phys. Rev. Lett. **83**, 186402 (2005).

[118] S. Ijima, Nature (London) **354**, 56 (1991).

[119] R. Egger and A. O. Gogolin, Phys. Rev. Lett. **79**, 5082 (1997).

[120] R. Egger and A. Gogolin, Eur. Phys. J. B **3**, 281 (1998).

[121] A. A. Odintsov and H. Yoshioka, Correlated electrons in carbon nanotubes, in *Low-Dimensional Systems: Interactions and transport properties*, edited by T. Brandes, volume 544 of *Lecture Notes in Physics*, page 97, Heidelberg, 2000, Springer.

[122] M. Bockrath et al., Nature (London) **397**, 598 (1999).

[123] H. Shiozawa et al., Physica B **351**, 259 (2004).

[124] J. Lee et al., Phys. Rev. Lett. **93**, 166403 (2004).

[125] A. Kiss et al., Phys. Rev. Lett. **107**, 187204 (2011).

[126] L. Balents, Orthogonality catastrophes in carbon nanotubes, in *Quantum physics at mesoscopic scale: proceedings of the XXXIVth Rencontres de Moriond, Les Arcs, France, January 23-30, 1999*, edited by D.-C. Glattli, M. Sanquer, and J. Thanh Vân Trâ'n, page 11, Les Ulis, 2000, EDP Sciences, cond-mat/9906032.

[127] N. Motoyama, H. Eisaki, and S. Uchida, Phys. Rev. Lett. **76**, 3212 (1996).

[128] J. C. Bonner and M. E. Fisher, Phys. Rev. **135A**, 640 (1964).

[129] D. A. Tennant, R. A. Cowley, S. E. Nagler, and A. M. Tsvelik, Phys. Rev. B **52**, 13368 (1995).

[130] I. A. Zaliznyak, Nature Materials **4**, 273 (2005), cond-mat/0504375.

[131] B. Lake, D. A. Tennant, and S. E. Nagler, Phys. Rev. Lett. **85**, 832 (2000).

[132] B. Lake, D. A. Tennant, C. D. Frost, and S. E. Nagler, Nature Materials **4**, 329 (2005).

[133] P. R. Hammar et al., Phys. Rev. B **59**, 1008 (1999).

[134] M. B. Stone et al., Phys. Rev. Lett. **91**, 037205 (2003).

[135] Görlitz et al., Phys. Rev. Lett. **87**, 130402 (2001).

[136] M. Köhl, T. Stöferle, H. Moritz, C. Schori, and T. Esslinger, Applied Physics B **79**, 1009 (2004).

[137] S. Richard et al., Phys. Rev. Lett. **91**, 010405 (2003).

[138] J. L. Roberts et al., Phys. Rev. Lett. **81**, 5109 (1998).

[139] S. Inouye et al., Nature (London) **391**, 151 (1998).

[140] B. Paredes et al., Nature (London) **429**, 277 (2004).

[141] T. Kinoshita, T. Wenger, and D. S. Weiss, Phys. Rev. Lett. **95**, 190406 (2005).

[142] T. Kinoshita, T. Wenger, and D. Weiss, Science **305**, 5687 (2004).

[143] I. Bouchoule, N. J. Van Druten, and C. I. Westbrook, Atom chips and one-dimensional bose gases, in *Atom Chips*, edited by J. Reichel and V. Vuletic, chapter 11, Wiley-VCH Verlag, Weinheim, 2011, arXiv:0901.3303.

[144] A. H. van Amerongen, J. J. P. van Es, P. Wicke, K. V. Kheruntsyan, and N. J. van Druten, Phys. Rev. Lett. **100**, 090402 (2008).

[145] E. Haller et al., Nature (London) **466**, 597 (2010).

[146] S. Rapsch, U. Schollwöck, and W. Zwerger, Europhys. Lett. **46**, 559 (1999).

[147] E. Orignac and T. Giamarchi, Phys. Rev. B **57**, 5812 (1998).

[148] R. Citro and E. Orignac, Phys. Rev. B **65**, 134413 (2002).

[149] P. Lecheminant and E. Orignac, Phys. Rev. B **65**, 174406 (2002).

[150] E. Orignac, R. Citro, S. Capponi, and D. Poilblanc, Phys. Rev. B **76**, 144422 (2007).

[151] M. Klanjsek et al., Phys. Rev. Lett. **101**, 137207 (2008), arXiv:0804.2639.

[152] H. Tsunetsugu, M. Troyer, and T. M. Rice, Phys. Rev. B **49**, 16078 (1994).

[153] F. D. M. Haldane, Phys. Rev. Lett. **50**, 1153 (1983).

[154] H. Watanabe, K. Nomura, and S. Takada, J. Phys. Soc. Jpn. **62**, 2845 (1993).

[155] S. P. Strong and A. J. Millis, Phys. Rev. Lett. **69**, 2419 (1992).

[156] S. P. Strong and A. J. Millis, Phys. Rev. B **50**, 9911 (1994).

[157] H. J. Schulz, Phys. Rev. B **34**, 6372 (1986).

[158] S. Takada and H. Watanabe, J. Phys. Soc. Jpn. **61**, 39 (1992).

[159] T. Kennedy and H. Tasaki, Phys. Rev. B **45**, 304 (1992).

[160] M. P. M. D. Nijs and K. Rommelse, Phys. Rev. B **40**, 4709 (1989).

[161] M. Oshikawa, J. Phys. C **4**, 7469 (1992).

[162] D. G. Shelton, A. A. Nersesyan, and A. M. Tsvelik, Phys. Rev. B **53**, 8521 (1996).

[163] I. Affleck, T. Kennedy, E. H. Lieb, and H. Tasaki, Phys. Rev. Lett. **59**, 799 (1987).

[164] I. Affleck, T. Kennedy, E. H. Lieb, and H. Tasaki, Commun . Math. Phys. **115**, 477 (1989).

[165] A. Nersesyan and A. M. Tsvelik, Phys. Rev. Lett. **78**, 3939 (1997), ibid. , **79**, E 1171.

[166] M. Greven, R. J. Birgeneau, and U. J. Wiese, Phys. Rev. Lett. **77**, 1865 (1996).

[167] T. K. Ng, Phys. Rev. B **50**, 555 (1994).

[168] S. Eggert and I. Affleck, Phys. Rev. B **46**, 10866 (1992).

[169] S. Eggert and I. Affleck, Phys. Rev. Lett. **75**, 934 (1995).

[170] A. M. Tsvelik, Phys. Rev. Lett. **69**, 2142 (1992).

[171] R. Z. Bariev, Teor. Mat. Fiz. **40**, 95 (1979), [Theor. Math. Phys. **40** 623 (1980)].

[172] R. Z. Bariev, Teor. Mat. Fiz. **42**, 262 (1980), [Theor. Math. Phys. **42** 173 (1980)].

[173] R. Z. Bariev, Teor. Mat. Fiz. **77**, 127 (1988), [Theor. Math. Phys. **77** 1090 (1989)].

[174] S. Ghoshal and A. Zamolodchikov, Int. J. Mod. Phys. A **9**, 3841 (1994), hep-th/9306002.

[175] R. Konik, A. LeClair, and G. Mussardo, Int. J. Mod. Phys. A **11**, 2765 (1996), hep-th/9508099.

[176] E. Polizzi, F. Mila, and E. S. Sorensen, Phys. Rev. B **58**, 2407 (1998).

[177] Ö. Legeza and J. Sólyom, Phys. Rev. B **59**, 3606 (1999).

[178] G. I. Japaridze and A. A. Nersesyan, JETP Lett. **27**, 334 (1978).

[179] V. L. Pokrovsky and A. L. Talapov, Phys. Rev. Lett. **42**, 65 (1979).

[180] R. Chitra and T. Giamarchi, Phys. Rev. B **55**, 5816 (1997).

[181] A. Furusaki and S.-C. Zhang, Phys. Rev. B **60**, 1175 (1999), cond-mat/9807375.

[182] T. Giamarchi and A. M. Tsvelik, Phys. Rev. B **59**, 11398 (1999), cond-mat/9810219.

[183] H. J. Schulz, Phys. Rev. B **22**, 5274 (1980).

[184] F. D. M. Haldane, J. Phys. A **15**, 507 (1982).

[185] S. Sachdev, T. Senthil, and R. Shankar, Phys. Rev. B **50**, 258 (1994).

[186] B. C. Watson et al., Phys. Rev. Lett. **86**, 5168 (2001).

[187] G. Chaboussant et al., Eur. Phys. J. B **6**, 167 (1998).

[188] F. Mila, Eur. Phys. J. B **6**, 201 (1998).

[189] S. R. White, Phys. Rev. Lett. **69**, 2863 (1992).

[190] S. R. White, Phys. Rev. B **48**, 10345 (1993).

[191] N. Shibata, A. Tsvelik, and K. Ueda, Phys. Rev. B **56**, 330 (1997).

[192] S. R. White, I. Affleck, and D. J. Scalapino, Phys. Rev. B **65**, 165122 (2002).

[193] T. Hikihara and A. Furusaki, Phys. Rev. B **63**, 134438 (2001).

[194] H. J. Schulz, Phys. Rev. Lett. **77**, 2790 (1996).

[195] B. Thielemann et al., Phys. Rev. B **79**, 020408 (2009).

[196] M. Klanjsek et al., Phys. Status Solidi B **247**, 656 (2010), Proceedings of International Conference on Quantum Criticality and Novel Phases, Dresde, 2009.

[197] P. Bouillot et al., Phys. Rev. B **83**, 054407 (2011), arXiv:1009.0840.

[198] I. Dzyaloshinskii, J. Phys. Chem. Solids **4**, 241 (1958).

[199] T. Moriya, Phys. Rev. **120**, 91 (1960).

[200] T. Kaplan, Z. Phys. B **49**, 313 (1983).

[201] L. Shekhtman, O. Entin-Wohlman, and A. Aharony, Phys. Rev. Lett. **69**, 836 (1992).

[202] L. Shekhtman, A. Aharony, and O. Entin-Wohlman, Phys. Rev. B **47**, 174 (1993).

[203] D. Dender, P. R. Hammar, D. H. Reich, C. Broholm, and G. Aeppli, Phys. Rev. Lett. **79**, 1750 (1997).

[204] M. Oshikawa and I. Affleck, Phys. Rev. Lett. **79**, 2883 (1997).

[205] I. Affleck and M. Oshikawa, Phys. Rev. B **60**, 1039 (1999), Phys. Rev. B **62**, 9200(E) (2000).

[206] D. N. Aristov and S. V. Maleyev, Phys. Rev. B **62**, R751 (2000).

[207] S. A. Zvyagin, A. K. Kolezhuk, J. Krzystek, and R. Feyerherm, Phys. Rev. Lett. **93**, 027201 (2004).

[208] S. A. Zvyagin, A. K. Kolezhuk, J. Krzystek, and R. Feyerherm, Phys. Rev. Lett. **95**, 017207 (2005).

[209] S. A. Zvyagin et al., Phys. Rev. B **83**, 060409 (2011).

[210] M. Kohgi et al., Phys. Rev. Lett. **86**, 2439 (2001).

[211] R. Matysiak, G. Kamieniarz, P. Gegenwart, and A. Ochiai, Phys. Rev. B **79**, 224413 (2009).

[212] M. Kenzelmann, Y. Chen, C. Broholm, D. H. Reich, and Y. Qiu, Phys. Rev. Lett. **93**, 017204 (2004).

[213] S. Bertaina, V. A. Pashchenko, A. Stepanov, T. Masuda, and K. Uchinokura, Phys. Rev. Lett. **92**, 057203 (2004).

[214] M. Herak et al., Phys. Rev. B **84**, 184436 (2011).

[215] I. Umegaki, H. Tanaka, T. Ono, H. Uekusa, and H. Nojiri, Phys. Rev. B **79**, 184401 (2009).

[216] I. Umegaki, H. Tanaka, T. Ono, M. Oshikawa, and K. Sakai, Phys. Rev. B **85**, 144423 (2012).

[217] A. M. Tsvelik, Phys. Rev. B **42**, 10499 (1990).

[218] M. Clémancey et al., Phys. Rev. Lett. **97**, 167204 (2006).

[219] S. Miyahara et al., Phys. Rev. B **75**, 184402 (2006).

[220] S. Capponi and D. Poilblanc, Phys. Rev. B **75**, 092406 (2007), cond-mat/0612162.

[221] G. Chaboussant et al., Eur. Phys. J. B **6**, 167 (1998).

[222] P. A. Fleury and R. Loudon, Phys. Rev. **166**, 514 (1968).

[223] B. S. Shastry and B. I. Shraiman, Phys. Rev. Lett. **65**, 1068 (1990).

[224] P. J. Freitas and R. R. P. Singh, Phys. Rev. B **62**, 14113 (2000), cond-mat/0004477.

[225] Y. Natsume, Y. Watabe, and T. Suzuki, J. Phys. Soc. Jpn. **67**, 3314 (1998).

[226] V. Gritsev, A. Polkovnikov, and E. Demler, Phys. Rev. B **75**, 174511 (2007).

[227] E. Orignac and R. Chitra, Phys. Rev. B **70**, 214436 (2004).

[228] R. Peierls, *Quantum Theory of Solids*, chapter 5, page 108, Oxford University Press, Oxford UK, 1955.

[229] P. Pincus, Solid State Commun. **4**, 1971 (1971).

[230] G. Beni and P. Pincus, J. Chem. Phys. **57**, 3531 (1972).

[231] E. Pytte, Phys. Rev. B **10**, 4637 (1974).

[232] M. C. Cross and D. S. Fisher, Phys. Rev. B **19**, 402 (1979).

[233] J. P. Pouget, Eur. Phys. J. B **20**, 321 (2001).

[234] J. W. Bray et al., Phys. Rev. Lett. **35**, 744 (1975).

[235] I. S. Jacobs et al., Phys. Rev. B **14**, 3036 (1976).

[236] S. Huizinga et al., Phys. Rev. B **19** (1979).

[237] A. Maaroufi, S. Flandrois, G. Fillion, and J. P. Morand, Mol. Cryst. Liq. Cryst. **119**, 311 (1985).

[238] J. P. Pouget et al., Mol. Cryst. Liq. Cryst. **79**, 129 (1982).

[239] R. Laversanne, C. Coulon, B. Gallois, J. P. Pouget, and R. Moret, J. de Phys. (Paris) Lett. **45**, L393 (1984).

[240] Q. Liu, S. Ravy, J. P. Pouget, C. Coulon, and C. Bourbonnais, Synth. Met. **56**, 1840 (1993).

[241] J. P. Boucher and L. P. Regnault, J. Phys. I (France) **6**, 1939 (1996).

[242] G. Caimi, L. Degiorgi, N. N. Kovaleva, P. Lemmens, and F. C. Chou, Phys. Rev. B **69**, 125108 (2004).

[243] E. Orignac, Eur. Phys. J. B **39**, 335 (2004).

[244] T. Papenbrock, T. Barnes, D. J. Dean, M. V. Stoitsov, and M. R. Strayer, Phys. Rev. B **68**, 24416 (2003).

[245] G. Uhrig, F. Schönfeld, M. Laukamp, and E. Dagotto, Eur. Phys. J. B **7**, 67 (1999).

[246] S. Takayoshi and M. Sato, Phys. Rev. B **82**, 214420 (2010).

[247] M. Tinkham, *Introduction to Superconductivity*, McGraw Hill, New York, 1975.

[248] R. Citro, E. Orignac, S. De Palo, and M.-L. Chiofalo, Phys. Rev. A **75**, 051602(R) (2007).

[249] P. Pedri, S. De Palo, E. Orignac, R. Citro, and M. L. Chiofalo, Phys. Rev. A **77**, 015601 (2008).

[250] S. De Palo, E. Orignac, R. Citro, and M. L. Chiofalo, Phys. Rev. B **77**, 212101 (2008).

[251] R. Citro, S. D. Palo, E. Orignac, P. Pedri, and M. Chiofalo, New J. Phys. **10**, 045011 (2008).

[252] T. Lahaye et al., Nature (London) **448**, 672 (2007).

[253] M. Lu, S. H. Youn, and B. L. Lev, Phys. Rev. Lett. **104**, 063001 (2010).

[254] M. A. Cazalilla, Phys. Rev. A **70**, 41604 (2004).

[255] S. Baroni and S. Moroni, Phys. Rev. Lett. **82**, 4745R (1999).

[256] E. Orignac and T. Giamarchi, Phys. Rev. B **64**, 144515 (2001).

[257] R. M. Bradley and S. Doniach, Phys. Rev. B **30**, 1138 (1984).

[258] M. Kardar, Phys. Rev. B **33**, 3125 (1986).

[259] E. Granato, Phys. Rev. B **42**, 4797 (1990).

[260] D. Jaksch and P. Zoller, New J. Phys. **5**, 56 (2003).

[261] K. J. Günter, M. Cheneau, T. Yefsah, S. P. Rath, and J. Dalibard, Phys. Rev. A **79**, 011604 (2009).

[262] Y.-J. Lin, R. L. Compton, K. Jiménez-García, J. V. Porto, and I. B. Spielman, Nature (London) **462**, 628 (2009).

[263] E. Orignac and T. Giamarchi, Phys. Rev. B **64**, 144515 (2001).

[264] F. D. M. Haldane, P. Bak, and T. Bohr, Phys. Rev. B **28**, 2743 (1983).

[265] C. Denniston and C. Tang, Commensurability in one dimension and the josephson junction ladder, cond-mat/9711049, 1997.

[266] X. Deng, R. Citro, A. Minguzzi, and E. Orignac, Phys. Rev. A **78**, 013625 (2008).

[267] X. Deng, R. Citro, A. Minguzzi, and E. Orignac, Eur. Phys. J. B **68**, 435 (2008), (Proceedings of BEC2008, Grenoble).

[268] S. Aubry and G. André, Ann. Isr. Phys. Soc. **3**, 113 (1980).

[269] D. J. Thouless, Phys. Rep. **13**, 93 (1974).

[270] I. M. Lifshitz, L. P. Pastur, and S. Gredeskul, *Introduction to the theory of disordered systems*, Wiley and Sons, New York, 1988.

[271] G. Roati et al., Nature (London) **453**, 895 (2008).

[272] G. Roux et al., Phys. Rev. A **78**, 023628 (2008).